Distribution Agreement

In presenting this thesis or dissertation as a partial fulfillment of the requirements for an advanced degree from Emory University, I hereby grant to Emory University and its agents the non-exclusive license to archive, make accessible, and display my thesis or dissertation in whole or in part in all forms of media, now or hereafter known, including display on the world wide web. I understand that I may select some access restrictions as part of the online submission of this thesis or dissertation. I retain all ownership rights to the copyright of the thesis or dissertation. I also retain the right to use in future works (such as articles or books) all or part of this thesis or dissertation.

Signature:

_____ _____

Udaya Shankari Rangaswamy Date

MHV68 M2 Manipulation of B cell signaling

By

Udaya Shankari Rangaswamy

Doctor of Philosophy

Graduate Division of Biological and Biomedical Sciences

Microbiology and Molecular Genetics

_____

Samuel H. Speck, Ph.D.

Advisor

_____

Max D. Cooper, M.D.

Committee Member

_____

Arash Grakoui, Ph.D.

Committee Member

_____

Joshy Jacob, Ph.D.

Committee Member

_____

David Steinhauer, Ph.D.

Committee Member

Accepted:

_____

Lisa A. Tedesco, Ph.D.

Dean of the James T. Laney School of Graduate Studies

_____

Date

MHV68 M2 Manipulation of B cell signaling

By

Udaya Shankari Rangaswamy
B.Tech., Anna University, 2006

Advisor: Samuel H. Speck, Ph.D.

An abstract of
A dissertation submitted to the Faculty of the
James T. Laney School of Graduate Studies of Emory University
in partial fulfillment of the requirements for the degree of
Doctor of Philosophy
in
Graduate Division of Biological and Biomedical Sciences
Microbiology and Molecular Genetics

2014

ABSTRACT

MHV68 M2 Manipulation of B cell signaling

By Udaya Shankari Rangaswamy

Gammaherpesviruses, members of the *Herpesviridae* family, are found in a wide variety of mammalian species and are characterized by their ability to establish life-long infections in their host. The human gammaherpesviruses Epstein-Barr Virus (EBV) and Kaposi's Sarcoma-Associated Herpesvirus (KSHV) are associated with several lymphoid disorders and carcinomas. Murine gammaherpesvirus68 (MHV68) is a well-characterized rodent model of gammaherpesvirus infection that is used to study various features of infection such as acute replication, latency, reactivation, host defense and lymphomagenesis. While latency is established in cell types such as B cells, macrophages, dendritic cells and lung epithelial cells, the long-term primary latent reservoir of MHV68 is memory B cells, similar to EBV. M2 is a MHV68 gene product that is required for efficient establishment of latency and reactivation from latency. M2 expression leads to increased IL-10 levels in primary murine B cells. In the first part, I characterized the signaling mechanism utilized by M2 to induce IL-10. Using an inducible B cell expression system, I demonstrate that M2 induces IRF4 in a manner partially dependent on the NFAT pathway to induce IL-10 expression. I also show that IRF4 is required for efficient establishment of latency and for reactivation from latency. In the second part, I show that Y129 is the critical residue of M2 absolutely required for IL-10 production and IRF4 expression *in vitro*; and establishment of latency, reactivation and plasma cell differentiation *in vivo.* Finally, using gene expression data from a microarray analysis, I wanted characterized IL-10 independent genes modulated by M2 and identified Suppressor of Cytokine Signaling-2 (SOCS2) as one such gene. Additionally, I show that M2 interacts and co-localizes with SOCS2. Taken together, this thesis work has identified key molecular players in the host signaling pathway(s) modulated by M2 which will aid in understanding the host evasion strategies utilized by this family of viruses to modulate B cell signaling to their benefit.

MHV68 M2 Manipulation of B cell signaling

By

Udaya Shankari Rangaswamy
B.Tech., Anna University, 2006

Advisor: Samuel H. Speck, Ph.D.

A dissertation submitted to the Faculty of the
James T. Laney School of Graduate Studies of Emory University
in partial fulfillment of the requirements for the degree of
Doctor of Philosophy
in
Graduate Division of Biological and Biomedical Sciences
Microbiology and Molecular Genetics

2014

ACKNOWLEDGEMENTS

To begin with, I owe an awful lot of gratitude to Sam, my scientific guru and a phenomenal one at that. He was instrumental in several stages of my scientific career, particularly in pushing my transition from the nutrition program to MMG. When it comes to science itself, he is such a thorough and rigorous scientist, and has taught me that the right way to do science is to 'simply do it right' (and also perhaps, to make sure it fits the Swiss-cheese approach). He has also given me complete freedom to test my hypotheses and the most important of all – the big bucks to do the research I want. His confidence in me when he says 'you'll figure it out', has taught me to be the better scientist I am today, compared to 6 years ago (when I didn't even know what an inducible expression system was). His patience and encouragement have kept me interested in research even when nothing seemed to work. Thanks a bunch, Sam.

I would also like to thank my committee members for providing valuable suggestions during committee meetings. In particular, Arash-for being a great believer in me, Max- for always having the door open when I need advice on science or career, Dave- for signing any paperwork I need without thinking twice and Joshy- for your advice on experiments especially during the early stages of my PhD when things weren't moving along as expected. Thank you all so much. I could not have asked for a better committee.

The Speck lab members – both past and present have been an extraordinary set that I am grateful to have met. I would like to particularly thank Andrea, my mini mentor, for having taught about all things M2 and her snippets on how to deal with life when M2 fails you. Other members - Liang, Laurie, Craig, Chris, Clint, Katy, Brian, Francine, Tanu, Nalini, Aarthi and Shariya – thanks a lot for all the fun times in the lab and for the random brainstorming sessions on science. Brigid and Caline – I am really glad to have met you both and hope that our friendship outside of lab continues.

Last, but not the least, my pillar of strength, my family and friends without whom this would not be possible. I am extremely grateful to - my parents and my paati (grandma), for their unfaltering faith in me, even though they have no idea what I am doing; my husband, Ilango- for his patience and support through our 'what-seems-forever' long distance relationship; my sister, Poorni for always pampering me when needed; and my niece, Ratria for being my joyful distraction away from science. My local and global friends, Archu, Vivi, Sowmiya, Nandy, Janani and Kumudha - you guys have shown me that distance doesn't matter when it comes to friendship. Finally, I would like to dedicate this thesis to Latha chithi, my almost-surrogate mom, who would have perhaps been the proudest aunt in this world.

TABLE OF CONTENTS

Chapter IV - MHV68 M2 protein increases SOCS2 levels to modulate IFNγ signaling independent of IL-10 induction

Chapter V – Summary, Future directions and conclusions

LIST OF FIGURES AND TABLES

Chapter I

Chapter II

Chapter III

Chapter IV

CHAPTER I

INTRODUCTION

I. Herpesviruses

1. An overview

Herpesviruses, belonging to the family *Herpesviridae,* are ubiquitous viruses with large double stranded DNA genomes. The spherical virion consists of the following: a core that contains the viral DNA, a capsid with an icosahedral symmetry, a tegument containing up to 30 proteins with regulatory functions and a surrounding lipid envelope that is closely associated with the tegument. A characteristic feature of all herpesviruses is their ability to establish a quiescent infection, termed latency, in which there is no progeny virus being produced. During this period, the virus is maintained as an episome in the nucleus of an infected cell. Upon certain stimuli, latency is interrupted, followed by expression of viral genes and production of progeny virus, in a process termed reactivation (reviewed in [1]).

Based on their morphology and biological characteristics, the members of this family broadly fall into three diverse subfamilies –alpha (α)-, beta (β), and gamma (γ)-herpesviruses. The primary attribute used for classification into these subfamilies is their tissue tropism for establishment of latency. The alphaherpesviruses are neurotropic and the human members of this family include herpes simplex virus-1 (HSV-1) that causes cold sores, HSV-2- the causative agent of genital ulcers and Varicella-Zoster Virus (VZV) that causes chickenpox/shingles (reviewed in [2]). The betaherpesviruses establish latency in the cells of monocytic lineage. For example, the human cytomegalovirus (HCMV) is found in granulocyte-macrophage progenitors [3]. The gammaherpesviruses are lymphotropic viruses primarily establishing latency in

lymphocytes. The human gammaherpesvirus Epstein-Barr Virus (EBV), for example, establishes latency in B lymphocytes (reviewed in [4]).

2. The Gammaherpesvirus Family

Unlike the alpha- or the beta- herpesviruses, the gammaherpesviruses share considerable sequence homology between different members of their family, possess very strict species-specific tropism and are tightly linked with the development of a wide variety of lymphoid and non-lymphoid cancers. Based on phylogenetic data, the gammaherpesviruses are further divided into two genera – γ1 herpesviruses (or lymphocryptoviruses) represented by EBV and genetically similar viruses in the Old World Primates [5] and γ2 herpesviruses (or rhadinoviruses), of which Kaposi's Sarcoma associated herpesvirus (KSHV) is a typical example [6]. Rhadinoviruses have been isolated from a broad range of species ranging from mice to mammals. Their species tropism can extend to T cells as well, in the case of Herpesvirus Saimiri (HVS) that infects New World squirrel monkeys (reviewed in [7]).

Another striking feature of the human gammaherpesviruses EBV and KSHV is their link with the development of a multitude of proliferative diseases such as lymphomas and carcinomas. EBV is associated with the following neoplastic diseases : the development of all cases of nasopharyngeal carcinomas [8], majority of the cases of post-transplant lymphoproliferative disorders (PTLD) [9,10], a subset of Hodgkin's lymphomas and T- cell lymphomas , and all cases of endemic Burkitt's lymphoma (reviewed in [11,12]). Likewise, KSHV is present in all cases of Kaposi's sarcoma [6], and is linked to primary effusion lymphomas (PEL) and Multicentric Castleman's disease (reviewed in [13,14]). Due to their potent oncogenic properties, the gammaherpesviruses have gained a lot of attention. However, due to the species-specific nature of this family of viruses, there is lack of comprehensive knowledge about the molecular determinants of the oncogenic processes and the pathogenesis of infection associated with this

virus family. The animal models utilizing primates are hampered by the increased expenses associated with the maintenance of primates as well as the availability of resources such as knockout models and antibodies.

3. MHV68 infection of mice – a small animal model to study gammaherpesviruses

Infection of mice with murine gammaherpesvirus 68 (MHV68) has gained a favorable response in the scientific community as a small animal model for the study of gammaherpesvirus pathogenesis. Murine gammaherpesvirus 68 (also called as MHV68, MuHV4 and γHV68) was originally isolated from bank voles and field mice in Slovakia and recently shown to be endemic to wood mice [15-17]. MHV68 infects common laboratory mice efficiently, allowing investigators to study the virus in a natural host. The natural route of transmission is currently under debate –initial attempts to determine horizontal transmission have been unsuccessful [18] and a recent study demonstrated a sexual transmission route from intranasally infected females to males in laboratory mice [19]. However, inoculation via an intranasal route is generally an accepted as an infection route to study MHV68 pathogenesis and host response. It is to be noted that other routes such as intraperitoneal route of infection have been investigated by our lab and others, and found to mildly affect the kinetics of infection, particularly in the case of certain mutant viruses [20-22].

Sequence analysis identified MHV68 to be a member of the rhadinovirus genera, being more similar to HVS and KSHV, than to EBV[23]. Comparison of the genome organization identified that MHV68 shared a well-conserved sequence homology in about sixty-three of the eighty MHV68 genes to other rhadinoviruses (KSHV and HVS) and were designated identities based on their homolog. Interestingly, there were about fourteen open reading frames (ORFs) detected that were largely MHV68-specific, and designated M1-M14[23] . Some of these genes have been extensively characterized and shown to be primarily involved in aspects of chronic

infection such as immune modulation, latency, reactivation, etc (reviewed in [24]). One such gene M2, identified in the left end of the genome, is the focus of study in this dissertation. Importantly, a number of studies aiming at identifying genes important for replication have demonstrated that the unique genes are dispensable for acute replication [25,26].

Upon intranasal infection of mice with MHV68, there is an acute phase characterized by productive replication in the lung in the alveolar epithelial cells and lung mononuclear cells [27] which is cleared by 10-12 days post infection [28]. The infection then spreads to the spleen where the virus induces a CD4+ T cell dependent splenomegaly [29]. Trafficking to the spleen requires B cells as observed by a lack of latency establishment in mice lacking B cells [30], but this defect can be overcome by infecting mice intraperitoneally, even at a low dose of 100PFU [31]. In the spleen, the virus undergoes a short replication phase that follows establishment of latency primarily in B lymphocytes, as well as in macrophages and dendritic cells [32-35], that lasts for the lifetime of the animal. As in the case of EBV, the long-term reservoir for latency is the class-switched memory B cells [33,36]. Notably, lung epithelial cells as well as B cells in the lung also harbor latency [37,38] and a recent study shows lung endothelial cells could also act as a site of persistence [39].

As in the case of the human gammaherpesviruses, MHV68 is not tumorigenic upon infection of immunocompetent mice, and the mice remain asymptomatic up to two years post-infection. BALB/c mice infected with MHV68 have shown a ~9% incidence of mild-high grade lymphomas in a three-year period, potentially due to the genetics of BALB/c mice compared to other strains examined [40]. However, in an immune compromised setting, elicited by treatment of infected mice with cyclosporine, there was an increase in the frequency of lymphoproliferative disorder (LPD) [40]. Furthermore, in a comparative study examining the infection of MHV68 in β2 microglobulin knockout (β2m-/-) mice in two different mice backgrounds, the authors found that when compared with the 129/Pas β2m-/- mice, BALB/c β2m-/- mice had a higher incidence

and faster development of B cell lymphomas and lymphoproliferative lesions termed atypical lymphoid hyperplasia (ALH) [41]. This illustrates that the genetic background as well as the host immune status play a critical role in elucidating the molecular mechanisms of lymphomagenesis. Importantly, MHV68 does not transform primary murine B cells in culture and therefore, much of the *in vitro* data on MHV68 genes was obtained using the S11 latently infected cell line [42]. This cell line was isolated from the lymphoma of a latently infected BALB/c mouse and shown to maintain the MHV68 genome in an episomal form capable of reactivation with a chemical inducer, namely phorbol 12-myristate 13-acetate (PMA, also called TPA) [43,44]. Of particular interest is a recent study showing that infection of murine fetal liver cells by MHV68 resulted in immortalization and differentiation of these cells into B cell plasmablasts. Furthermore, these transformed cells were capable of inducing lymphomas when injected into immunocompromised mice [45]. This experimental system opens new possibilities for examination of viral genes required for lymphomagenesis and host factors critical for the transformation process.

4. MHV68 M2- a unique latency and reactivation associated gene

As mentioned above, sequencing of the MHV68 genome revealed a set of unique genes that were largely dispensable for lytic replication. A subset of these genes and their associated functions are as follows: the secreted M1 gene possesses superantigen like properties inducing expansion of a Vβ4(+) CD8(+) T cell subset [46], the M2 gene is a B cell modulatory protein with functions in latency and reactivation, the secreted product of the M3 gene is an immunomodulatory protein that binds CC chemokines, but not CXC chemokines [47-49], and the secreted M4 protein is required for establishment of latency at early times post infection in the spleen [50]. Perhaps, the most studied gene among the unique genes of MHV68 is M2, given its multifaceted roles in MHV68 pathogenesis and B cell signaling (see description below).

The gene that is the subject of this dissertation, M2, was first hypothesized to be a candidate latency associated gene in a reverse transcriptase PCR screen to identify latency and lytic associated transcripts from MHV68 infected mice and in the latently infected *in vitro* B cell tumor line S11 [44,51,52]. Although M2 possesses no homology to any known cellular or viral protein, it contains several PxxP motifs that are capable of binding cellular proteins that contain SH3 interaction domains. M2 also contains two closely spaced tyrosines, at positions 120 and 129, which are potential targets of SH2 containing cellular proteins (Figure 1). This suggested that M2 acts as a scaffolding protein that can bring together cellular proteins during certain cellular processes such as activation, interaction, etc. To this end, several studies have been done to tease apart the biochemical functions of M2.

a) Biochemistry of M2

Upon overexpression of M2 in the A20 B cell line and NIH 3T3 fibroblasts, there is downregulation of STAT1 and/or STAT2, leading to inhibition of IFNα/β as well as IFNγ signaling [53]. M2 expression in A20 cells also showed that it interacts with the (damage-induced DNA Binding protein-1) DDB1/COP9/Cullin repair complex and the ATM DNA damage signal transducing protein to inhibit DNA-damage induced apoptosis [54]. Consistent with this observation, using a yeast two hybrid screen, *Madureira et al* showed that M2 interacts with the Vav1 and Vav2 nucleotide GEF(Guanine nucleotide Exchange Factors) proteins[55]. It was also shown that upon BCR crosslinking, M2 expression in the WeHI B cell line resulted in diminished cell cycle arrest and apoptosis [55], perhaps by its association with the DDB1/COP9/Cullin complex. M2 can phosphorylate Vav, leading to downstream activation of Rac1 and formation of a trimolecular complex with Vav and Fyn [56]. The authors also show that one of the PxxP motifs in the C-terminal end of M2 is essential for this complex formation[56]. Consistently, infection of Vav1-/- or Vav2-/- mice with wild type virus resulted in accumulation of the virus in the germinal

centers, indicating that Vav proteins are required for efficient latency establishment[56]. In a follow-up study, the authors show that this complex formation also requires the tyrosines at positions 120 and 129 of M2 [57]. In this study, the authors show that M2 is phosphorylated at Y120 in a constitutive fashion upon expression in the A20 B cells, and that the phosphorylated M2 serves to bring together the complexes of Vav and Fyn[57]. Furthermore, upon infection of Balb/c mice, a mutant virus in which Y120 and Y129 are mutated to phenyalanine behaved similar to a M2 null virus with respect to establishment of latency, indicating that the tyrosine(s) are critical for M2 mediated functions [57](further described in Chapter 3).

M2 expression in primary murine B cells leads to increased proliferation, and survival along with increased secretion of IL-10 in culture supernatants. Consistently, when infected with a M2 null virus, mice have decreased serum IL-10 levels, along with elevated cytotoxic T-cell responses [58] indicating that M2 mediated IL-10 production plays a pivotal role in dampening of the immune response. M2 expressing cells also down-regulate B220, MHC II, IgD along with upregulation of GL7 and IgG (surface as well as secreted), indicating that M2 expressing cells differentiate towards a plasmablast phenotype. Furthermore, M2 expression in a lymphoma cell line BCL1-3B3, capable of plasma cell differentiation upon certain stimuli [59], leads to differentiation into plasma cells, as confirmed by increase in size of cells, upregulation of IRF4, Blimp-1,XBP-1 and J-chain transcripts as well as increased IgG and IgM secretion [60]. A recent study on characterization of M2 interacting partners identified that Y120 of M2 binds Vav, NCK1, Src family kinases and p85α whereas Y129 preferentially bound PLCγ2, SHP2 as well as p85α [61], indicating that M2 is capable of interacting with multiple proteins involved in the B cell signaling cascade (Figure 1). These data indicate a complex role for M2 in modulation of B cell signaling. The *in vivo* implications of some of these interactions are yet to be determined.

b) In vivo roles of M2

The wealth of biochemical studies on M2 function has been instrumental in showing that M2 acts as a scaffolding protein bringing together B cell signaling molecules importantly Vav, Fyn and PLCγ2 among others. These *in vitro* studies have been rightfully complemented by a vast number of *in vivo* studies that aimed to dissect the role of M2 in MHV68 biology. M2 contains a CD8+ T cell epitope [44] that elicits a B cell dependent, CD8+T cell response to MHV68 infection peaking at 14 days post infection (dpi) [62]. Analysis of an M2 null virus showed that M2 is dispensable for acute replication in the lungs and spleen following intranasal (IN) infection [20,21,63]. Upon IN infection at a high dose of $4x10^5$ PFU, there was a defect in the establishment of latency, as well as reactivation from latency in the spleen at 16 days post infection (dpi), which was largely resolved by 42 dpi. Interestingly, upon infecting intraperitoneally (IP) at a high dose of 10^6 PFU, there was no defect in the establishment of latency at the spleen or peritoneal exudate cells (PECs) [20]. Importantly, there was a striking defect in reactivation from latency upon high dose IN infection, but not IP infection [20].

A careful examination of the dose and route specific phenotypes of the M2 null virus showed that the striking defect in establishment of latency exists only upon IN administration of a low dose of 100PFU, and that the defect can be partially overcome by administering either a high dose $4x10^5$ PFU IN or with a low dose of 100PFU given IP [21]. However, even under conditions where the M2 null virus can establish efficient latency in splenocytes, there was a significant defect in the ability of the virus to reactivate. These data indicate that the requirement for M2 *in vivo* is two-fold – at a latency establishment phase and a reactivation phase. Furthermore, M2 is required for the efficient transition of infected B cells from the germinal center cells to the memory B cell reservoir [21,64]; further emphasizing that M2 manipulates B cell signaling for efficient latency establishment. In an elegant study employing a recombinant yellow fluorescent

protein (YFP) tagged virus, *Liang et al* [60]showed that at the peak of latency, there was no difference in the percentage of virus infected cells with a germinal center phenotype ($GL7^{+}CD95^{+}$) between wild type virus and a M2 null virus. On the other hand, there was a remarkable difference in the frequency of infected cells with a plasma cell phenotype ($B220^{low}$, $CD138^{hi}$) ([60] and personal observations). In the same study, sorting of infected plasma cells showed that these cells represent majority of the reactivating cells at the peak of latency, strongly linking plasma cell differentiation to virus reactivation [60]. Taken together, the studies on MHV68 M2 direct to a role for M2 in modulation of the host cell signaling during infection to establish an efficient infection.

II. B cell signaling and differentiation

1. An overview

The B cell receptor (BCR) complexes consist of the antigen binding cell surface immunoglobulin and the invariant chains Igα/Igβ which contain immunotyrosine activation motifs (ITAM) responsible for signaling. Upon crosslinking of the B cell receptor (BCR) with antigen, the closely spaced tyrosines on the ITAMs get phosphorylated by the receptor associated tyrosine kinases, namely Src family kinases (reviewed in[65,66]).The phosphorylated tyrosines of the ITAMs then recruit and bind the SH2 domains of a second kinase, termed the Syk kinase, which can then auto phosphorylate and activate the adaptor protein B cell linker protein (BLNK), which initiates a rather coordinated cascade of signaling events downstream of the BCR (reviewed in[67,68]). Downstream signaling involves activation of several proteins that bind phosphorylated tyrosines via SH2 domains, such as the enzyme PLCγ2 among others, mediating downstream nuclear signals that activate the key transcription factors NF-κB, NFAT, AP-1, ERK, etc. PLCγ2 activation results in production of the second messengers inositol-1,4,5-trisphosphate (IP3) and diacylglycerol (DAG) (reviewed in [69]). IP3 then binds to its receptors in the ER

membrane resulting in the release of Ca^{2+} from the ER. This transient increase in Ca^{2+} levels results in the activation of the NF-κB pathway [70]. When the ER stores get depleted, there is an increase in the Ca^{2+} from extracellular stores, that leads to activation of the Calcineurin-NFAT pathway[71,72] (Figure 2).

2. Signaling molecules of Gammaherpesviruses

The human gammaherpesviruses are notorious for encoding proteins that deregulate the host signaling machinery in order to survive successfully in their hosts. Some of these proteins also possess transformation capacities along with their signaling properties. EBV encodes the latent membrane proteins, LMP-1 and LMP2a, both of which are capable of modulating B cell signaling by mimicking constitutive CD40 or BCR signaling, respectively [73-75]. LMP-1 possesses transforming capability [76] whereas no such role has been identified for LMP2a. Both of these proteins can activate the PI3K pathway and LMP1 primarily mediates its functions by activation of the NFκB pathway [77-82]. KSHV encodes K1, a transforming protein [83] which contains an ITAM motif capable of propagating signals that result in activation of the NFAT pathway primarily [83-85], and NFκB pathway in some cases [86]. Similar to LMP1, signaling via K1 is constitutive [83,84]. KSHV also encodes K15, in the 3' end of the genome, in a location similar to that of EBV LMP2a. The functions of K15 include inhibition of BCR signaling and activation of the MAPK and NFκB pathways [87-89]. Notably, the primate herpesvirus HVS encodes STP, which is capable of transformation [90,91] as well as signaling via NFκB [92] in a fashion similar to that of EBV LMP-1 and KSHV K1. Indeed, it was shown that K1 can effectively substitute for STP for its oncogenic potential [83]. HVS also encodes another transforming protein, Tip, which interacts with Lck, a TCR associated kinase leading to deregulated TCR signal transduction and constitutive STAT3 activation [93-95]. Of particular note, upon collinear alignment of the genomes of herpesviruses, the location of MHV68 M2 is

very similar to that LMP1, K1 and STP. Interestingly, as mentioned above, although M2 is not found on the plasma membrane of the B cells [53], it does associate with membrane associated receptor tyrosine kinases such as Src family kinases [57,61].

Importantly, the gammaherpesviruses also encode viral cytokines that are homologous to their cellular counterparts. EBV encodes vIL-10[96], capable of transforming B lymphocytes [97]. The functions of vIL-10 include inhibition of IFNγ and IL-2 production [98], downregulation of MHC I by inhibition of TAP transporter protein [99], reduced antigen presentation by monocytes by downregulation of MHC II [98]. The myriad functions of vIL-10 indicate that EBV has evolved to encode this viral protein to create a cellular environmental niche that lets it survive in the host by suppressing the host response. KSHV encodes a vIL-6 cytokine that can induce B cell proliferation as well as IL-6 production by PEL cells [100,101]. vIL-6, in contrast to cellular IL-6, signals primarily through the gp130 subunit of the IL6 receptor(IL6R) independent of the IL6Rα subunit [102]. KSHV also encodes several chemokines namely, vCCL1, vCCL2 and vCCL3 (also termed vMIPI, vMIPII and vMIPIII, respectively), that are homologous to cellular CC chemokines capable of binding CC chemokine receptors (CCRs). These viral chemokines collectively seem to act by inducing angiogenic properties leading to KS progression (reviewed in [103-106]). In contrast to the human gammaherpesviruses, MHV68 does not encode any cytokine or chemokine homolog, but the high levels of IL-10 induction along with increased IL-6, IL-2 and MIP1α [58] upon expression of M2 indicates that MHV68 may have evolved to encode M2 as a multifunctional protein that combines redundant functions of some of their human counterparts .

3. IL-10 – role in B cells

IL-10 is a pleiotropic cytokine originally identified as a T_h2 cytokine that is capable of inhibiting T_h1 cells [107,108], but later known to be produced by most types of cells of the

immune system namely B cells,T_h1, T_h17, Treg, CD8+ T cells, DCs, macrophages, mast cells, NK cells, neutrophils and eosinophils (reviewed in [109]). The various functions of IL-10 are illustrated in Figure 3.

B cells can secrete IL-10 as well as respond to IL-10 in an autocrine fashion[110]. Exogenous IL-10 enhances human B cell proliferation, class-switching and differentiation into antibody secreting cells [111-114]. Reports on the ability of IL-10 to enhance differentiation of murine B cells are unclear, although it is shown to enhance survival and proliferation of murine B cells [115,116]. IL-10 production in mice was initially thought to be restricted to $CD5^+$ B-1 B cells in the peritoneal cavity [117-119], implicating a role for IL-10 in B-1 B cell development. However, there is a mounting evidence for a regulatory subset of B cells in mice and humans that is characterized by the ability to produce IL-10. These cells, termed B_{regs} are shown to play regulatory roles in several models of autoimmunity, inflammatory bowel disease, cancer, etc [120-129]. However, there are no reports on the transcription factors that are responsible for differentiation of naïve B cells into B_{regs}. There is also considerable debate about the surface markers used to differentiate these subsets in mice and humans and a clear picture is yet to emerge on the differentiation state of this specialized B cell subset. M2 expressing cells produce significant amounts of IL-10 [58], undergo proliferation and survive better. This indicates that perhaps, IL10 is made by M2 expressing cells to enhance their survival and create an immunosuppressive environment where cell types other than the M2 expressing B cells are suppressed. By initiating this scenario, the virus ensures that the latent reservoir for the virus is amplified (Figure 4).

4. Plasma cell differentiation – an overview

B cell development begins in the bone marrow where hematopoetic stem cells give rise to lymphocyte precursors that undergo rearrangements of their V, D and J gene segments to produce

immature B cells expressing surface IgM [130]. The immature B cells then exit the bone marrow and migrate to secondary lymphoid organs, such as the spleen, where they become mature B cells [131]. In the spleen, depending on the environmental signal, they can either become a marginal zone B cell or a naïve follicular B cell. Marginal zone B cells are a small fraction of B cells which represent the early antibody responders to certain pathogens. They primarily depend on T-independent antigens, although they are capable of making antibodies to some T dependent antigens as well (reviewed in [132]). Upon encounter with an antigen and with T-cell help, the follicular B cells can either become short-live plasma cells producing IgM primarily, or form germinal centers. In the germinal centers, these cells undergo several rounds of proliferation, somatic hypermutation and class switch recombination (reviewed in [133]) . Cells then exit the germinal center either as memory B cells with high affinity for the target antigen, or as long-lived plasma cells, some of which home to the bone marrow and secrete high affinity antibodies that last up to a year[134,135]. The regulation of plasma cell development is controlled by a tightly coordinated set of transcription factors that act to either inhibit plasma cell differentiation (to maintain B cell identity) or promote plasma cell differentiation (by repression of B cell identity). The major transcription factors that promote plasma cell differentiation are interferon regulatory factor 4 (IRF4) (described below), B lymphocyte induced maturation protein (Blimp-1), and X-box binding protein-1 (XBP-1) [59,136-140].

a) IRF4 in plasma cell differentiation

Interferon regulatory factor 4 (IRF4) is a member of the IRF family that is specifically expressed by cells of the immune system. It is highly upregulated upon activation of T and B cells. Analysis of IRF4-/- mice revealed that IRF4 is required in several aspects of mature T and B cell functions, namely activation and antibody responses [141]. IRF4 is expressed in all stages of B cells except in germinal center cells [142], potentially due to the high levels of expression of

microphthalmia-associated transcription factor (MITF), that inhibits IRF4 in the germinal center [143]. The role of IRF4 in germinal center formation is currently unclear –*Irf4*$^{fl/-}$Cγ1-Cre mice in which IRF4 is deleted post GC formation display normal GC responses [140] compared to *Irf4*$^{fl/fl}$CD19-Cre mice which have a severe defect in GC formation [144]. Based on current evidence, it appears that IRF4 is required for formation of a GC but perhaps not for maintenance of a GC reaction. While the role of IRF4 in the GC reaction is unclear, several lines of evidence show that IRF4 is absolutely required for 1) class switch recombination by induction of *Aicda* expression and 2)plasma cell differentiation, potentially by directly upregulating the levels of Blimp-1, the master regulator of plasma cell development [139,140,144-146]. IRF4 is also required for the transcriptional regulation of several B cell differentiation associated molecules, namely Igκ light chain enhancer, CD23,CD20 and MHC-I (reviewed in [147,148]). Consistent with the requirement of IRF4 regulation of B cell differentiation, it is also required for T cell differentiation [149-152] and development by regulating the transcription of several cytokines, namely IL-10 and IL-4 [153,154]. Given the ability of IRF4 to modulate expression of a vast majority of cytokines in T cells, it seems possible that it may do so in B cells as well.

b) Plasma cell differentiation associated reactivation in gammaherpesviruses

Early studies in EBV implicated that differentiation to a plasma cell might be a trigger to initiate reactivation of EBV genome positive B cells [155]. In healthy human carriers, tonsillar plasma cells are reactivated to produce virus. Furthermore, BZLF-1(also called Zta is the lytic transactivator protein of EBV) promoter activity was high in plasma cells that arose from differentiation of a memory B cell *in vitro* [156]. Indeed, it was shown that the plasma cell associated factor XBP-1s can transactivate the BZLF-1 promoter [157,158]. This applies in the case of KSHV as well. XBP-1 can also transactivate the promoter of KSHV/Rta, the lytic transactivator protein, to induce reactivation [159,160]. A gene expression analysis aimed to

identify the B cell developmental stage of PEL cells identified that the profile fits closely to that of plasma cells, with a decreased expression profile of mature B cell genes [161]. Importantly, in both EBV and KSHV, the reactivation trigger seemed to be the cellular transcription factor, XBP-1 that was capable of initiating the lytic transactivation cycle. It seems intriguing that the virus depends on a host factor (XBP-1) to initiate reactivation. Interestingly, in the case of MHV68, plasma cell differentiation is linked to reactivation from latency. At the peak of latency, when purified from total splenocytes, the infected plasma cell population represented the major reservoir of reactivating cells in an *ex-vivo* explant reactivation assay. Notably, infection with a mutant virus lacking the M2 gene was severely compromised or plasma cell differentiation, indicating that M2 was required for efficient plasma cell differentiation. Consistently, expression of M2 resulted in differentiation of a BCL-1 lymphoma cell line into plasma cells [60], as well as differentiation of primary murine B cells to a pre-plasma memory phenotype [58]. This strongly suggests that the human gammaherpesviruses may also encode proteins that can cause plasma cell differentiation mediated reactivation. The likely targets for EBV include the LMP proteins and vIL-10 and K1 for KSHV.

Given the importance of plasma cell differentiation in reactivation of gammaherpesviruses, we wanted to determine how MHV68 M2 facilitated plasma cell differentiation. Since M2 mediated IL-10 as well as induced plasma cell differentiation, we aimed to identify the signaling mechanisms of M2 leading to IL-10 expression and/or plasma cell differentiation. We also wanted to identify potential residues on M2 that are critical for induction of IL-10. These studies will help in identifying the cellular players that play important roles in gammaherpesvirus biology, particularly in reactivation.

FIGURES

Figure 1

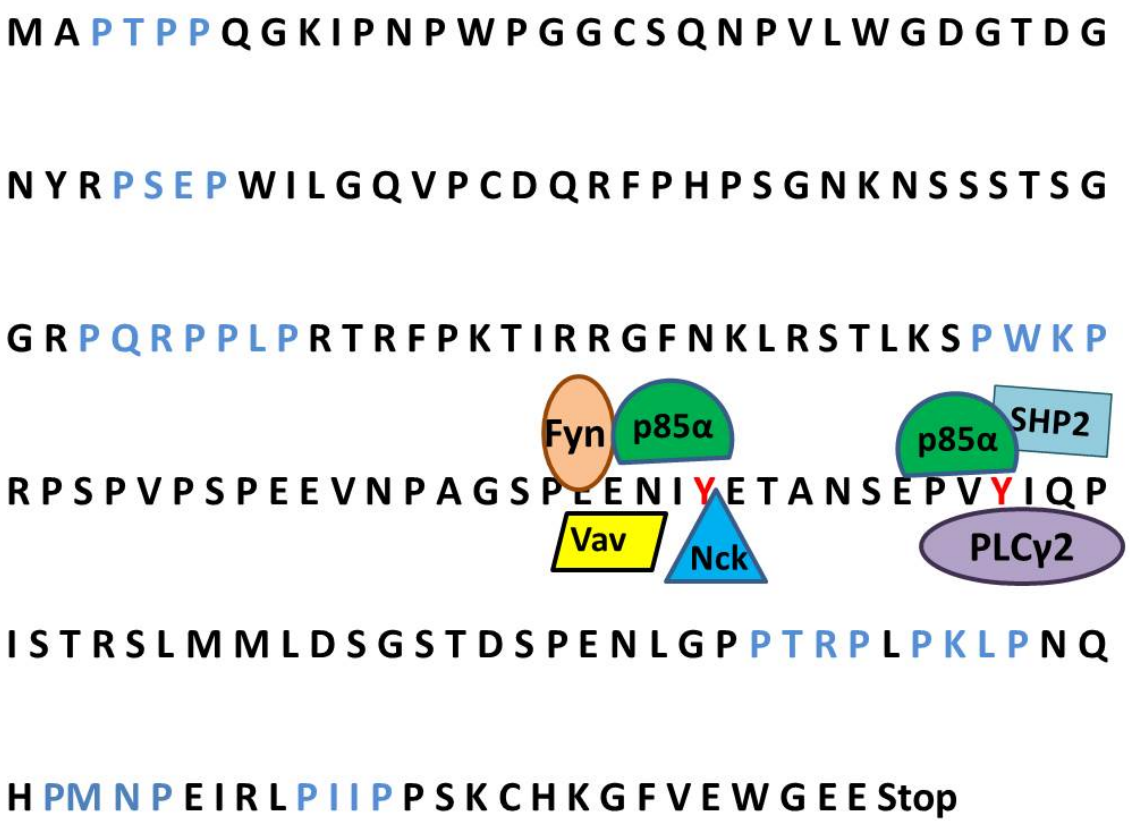

Figure 2

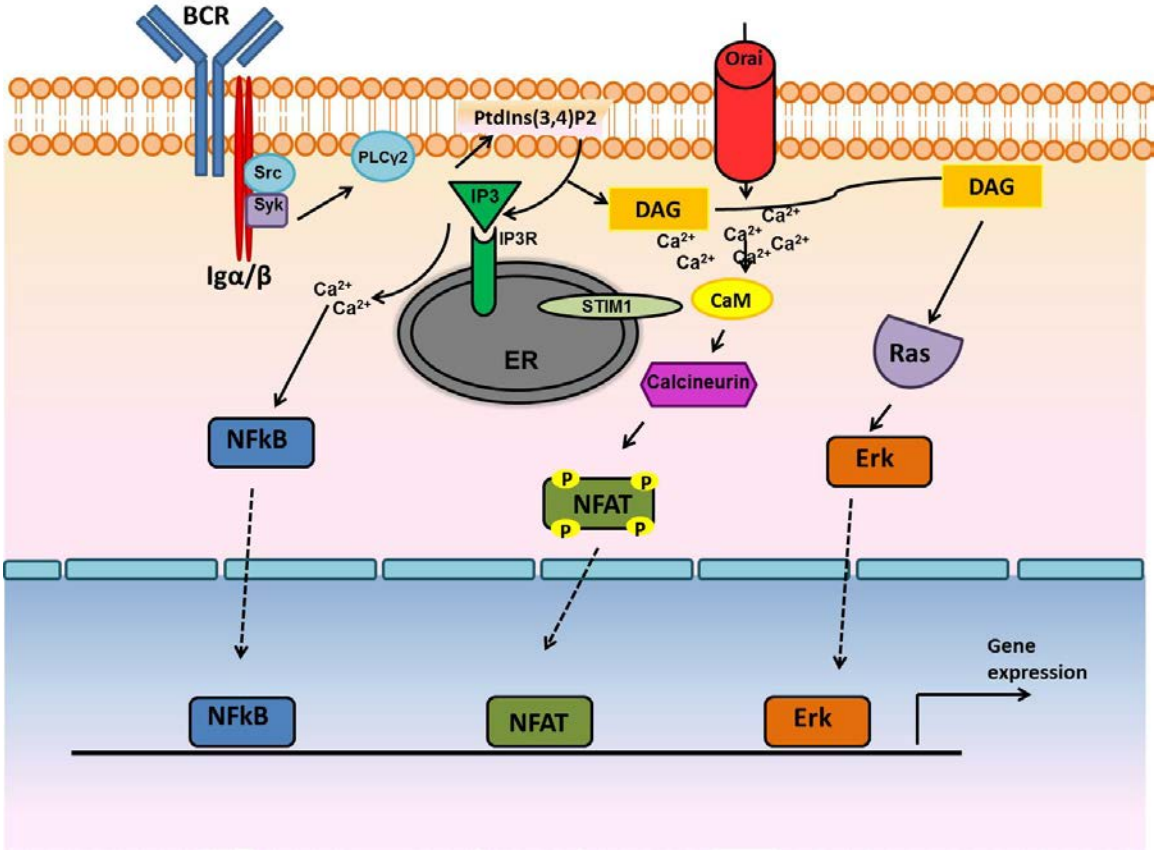
BCR
Orai
PtdIns(3,4)P2
PLCγ2
Src
Syk
IP3
IP3R
DAG
DAG
Ca2+
Ca2+
Ca2+
Ca2+
Ca2+
Ca2+
Ca2+
Ca2+
Igα/β
STIM1
CaM
ER
Calcineurin
Ras
NFkB
NFAT
Erk
P
P
P
P
Gene
expression
NFkB
NFAT
Erk

Figure 3

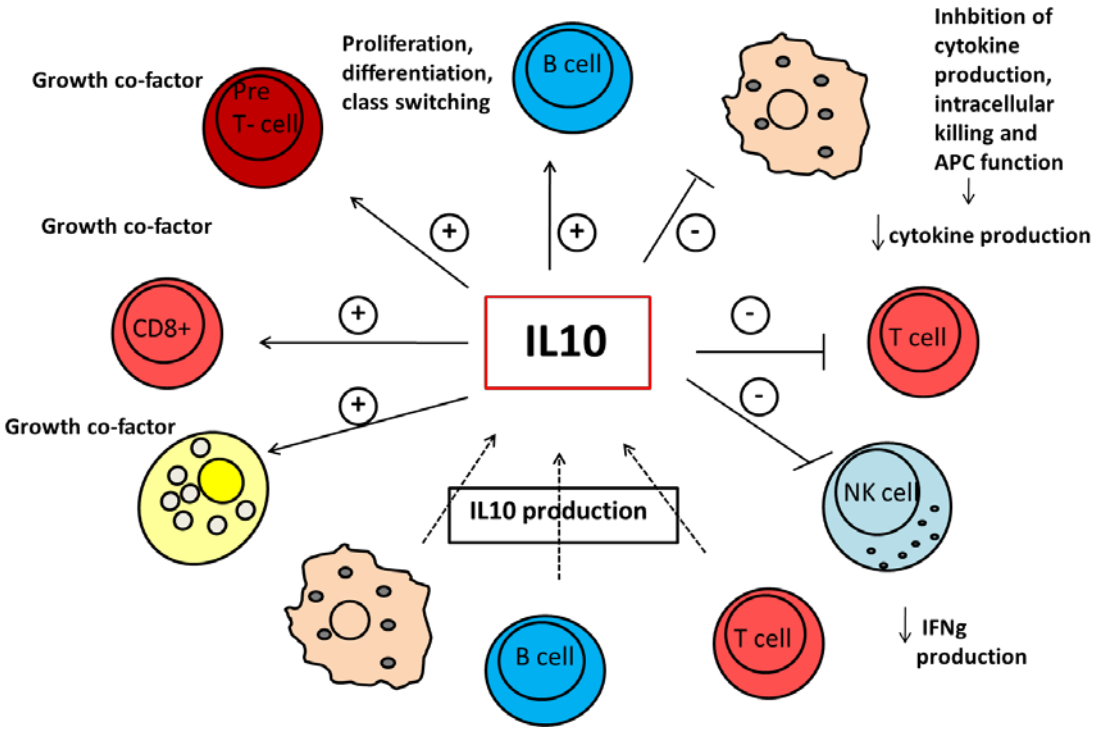
Growth co-factor
Pre T- cell
Proliferation, differentiation, class switching
B cell
Inhbition of cytokine production, intracellular killing and APC function
cytokine production
Growth co-factor
CD8+
IL10
T cell
Growth co-factor
NK cell
IL10 production
B cell
T cell
IFNg production

Figure 4

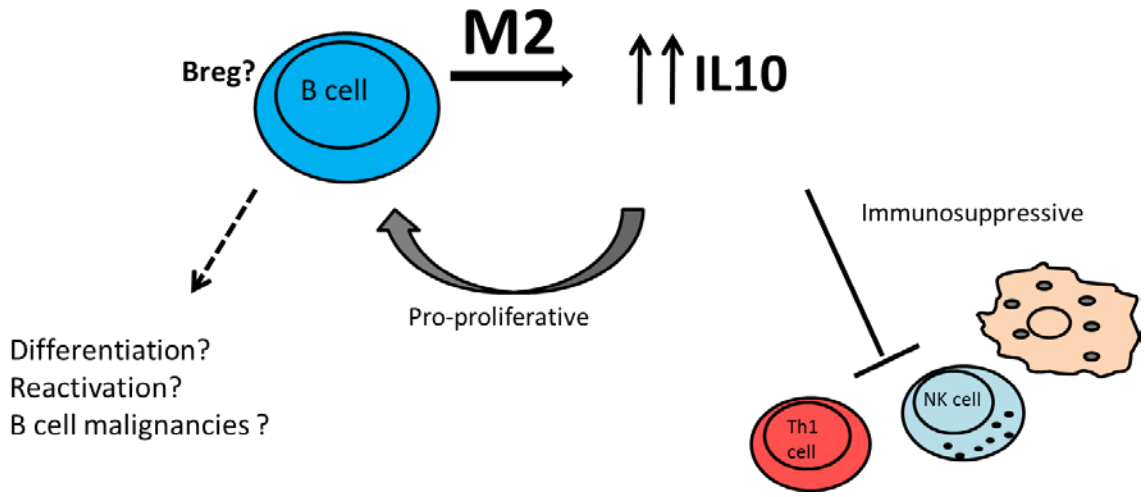
Breg?
B cell
M2
IL10
Immunosuppressive
Pro-proliferative
Differentiation?
Reactivation?
B cell malignancies ?
NK cell
Th1 cell

FIGURE LEGENDS

Figure 1. Amino acid sequence of M2. The amino acid sequence of M2 is shown. The PxxP motifs capable of interacting with SH3 domain containing cellular proteins are shown in blue. The two tyrosines are shown in red. The proteins shown to interact with each of the tyrosines are depicted by colored blocks. The blocks do not indicate a complex formation and only represent that the tyrosine is capable of interacting with each molecule individually. Adapted from [162].

Figure 2.B cell signal transduction. BCR crosslinking follows a series of events where the ITAMs of Igα/β interact with Src family kinases and Syk kinase, activate effector enzymes such as PLCγ2 which result in calcium immobilization from ER stores, eventually resulting in NFκB activation. Extracellular calcium flux via Orai channels results in a sustained calcium increase that is sensed by Calcineurin leading to NFAT activation. Other pathways shown involve activation of ERK pathway upon DAG activation of Ras family members. Adapted from [163].

Figure 3. IL-10 Is a pleiotropic cytokine. IL-10 is produced by different cell types such as T cells, B cells and macrophages. The effects of IL-10 on the different cell types indicated are shown. Adapted from [164].

Figure 4. Hypothesized roles for M2 mediated IL-10. Our working model for M2 mediated IL-10 functions is shown. Upon M2 expression in B cells, M2 induces IL-10 which enhances proliferation and survival of M2 expressing cells, as a means for efficient establishment of viral latency within the B cells. At the same time, IL-10 serves to dampen the immune response elicited by cell types such as T-cells, macrophages, etc. Thus, by expressing M2, the virus is able to create more reservoirs of latency where M2 is present, and in some instances, induce reactivation to seed new latency reservoirs.

CHAPTER II

Chapter II has been published in the Public Library of Science (Rangaswamy, U.S., and Speck S.H. (2014) Murine Gammaherpesvirus M2 Protein Induction of IRF4 via the NFAT Pathway Leads to IL-10 Expression in B Cells. PLoS Pathog. 2014 Jan;10(1):e1003858. doi: 10.1371/journal.ppat.1003858).

INTRODUCTION

Gammaherpesviruses are lymphotropic viruses that are associated with the development of lymphoproliferative diseases and lymphomas (reviewed in [165]). The two human γ-herpesviruses, Epstein Barr virus (EBV) and Kaposi's sarcoma-associated herpesvirus (KSHV), exhibit very narrow host tropism, making *in vivo* studies challenging and accentuating the need for relevant small animal models. One of the best-characterized animal models of gammaherpesvirus pathogenesis is murine gammaherpesvirus 68 (MHV68) infection of laboratory strains of mice [15,16]. Intranasal inoculation of mice with MHV68 results in an acute lytic phase in the lung that is largely cleared by days 10-12 post infection. Latency is established in the spleen and, similar to EBV, memory B cells are the primary long-term latency reservoir. Periodic reactivation results in productive infectious virus capable of reseeding new latency reservoirs. Efficient trafficking of MHV68 to the spleen requires B cells, as evidenced by the delayed kinetics of establishment of splenic latency in B cell-deficient mice [13,28,30,34].

Both EBV and KSHV encode genes that modulate the host B cell signaling to gain access to the latency reservoir. EBV encodes LMP1 and LMP2a, which mimic signals from CD40 and BCR respectively, and vIL-10- a homolog of cellular IL-10, capable of inducing B cell proliferation [166-168]. Similarly, KSHV encodes K1, a constitutive BCR mimic that functions to activate the PI3K and NFAT signaling pathways [83,85]. MHV68 does not encode clear

homologs of these viral proteins, but the functions of the latency associated M2 gene product closely resemble those of EBV LMP2a and KSHV K1. The M2 ORF is not required for acute replication in the lung, but it is essential (in a dose and route dependent manner) for efficient establishment of latency in the spleen. Furthermore, under conditions where M2 null MHV68 mutants establish latency, a significant defect in reactivation from B cells is observed [20,21]. Consistent with this finding, M2 is required for efficient differentiation of MHV68 infected B cells to plasma cells *in vivo,* and M2 over-expression can drive plasma cell differentiation *in vitro* in a B lymphoma cell line [60]. Furthermore, M2 expression in primary murine B cells leads to proliferation, IL-10 expression and differentiation to a pre-plasma, memory B cell phenotype [58]. Although M2 is not homologous to any cellular or viral protein, it contains two tyrosines and nine PxxP motifs that can bind SH2 and SH3 containing cellular proteins respectively [162]. Indeed, Tyr^{120} and Tyr^{129} of M2 can bind the SH2 domains of Fyn and Vav1 forming a trimolecular complex, resulting in the phosphorylation of Vav1 by Fyn [57]. Moreover, *in vivo* analyses have shown that Tyr^{120} and Tyr^{129} are required for efficient reactivation from latency in splenocytes [162]. M2 has also recently been shown to interact with, and drive phosphorylation of PLCγ2, as well as inhibit downstream Akt pathway activation [61]. While M2 forms multiprotein complexes, detailed analyses of the functional consequences associated with such interactions and downstream signaling events is lacking.

Crosslinking of the B cell receptor (BCR) follows a highly coordinated cascade of intracellular events resulting in the formation of a microsignalosome, primarily consisting of Lyn (a Src family kinase), Syk, BLNK, PLCγ2, PI3K and Vav ([67,68] and reviewed in [66] and [65]). Activation of PLCγ2 results in the hydrolysis of PtdIns-4, 5-P2 to IP3 and DAG. Binding of IP3 to its receptor on the endoplasmic reticulum (ER) membrane leads to release of Ca^{2+} from the ER stores. Upon depletion of the ER Ca^{2+} stores, an influx of extracellular calcium occurs, termed Store Operated Calcium (SOC) flux leading to activation of the calcineurin-NFAT

pathway. The NFAT (Nuclear Factor of Activated T cells) family of transcription factors is a key player in the regulation of gene transcription in response to a variety of immune signals. Originally identified as a T-cell specific factor required for the transcription of the IL-2 promoter, the five different family members – NFATc1 (also known as NFAT2), NFATc2 (also known as NFAT1), NFATc3 (also known as NFAT4), NFATc4 (also known as NFAT3) and NFAT5 are widely expressed in most cell types and act in response to calcium mobilization (with the exception of NFAT5) (reviewed in [169]). The role of NFAT family members in B cells has only recently been appreciated. *In vivo* ablation of NFATc1 results in defective B1a B cell development [170]. Interestingly, mice lacking the regulatory subunit of calcineurin (Cnb1) in B cells exhibit impaired class switching by T-independent type II antigens and defective proliferation upon BCR engagement. These mice have a defect in plasma cell responses (potentially due to lack of sufficient IRF4 expression by these mice) [171], which is reminiscent of a phenotype of M2 null MHV68.

Interferon Regulatory Factor 4 (IRF4), a member of the IRF family of transcription factors, is expressed upon activation of T and B cells. In B cells, IRF4 is expressed in all stages of B cell development except germinal center B cells, and is highly expressed in terminally differentiated plasma cells (reviewed in [148]). Notably, IRF4 is required for class switch recombination and plasma cell differentiation [139,140]. In T cells, IRF4 is required for lineage commitment by controlling the regulation of several cytokines [149,153,172-175], but it still remains unknown whether it plays any such role in cytokine expression by B cells. Interleukin-10 (IL-10), despite its initial identification as a T_h2 specific cytokine, has a broad expression pattern including T_h1, T_h2, T_h17, T_{reg} and B cells. In human B cells, IL-10 has roles in activation, proliferation, immunoglobulin production and differentiation [113,176-178], while the role of murine IL-10 in B cell differentiation is unclear.

In this study, we have identified a key host signaling pathway activated by MHV68 M2 to drive IL-10 expression. We show that M2 signals via the NFAT regulatory network to induce expression of IRF4 which activates the IL-10 promoter. Our study is the first known description of a direct role for IRF4 in IL-10 expression from B cells.

MATERIALS AND METHODS

Cell lines. The M12 murine B cell lymphoma cell line was used as the parent cell line for the development of an inducible cell system that expresses M2 conditionally. The inducible cell line was made according to manufacturer's instructions (Clontech). Briefly, the M12 cell line was transiently transfected with the pCMV-TetON regulator plasmid containing the TetON regulator driven by a CMV IE promoter. The cells were selected with G418 at a concentration of 1mg/mL. Stable cells that were resistant to G418 were expanded and plated in a limiting dilution manner to obtain single cell clones. Clonal cells were screened for their ability to express TetON by a transient transfection with the pTRE3G-luciferase plasmid that contains the tetracycline response element driving luciferase activity. Clones that exhibit highest luciferase activity only in the presence of doxycycline (a tetracycline analog) were chosen. This cell line designated C30p, was used as a parental cell line to account for any phenotypes associated with doxycycline treatment. C30p cells were transfected with the pTRE3G-mCherry-IRES-M2 plasmid along with a linear hygromycin selection marker. Stable bulk cells (termed C30bulk) that were resistant to hygromycin (400μg/mL) were plated in a limiting dilution manner to obtain single cell clones. Clonal cells were screened by doxycycline (500ng) treatment followed by visualization of mCherry expression. Cell lines A20, M12 and its derivatives (C30p, DS10, DS14 and DS15) were grown in complete RPMI-1640 (cRPMI) supplemented with 10% FCS, 100U/mL penicillin, 100mg/mL streptomycin, 2mM L-glutamine and 50mM β-mercaptoethanol. P3X63Ag8 (ATCC-TIB-9), BCL1-3B3 and primary murine B cells were cultured in complete RPMI-1640 along with 10mM non-essential amino acids, 1mM sodium pyruvate and 10mM HEPES. NIH 3T12 cells used to grow virus stocks and Mouse Embryonic Fibroblasts (MEFs) used to measure reactivating virus from splenocytes were maintained in complete DMEM (Dulbecco's Modified Eagle Medium) medium supplemented with 10% FCS, 100U/mL penicillin, 100mg/mL streptomycin and 2mM L-glutamine. Cells were routinely counted using trypan blue exclusion method.

Mice and virus infections. M2stop.HY and M2MR.HY viruses were created using the galK mediated λRed recombineering as described previously [167,179].The MHV68-H2bYFP BAC described in Collins et al [180] was used as a backbone to create a M2/galK intermediate BAC where the M2 ORF was replaced with a galK cassette. The M2/galK intermediate was made by amplifying the galK gene from pGalK using the following primers – gK-M2-FP (5'-tggaggggtttcaacaggcactagtctgatgaggtttcgttttcaggta TCAGCACTGTCCTGCTCCTT-3') and gK-M2-RP (5'-tccaggcgtgtttaaagaaaaagtta tgttctgcgttagcaccttcactgCCTGTTGACAATTAATCATC GGCA-3'). These primers contain 50bp homology arms that flank the M2 ORF. The resulting PCR product was transformed into the SW102/H2bYFP cells and screened by positive selection on minimal media containing galactose as the carbon source. Following confirmation of the M2/galK intermediate by restriction digest, the galK region was swapped out and replaced with either M2 or M2stop containing PCR products amplified from pMIT-M2 or pMIT-M2stop plasmids using the same homology arms used for generating the M2/galK intermediate: M2-FP (5'-tggaggggtttcaacaggcactagtctgatgaggtttcgttttcaggta ATGGCCCCAACACCCCCACA-3') and M2-RP (5'- tccaggcgtgtttaaagaaaaagt tatgttctgcgttagcaccttcactgTTATATAT AGCGATAGGTAT CCTCCTCG – 3'). PCR products were electroporated into the M2/galK intermediate and recombinants were selected on minimal plates containing glycerol and 2-deoxy-D-galactose. Potential colonies were screened by colony PCR and confirmed by sequencing prior to final confirmation by Southern blotting (data not shown).

Eight-12 week old C57BL6/J mice (Jackson Labs) were used for harvesting splenocytes for retroviral transductions and for infections with M2stop.HY and M2MR.HY. $IRF4^{fl/fl}$ mice have been previously described [140] and were purchased from Jackson Labs (catalog no. 009380). Mice were housed and maintained at the Whitehead vivarium according to Emory University and IACUC (International Animal Care and Use Committee) guidelines. Both male and female mice were used since we did not observe any significant gender specific differences in

our preliminary latency or reactivation analyses. Mice were anesthetized using isoflourane before infecting with either 1000PFU of MHV68-Cre or MHV68-WT virus (described in [166]) in 20μLcomplete DMEM via the intranasal route.

Limiting dilution analyses for assessing ex-vivo MHV68 reactivation and establishment of MHV68 latency. To determine the frequency of latently infected splenocytes, a limiting dilution, single-copy sensitive nested PCR assay was performed as previously described [31,34,35]. Briefly, frozen splenocytes were thawed, counted and washed in isotonic buffer prior to plating in serial three-fold dilutions onto a background of 10^4 uninfected 3T12 cells in 96-well plates. Following lysis using a proteinase K mediated digestion step for 6-12 hours, the samples were subject to two rounds of nested PCR. Twelve PCRs were performed for each dilution for a total of six dilutions starting with 10^4 cells. Each PCR plate contained control reactions that contained 0, 0.1,1, or 10 copies of plasmid DNA in a background of uninfected cells. Products were analyzed on a 2% agarose gel. To determine the frequency of splenocytes capable of reactivating virus from latency, a limiting dilution ex-vivo reactivation assay was performed as previously described [31,34,35]. Briefly, splenocytes from infected mice were plated in a two-fold serial dilution fashion (starting with 10^5 splenocytes per well) on to MEF monolayers in 96-well tissue culture plates. Twenty-four wells were plated per dilution and 12 dilutions were plated per sample. Wells were scored microscopically for cytopathic effect (CPE) at 14-21 days post-explant. Preformed infectious virus was detected by plating parallel samples of mechanically disrupted cells onto MEF monolayers alongside intact cells.

Immunoblotting and antibodies. Western blotting was performed by standard Lamelli protocol. Approximately $5x10^5$ cells per condition were harvested, washed once with PBS and resuspended in an appropriate volume of lysis buffer containing 50mM Tris-HCl,150mM NaCl,1mM EDTA and 0.1 % TritonX-100 supplemented with Complete mini-EDTA-free protease inhibitor tablet

(Roche) and 1mM NaF and 1mM Na_3VO_4. The amount of protein in lysates was quantified using DC protein assay (Bio-Rad). For immunoblots using primary B cells, 10μg protein was loaded per well. For cell lines, $5x10^5$ cell equivalents (unless when noted) were directly lysed in equivalent volumes of lysis buffer and 2X Lamelli buffer, boiled at 100°C for 5-10 minutes and resolved by SDS-PAGE. SDS-PAGE gels were transferred on to nitrocellulose membranes using a semi-dry apparatus (Bio-Rad).Blots were blocked with 5% milk in TBS-Tween (TBST) for one hour at room temperature followed by three washes in TBST. Primary antibodies were diluted in blocking buffer and incubated overnight at 4°C. Following overnight incubation, the blots were washed three times with TBST, incubated with secondary antibodies for one hour at room temperature followed by three washes in TBST. The blots were developed using Supersignal West Pico Chemiluminescent substrate (Pierce). Antibodies used include: goat anti-IRF4 (M17), NFATc1 (7A6), NFATc2 (4G6-G5) from Santa Cruz biotechnology (used at a 1:200 dilution), rabbit polyclonal AU1 from Covance (1:1000), mouse monoclonal β-Actin from Sigma (1:10000). All secondary antibodies were from Jackson immunoresearch.

Plasmids and luciferase constructs. pNFAT-luc, pNFkB-luc, pAP-1-luc and pFC-MEKK were obtained from (Agilent technologies) as part of the PathDetect Signal Transduction Pathway cis-reporting systems. pNFAT-luc contains 4X repeats of NFAT enhancer element sequence upstream of a luciferase reporter gene. pNF-kB-luc contains 5X repeats of the NFκB enhancer element upstream of a luciferase reporter gene. pAP-1 reporter plasmid contains 7X repeats of the AP-1 enhancer element upstream of a luciferase reporter gene. pISRE-luc reporter plasmid contains 5X repeats of an ISRE enhancer element upstream of a luciferase reporter gene. pFC-MEKK is a positive control expression plasmid that contains the activating MEKK kinase controlled by a constitutive CMV promoter. IκBαM is a negative control plasmid that expresses a mutant form of the IκB kinase.

The full length IL-10 promoter pGL2B-1538/+64, designated here as IL10pFL-luc, described in [181] was a courtesy of Dr.Stephen Smale, obtained from Addgene (Addgene plasmid 24942). The IL-10promoter constructs containing CNS9 and CNS3 elements, designated IL10pCNS3-luc and IL10pCNS9-luc were constructed by inserting the DNA fragments containing CNS3 or CNS9 into the full length IL-10promoter construct via MluI and XhoI as described in [182]. The DNA fragments containing CNS3 and CNS9 elements were PCR amplified from genomic DNA from naïve C57BL6 splenocytes. The primers used were CNS3 forward: 5' GTGGTCATTTTTTCAGTAAGACC 3', CNS3 reverse: 5'CCTAACCTTTCATCTCACAG 3', CNS9 forward: 5'CGCTCTTC CGAATAGATGTGGT3', CNS9 reverse: 5'CCGCACTCCGAT GTATTAGTTCC3'. PCR products were cloned into pCR-BLUNT vector from Invitrogen to confirm sequence. Positive clones were PCR amplified, digested with MluI and Xho I and ligated into the full length promoter using MluI and XhoI sites.

pMSCV-M2-IRES-Thy1.1(pMIT-M2) and pMSCV-M2stop-IRES-Thy1.1(pMIT-M2stop) are described in [58]. pMSCV-IRES-GFP-Empty vector (pMIG-EV) and pMSCV-IRF4-IRES-GFP (pMIG-IRF4) plasmids were kind gifts from Dr.X.Liang. pRV-NFAT1, pRV-NFAT2 and IL2promoter-luc described in [144,183] were a courtesy of Dr.Anjana Rao, obtained from Addgene (Addgene plasmids 11100, 11101 and 12194 respectively).

Transfections. 1-1.5x10^6 B cells were centrifuged, washed once with PBS and resuspended in 100µL of Ingenio electroporation solution (MirusBio) or solution L (Lonza). Triplicate wells were used per condition. 5µg reporter DNA prepared using Qiagen endofree maxiprep kit was added to the electroporation mixture and nucleofected using Amaxa Nucleofector I system. For M12 cells and the inducible cell clones derived from M12 as the parental cells, the program T-20 was used. To account for variability with doxycycline treated and untreated samples, two reactions worth of cells were pooled prior to nucleofection. Upon nucleofection, the pooled

reactions were split into two, one receiving doxycycline while the other was left untreated. Reporter activity was measured after 48 hours as per manufacturer's instructions (Promega luciferase assay system).

Retrovirus production and transduction of primary B cells. Splenocytes were harvested from 9-12 week old C57BL6 mice (Jackson Labs), and primary B cells were isolated by immunomagnetic negative selection using the EasySep™ Mouse B Cell Enrichment Kit (Stem Cell Technologies) as per manufacturer's instructions. The purity of B cell isolation was routinely analyzed and found to be ≥ 95% as determined by staining for CD19 by flow cytometry. The cells were plated at $1x10^6$ cells/mL of a 24 well plate overnight with cRPMI containing 25μg/mL LPS (Sigma) prior to retroviral transduction. Retroviruses were prepared as described in [58]. Briefly, BOSC23 (ATCC) producer cells were plated at a density of $1.5x10^6$ cells per 60mM collagen coated dish (BD biosciences) overnight. After 18-24hours of plating, the cells were transfected with 5μg of either pMIT-M2 or pMIT-M2stop. Supernatants were harvested at 72 hours and used immediately or frozen at -80°C until ready for use. On the day of transduction, the retroviruses were centrifuged at 2000rpm for 10 minutes to remove any cellular debris and supplemented with 5μg/mL of polybrene. 750μL of the media was removed and replaced with 1mL of the retrovirus containing polybrene. The cells were spin infected for 2500 rpm for one hour at 30°C. Post-transduction, 750μL of the supernatant was removed from each well and 1mL of fresh media was added. Triplicate wells per condition were analyzed by flow cytometry at days 2-5 post-transduction.

Flow cytometry. Flow cytometry was performed as per standard procedure. Briefly, cells from triplicate wells per condition were washed once in FACS buffer (2% FBS in PBS) and incubated with Fc block (Rat anti-mouse CD16/CD32, eBioscience) for 10 minutes prior to surface staining with an antibody cocktail. The cells were washed two times with FACS buffer prior to analysis

on a BD LSRII flow cytometer. Antibodies used include: CD19-FITC, - APC, - PE, -PECy7 or -APC-Cy7, Thy1.1-APC, GL7-FITC, CD23-PE, IgD-FITC, B220-PECy7, CD138-APC, IA^b-PE (eBioscience or BD biosciences). Live dead analysis was routinely included using LIVE/DEAD® Fixable Violet Dead Cell Stain Kit (Invitrogen).

Intracellular staining for IRF4 was performed as described in [139] with minor modifications. Briefly, 5 $x10^6$ cells were surface stained for surface markers as described above. Live/dead analysis was included using Zombie Yellow™ fixable viability stain (Biolegend). After surface staining, cells were fixed with 1%(w/v) paraformaldehyde (Electron Microscopy Sciences) followed by permeabilization with 1X(0.05-0.15%) stock made from 10X saponin-based permeabilization and wash buffer(Invitrogen), diluted in FACS buffer. Cells were incubated overnight in 1X saponin buffer with an antibody cocktail containing a rabbit anti-GFP-FITC antibody at a dilution of 1:500 (Rockland Antibodies) and a polyclonal goat anti-IRF4 at a dilution of 1:100 (Santa Cruz Biotechnology) in the presence of 5% (v/v) normal donkey serum. Normal goat IgG (Santa Cruz Biotechnology) was used as an isotype control. Cells were washed two times with 0.5X saponin based wash buffer followed by incubation with an Alexa-647-coupled donkey anti-goat detection antibody (Jackson Immunoresearch). Cells were washed two times prior to analysis. Data was analyzed using FlowJo software (TreeStar, Inc.).

Drug treatments. Cyclosporin A (500ng/mL), FK-506 (1μM), EGTA (2.5mM), PMA (60ng/mL) and Ionomycin (1mM) were from Sigma. BAPTA-AM (5μM), PP2 (10μM) and PP3 (10μM) were from Calbiochem. The selection drugs, hygromycin and G418 were from Calbiochem and Cellgro, respectively. Doxycycline (5-500ng/mL) was from Clontech. The drugs were used at a final concentration as indicated within parentheses above. Cell viability upon drug treatment was assessed by trypan blue exclusion.

ELISA.ELISA for IL-10 was performed as per manufacturer's instructions (BD OptEIA™, BD Biosciences). Supernatants from cells were stored at -80°C prior to ELISA analysis.

Statistical analysis. Statistical data analysis was performed using GraphPad Prism software. Data shown represents one of at least triplicate experiments. Error bars represent standard error mean. Significance was determined by two-tailed, unpaired Student's t-test with a confidence level of 95%.

RESULTS

Generation of M2 inducible B cell lines that recapitulate M2 induction of IL-10 and IRF4.

M2 expression in primary murine B cells leads to high levels of IL-10 secretion in culture supernatants [58]. Since IL-10 production is a common evasion strategy used by human gammaherpesviruses [32,184], as well as a number of other viruses ([185-189] and reviewed in [190]), we wanted to understand and define the roles of key signaling intermediates that are involved in this progression to IL-10 expression. Due to the limited life-span of primary murine B cells in culture and availability of sufficient starting material to perform biochemical studies, we sought to study signaling networks affected by M2 in an established murine B cell line. Notably, our early attempts to overexpress M2 in murine B cell lines were inefficient and confounded by the fact that most murine B cell lines produce significant levels of IL-10. M2 over-expression in these systems resulted in only a modest increase in the level of IL-10, and identification of signaling intermediates was difficult, most likely due to the fact that M2 augments signaling pathways already activated in these cell lines. To overcome these technical challenges, and to express M2 in a temporal and conditional manner, we created inducible cell lines expressing M2 using the Tet-ON inducible system which allows expression of target genes in a doxycycline-dependent manner. For these studies we used the M12 murine lymphoma cell line to create the inducible M2 expression system. The rationale for using this cell line was two-fold: (i) this cell line is a mature B cell line that does not make any endogenous IL-10 and therefore, any IL-10 that we observe would be the result of M2 expression; and (ii) this cell line is amenable to both transient as well as stable transfection methods. To facilitate detection of M2 by immunoblotting, we introduced an AU1 epitope tag at the C-terminus of M2. In addition, the tetracycline regulated expression plasmid employed harbors a mCherry expression cassette upstream of an IRES

element that drives expression of the inserted M2 coding sequences. The latter facilitated screening of candidate M2 inducible clones (Figure 1A).

Several candidate clonal cell lines were generated using the inducible expression system, and these were screened for tightly regulated M2 expression. Among several clones tested, clones DS10, DS14 and DS15 were used for further analyses. As a control in all experiments outlined below, we used the parental clonal cell line, C30p, which stably expresses the tetracycline regulator protein (TetON) but does not contain the inducible M2 expression vector. This control was included to assess any effect that addition of doxycycline might have on these cells. Expression of the fluorescent protein mCherry was used as a visual measure for M2 expression, and ensured that all cells in a clonal population responded uniformly to doxycycline (dox) induction (Figure 1A). Furthermore, these cells express M2 only upon doxycycline addition, demonstrating tightly regulated expression of M2 without any detectable leaky basal expression (leaky expression of genes is commonly associated with such inducible systems) (Figure 1B). Importantly, we show that the clones DS10, DS14 and DS15 make IL-10 upon M2 induction by doxycycline (Figure 1C). Since this system recapitulates M2 induction of IL-10 in primary murine B cells, it provided an experimental model to further characterize the signaling events downstream of M2 leading to IL-10 production.

Based on our previous finding describing M2 driven-plasma cell differentiation [60], we also wanted to assess whether expression of M2 in this cell line led to changes in the expression of any plasma cell associated factors, namely IRF4, since we observed a robust increase in both transcript and protein levels in our previously analyses of BCL-1 cells expressing M2 [60]. Consistent with our previous analyses, expression of M2 led to a marked increase in the expression of IRF4 (Figure 1B, middle panel), indicating that M2 driven plasma cell differentiation is potentially a result of M2 modulating the levels of IRF4.

M2 induction of IL-10 and IRF4 involves activation of the NFAT pathway.

Biochemical characterization of M2 has revealed that M2 acts as an adaptor protein forming a trimolecular complex with Vav and Fyn [55-57]. Recently, it has been shown that M2 can also bind PLCγ2 - resulting in the inhibition of the Akt pathway [61]. These results, along with *in vivo* work demonstrating that M2 is required for the infected B cells to access the germinal center B cells, strongly suggest that M2 modulates B cell signaling - either by potentiating signals from the BCR or by modulating aspects of BCR-mediated signaling. To gain a better understanding of the major signaling pathways manipulated by M2, we sought to perform a luciferase assay based screen using the PathDetect Signal Transduction cis-reporting system (Agilent technologies). This system employs a collection of inducible reporter plasmids to assess activation of major signal transduction pathways. These reporter plasmids contain a luciferase reporter gene driven by a basic promoter element plus a defined inducible cis-enhancer element. Using these reporters and the inducible cell lines, we analyzed whether M2 induction by doxycycline modulates the key pathways (NFκB, NFAT, AP-1 and ISRE pathways) known to be important in immune response to viruses. When compared to the uninduced cells, the cells that received doxycycline treatment activated the NFAT pathway significantly (Figure 2A). Notably, this activation was of similar or greater magnitude compared to the positive control induction (i.e., treatment with a combination of PMA and ionomycin, well-characterized activators of NFAT pathway), indicating a robust induction of this pathway by M2 (Figure 2A). To verify that this effect was indeed due to M2 expression, rather than an unanticipated side effect of doxycycline addition, we performed the same experiment in the C30p parental cell line. Notably, in the C30p parental cells we failed to observe any impact of doxycycline on the NFAT pathway (Figure 2B), confirming that M2 directly activates the NFAT pathway. We also confirmed M2 induction of the NFAT pathway in another M2 inducible clonal cell line, DS15 (Figure 2C).

Analysis of NFkB reporter revealed weak activation by M2 (Figure 2D). However, it should be noted that established B cell lines in general have high basal levels of NFkB activity. Thus, it is perhaps not surprising that M2 can only modestly enhance this activity. Analyses of the AP-1 and ISRE reporters in the DS10 cell line failed to reveal any impact of M2 on these pathways (Figure 2E and 2F). It is to be noted that others have reported that M2 inhibits the ISRE pathway [53], but we believe that the discrepancy with our data is a reflection of the different cell lines used – perhaps coupled with differences in the experimental methods utilized. Our assay measures the ability of M2 to activate the described pathways in the absence of any external stimuli, while the other study showed that M2 represses ISRE activity in the presence of IFNα [53]. Since we are interested in examining the signaling mechanism(s) utilized by M2 in the absence of external stimuli, this pathway was not explored further. In T cells, several cytokine genes such as IL-2, IL-3, IL-4, TNF-α, GM-CSF, etc. are known to contain NFAT binding sites in their promoter/enhancer regions[154,183]. To determine whether M2 expression can activate a known NFAT-responsive gene, we performed a reporter assay using an IL-2 promoter driven luciferase construct in DS10 cells. As shown in Supplementary Figure 1, M2 expression upon doxycycline treatment activates the IL-2 promoter to about 14-fold over uninduced cells. This activity was inhibited upon cyclosporine A (CsA) treatment. Addition of PMA and Ionomycin served as a positive control. Consistent with this data, we have previously shown that transduction of primary murine B cells with a M2 expressing retroviral construct leads to about a 25-fold increase in IL-2 levels in culture supernatants compared to control supernatants on day 4 post-transduction [58]. This suggests that M2 expression in B cells utilizes similar signaling machinery as utilized by T cells to induce cytokine expression and a subsequent immune response.

M2 activation of the NFAT pathway is dependent on extracellular calcium flux and Src kinase activity.

CsA and FK506 are commonly used immunosuppressants that inhibit the Ca^{2+} dependent protein phosphatase calcineurin, which in turn inhibits the activation of NFAT pathway resulting in a global inhibition of T cell activation [191]. Therefore, we wanted to study whether the NFAT induction observed upon M2 expression occurred via the Ca^{2+}-calcineurin pathway as well. To this end, we performed a NFAT reporter assay in DS10 cells in the presence or absence of CsA and FK506. Doxycycline was added to cells 1 hour after nucleofection followed by addition of CsA or FK506 at 24 hours post-nucleofection. Luciferase activity was measured 48 hours post-nucleofection. To account for any toxicity resulting from the addition of the drugs, data is represented as fold over uninduced for each drug treatment. As shown in Figure 3A, both CsA and FK506 addition inhibited the activation of NFAT pathway mediated by M2, consistent with their roles in inhibition of the NFAT pathway. In contrast to NFκB activation that occurs as a result of intracellular calcium flux immediately following BCR engagement, activation of the NFAT pathway is dependent on a sustained calcium flux mediated by an influx of extracellular calcium (which occurs upon depletion of intracellular calcium stores) [70]. To examine whether M2 induction of the NFAT pathway is mediated by an intracellular or extracellular calcium flux, we performed the NFAT reporter assay in the presence of chelators of intracellular and extracellular calcium. BAPTA/AM [1,2-bis(2-aminophenoxy)ethane-*N,N,N′,N′*-tetraacetic acid tetrakis(acetoxymethyl ester)] is a membrane-permeable ester form of BAPTA that blocks an intracellular calcium flux, whereas EGTA (ethylene glycol-bis(2-aminoethylether)-*N,N,N′,N′*-tetraacetic acid) is a cell impermeable calcium chelator that inhibits an extracellular calcium flux. Addition of EGTA to culture medium abolished the activation of NFAT by M2, whereas addition of BAPTA/AM had no effect (Figure 3B). These results indicate that M2 activation of the NFAT pathway requires a sustained extracellular calcium flux, rather than a transient increase in intracellular calcium.

Based on previous studies describing the interaction of M2 with Src family kinase members and PLCγ2 [57,61], we were interested in determining whether any Src kinase family members play a role in NFAT activity mediated by M2. To this end, we performed a NFAT reporter assay in the presence of PP2, a potent and selective Src kinase family inhibitor. As a negative control, the kinase inhibitor PP3, which inhibits EGFR kinase, was used. Inhibition of Src kinase activity with PP2 abolished M2 mediated NFAT activity (Figure 3C) whereas NFAT activity induced by PMA/ionomycin was unaffected. This result suggests that interaction of M2 with a Src kinase is required for M2-mediated NFAT activation, but is not required for PMA/ionomycin mediated NFAT induction. The addition of PP3 did not affect NFAT activation mediated by M2 or PMA/ionomycin. It is to be noted that none of the drug treatments had a significant effect on the viability of the cells, as measured by trypan blue viability assay (Supplementary Figure 2D and 2E). The drug treatments also did not affect the levels of M2 expression as shown in Supplementary Figure 3A (for PP2 and PP3 treatment), 3C (for EGTA, BAPTA and FK506 treatment) and Figure 4B (for CsA treatment). Furthermore, to test the effect of inhibiting Src-kinase activity on the levels of IRF4 and IL-10, DS10 cells were treated with PP2 and PP3 in the presence or absence of doxycycline. Whole cell lysates were analyzed for IRF4 expression and the supernatants from the cells were tested for IL-10 levels by ELISA. Addition of PP2 resulted in a decrease in IRF4 expression (Supplementary Figure 3A) correlating with a decrease in IL-10 levels in culture supernatants (Supplementary Figure 3B). Taken together, these data suggest that interaction of M2 with a Src kinase is one of the initial events that drive induction of NFAT activity, IRF4 expression and IL-10 secretion. Additionally, addition of both EGTA and BAPTA caused a modest decrease in IRF4 levels (Supplementary Figure 3C, IRF4 short exposure). While it is expected for EGTA treatment to result in decreased IRF4 expression due to a defect in NFAT activation, we were surprised that BAPTA/AM addition also decreased in IRF4 expression. This is potentially due to the fact that addition of BAPTA/AM inhibits activation of the NFκB pathway, another major transcription factor controlling IRF4

expression [141,145,192]. We next assessed whether induction of M2 in the inducible cell lines leads to a change in the endogenous levels of NFAT proteins themselves. Among the different NFAT family members, NFATc1 and NFATc2 are the predominant species expressed in lymphocytes. Therefore, we measured the expression levels of both NFATc1 and NFATc2 in the DS10, DS14 and DS15 cell lines in the presence and absence of doxycycline. As a negative control, the C30p parental cell line was analyzed. We were unable to detect any NFATc2 in these lysates, possibly because this cell line does not express NFATc2 (data not shown). However, we detected low level expression of NFATc1 in the parental C30p and M2-inducible cell lines (Figure 3D, lanes 1-5). M2 expression resulted in an increase in the levels of NFATc1 (Figure 3D, lanes 6-8), indicating that in addition to activating the NFAT pathway, M2 expression also results in an increase in the levels of NFAT protein themselves, potentially driven by an increase in extracellular calcium flux.

M2 induction of IRF4 expression is partially mediated by NFAT activation.

IRF4, a critical player in plasma cell development as well as immunoglobulin class switch recombination [139,140], is strongly up-regulated upon M2 expression in the inducible cell lines (Figure 1B, middle panel). We hypothesized that M2-driven plasma cell differentiation is associated with IRF4 expression induced via the NFAT pathway. Notably, it has been demonstrated that mice deficient in Cnb1, the regulatory subunit of calcineurin phosphatase, have a defect in expression of IRF4 that is reflected by a decrease in plasma cell response to T dependent antigens [171]. To determine whether the NFAT pathway is involved in the induction of IRF4 expression by M2, we evaluated the expression of IRF4 upon treatment of M2 expressing cells with CsA. Pharmacological inhibition of the NFAT pathway with CsA in DS10 cells led to an ca. 50% decrease in the levels of IRF4 protein induced by M2 (Figure 4A, compare lanes 2 and 3). As a control, PMA/ionomycin treatment induced robust IRF4 expression in both DS10

and the parental C30p cell lines (Figure 4A, lanes 8 and 9). As a stimuli-independent positive control, we used whole cell lysates from a murine myeloma cell line P3X63Ag8 (termed P3XAg) that constitutively expresses IRF4. Consistent with this data, addition of FK506 also caused a decrease in IRF4 levels upon M2 expression (Supplementary Figure 3C, IRF4 long exposure). Duplicate immunoblots using lysates prepared at the same time and probed for M2 expression (using an antibody to the AU1 epitope tag) confirmed that expression of M2 itself was not affected upon CsA treatment (Figure 4B). In addition, since M2 induces IL-10 in DS10 cells, we analyzed the IL-10 levels in supernatants from cells used in Figure 4A. The addition of CsA to doxycycline treated DS10 cells resulted in a 9-fold reduction in IL-10 levels (Figure 4C). Together, these data suggest that M2 augments/mimics signaling from the BCR, by interacting with and signaling through Src family kinases and/or PLCγ2 to activate the NFAT pathway - leading to a strong upregulation of IRF4. While the NFAT pathway is not the only pathway required for M2-induced IRF4 expression or IL-10 levels, our data indicates that this pathway plays an important role in M2 function. Importantly, the modest induction of NFkB activity by M2 (Figure 2D) may also contribute, since expression of IRF4 has been shown to be activated by stimuli that activate the NFκB pathway [141,145,192].

Tyr^{120} and Tyr^{129} are required for M2 mediated NFAT activation and IRF4 expression.

Tyr^{120} and Tyr^{129} of M2 are differentially required for phosphorylation by Src family kinases and for forming multi-protein complexes with SH2 domain containing signaling intermediates such as PLCγ2, SHP2, etc. [57,61]. Tyr^{120} is the predominant tyrosine that is phosphorylated by Fyn, leading to a trimolecular complex between Vav1, Fyn and M2. While phosphorylation on Tyr^{129} is dispensable for this interaction, it is required for forming complexes with PLCγ2 and SHP2 [61]. In an effort to determine the roles of Tyr^{120} and Tyr^{129} (also called Y120 and Y129), we created M2 inducible cell lines as described above for wild type M2

expression, where the tyrosines 120 and 129 were mutated to phenylalanine (designated Y120F and Y129F). DS114 and DS119 are two independently derived cell lines with the mutation Y120F while DS201 and DS208 are independently derived cell lines with the mutation Y129F. These cell lines were assessed for their ability to activate the NFAT pathway using the NFAT reporter assay. As shown in Figure 5A, cell lines with either Y120F or Y129F mutations failed to activate the NFAT reporter compared to the wild type M2 expressing cell line DS10.Consistent with the hypothesis that NFAT activity is required, at least partly for IRF4 expression, we tested the ability of these cells to express IRF4 upon doxycycline induction of M2 expression. As shown in Figure 5B, none of the mutant cell lines showed an increase in IRF4 expression upon doxycycline induction (Figure 5B, middle panel). It is to be noted that none of the cell lines had a defect in expression of M2 – all expressed M2 at levels equivalent or slightly higher than the DS10 wild type M2 control cell line (Figure 5B, top panel). This suggests that the interaction of M2 with a SH2 domain containing protein(s), such as Src kinases and/or PLCγ2 and/or SHP2, plays a critical role in the initiation of signaling leading to NFAT activation and subsequent IRF4 expression.

IRF4 expression in B cells leads to IL-10 production.

IRF4 possesses a multifaceted role in T cell differentiation, particularly in T_h2, T_h17 and some aspects of T_{reg} development [149-151,154,172]. Based on this evidence in T cells, and because M2 expression leads to IRF4 as well as IL-10 expression, both of which are CsA sensitive, we wanted to investigate whether IRF4 expression leads to IL-10 production by B cells. To this end, we utilized the M2 inducible DS10 cell line transfected with either an empty vector, pMSCV-IRES-GFP (pMIG-EV), or an IRF4 expression construct, pMIG-IRF4, in the presence or absence of doxycycline. Expression of IRF4 alone resulted in significant levels of IL-10 secretion compared to supernatants from cells transfected with the empty expression vector (EV) (Figure 6A). Furthermore, M2 synergized with IRF4 to enhance the levels of IL-10 present in the

culture supernatant. To confirm our findings, as well as to eliminate the possibility that IL-10 expression observed in the DS10 cells was not due to leaky M2 expression in the absence of doxycycline, we overexpressed M2 or M2stop (negative control plasmid) with either the empty expression vector (EV) or an IRF4 expression construct in the M12 B cell line and monitored the levels of IL-10 by ELISA in the culture supernatants at 48 hours post-nucleofection (Figure 6B). Consistent with the results obtained in the DS10 inducible cell line, we observed that either M2 or IRF4 expression alone can induce IL-10, and together they synergize to increase the levels of IL-10 in the culture supernatants (Figure 6B).

In T cells it is known that IRF4 plays a role in activating IL-10 expression [172,182].Therefore, we investigated whether it holds true in B cells. To assess this, we used a previously described 1.6Kbp IL-10 promoter construct [181], IL-10pFL, as well as reporter constructs containing the 1.6Kbp promoter fragment along with upstream enhancer sequences from the IL-10 locus (termed CNS-3 and CNS-9) that have been described to be modulated by IRF4 in T cells [153,193]. First, we tested the 3 promoter constructs – full length (IL-10pFL), full length plus CNS-3 element (IL-10pCNS-3) and full length plus CNS-9 element (IL-10pCNS-9), for basal and M2-induced activity in the DS10 cells. Among the three constructs, the IL-10pCNS-9 construct exhibited the highest M2-induced activity (Supplementary Figure 4). Notably, the CNS-9 region contains three putative NFAT binding sites and two putative IRF binding sites [153]. Therefore, we used the IL-10pCNS-9 construct to further assess whether IRF4 modulates the activity of the IL-10pCNS-9 reporter construct in the DS10 cells. Expression of either M2 or IRF4 alone were able to induce activity of this promoter construct, while the combination of IRF4 and M2 further enhanced expression from this reporter (Figure 6C). However, unlike in T_h2 cells where NFATc2 synergizes with IRF4 in activating CNS-9 enhancer activity [153], co-expression of NFATc1 and IRF4 did not have an effect on IL-10 promoter activity (data not shown).

Since we have previously observed basal IL-10 levels in a variety of murine B cell lines routinely used in our lab, we were interested in determining whether there is a consistent correlation between IL-10 levels and IRF4 expression in established B cell lines. For this analysis we used A20, a mature B cell line known to secrete basal IL-10 [58], BCL-1-3B3 cell line, a leukemic cell line that can be differentiated *in vitro* to plasma cells [59], and P3X63Ag8, a mouse plasmacytoma/myeloma cell line that expresses high levels of endogenous IRF4. We harvested whole cell lysates, as well as culture supernatants, from these cells and performed ELISA for IL-10 and western blot analysis for IRF4 (Figure 6, panels D and E). As expected, the cell lines that expressed IRF4 exhibited high levels of basal IL-10 in their culture supernatants. In contrast, the M12 B cell line does not express any detectable IL-10 or IRF4 (Figure 6, panels D and E). Thus, at least in this limited survey of B cell lines, there is a consistent correlation between IRF4 expression and IL-10 levels. Based on these observations, we conclude that IRF4 can regulate the expression of IL-10 in B cells, a finding that will aid in understanding the roles of IRF4 in plasma cell development, isotype switching and cytokine regulation.

M2 induction of IL-10 in primary murine B cells involves NFAT activation.

The induction of IL-10 by M2 is most striking in primary murine B cells [58] where M2 expressing cells can induce up to 20-fold more IL-10 than control cells. Therefore, we wanted to confirm that our studies using the inducible cell line can be recapitulated in the primary murine B cells. Since nucleofection of primary murine B cells is extremely inefficient, we cannot perform a NFAT reporter assay in these cells. To get around this limitation, we sought to investigate the effect of pharmacological inhibition of the NFAT pathway in primary murine B cells that express M2 or the negative control. Primary murine B cells were isolated and stimulated overnight with LPS to induce cell proliferation, thereby making them conducive to retroviral transduction. The next day, the cells were transduced with retroviruses expressing either M2 or as a negative

control, M2stop. CsA was added to the culture media immediately after transduction and replenished again at day 3 after transduction. Surface Thy1.1 expression was monitored as a surrogate for M2 expression since the retroviral plasmid contains an IRES-Thy1.1 cassette downstream of M2. As we have previously described [58], M2 expressing cultures expanded in culture over time (Figure 7A), reaching almost 90% Thy1.1 positive by 5 days post-transduction compared to M2stop expressing cultures that remained at about 10-20% Thy1.1 positive from days 2 through 5 post-transduction. However, M2 expressing cultures that received CsA started off having similar frequencies of Thy1.1 positive cells as that of untreated cells, but had a striking defect in expansion of Thy1.1 positive population by 4 days post-transduction – ca. 84% of the cells being Thy1.1 positive in cultures that did not receive CsA compared to about 46% of cells being Thy1.1 positive in cultures that received CsA (Figure 7A, compare blue solid and dotted lines). This result indicates that the NFAT pathway is required, at least partially, for the expansion of M2 expressing cells (Figure 7A). In addition, there was a 12-fold decrease in the levels of IL-10 in culture supernatants from cells expressing M2 in the presence of CsA compared to M2 expressing cells without CsA on days 3 and 4 post-transduction (Figure 7B) and a 6-fold decrease on days 2 and 5 post-transduction. M2stop expressing cultures did not have a significant change in frequency of Thy1.1+ cells or IL-10 levels with or without CsA, although the CsA treated cultures expressed slightly lower levels of IL-10 (less than 2-fold), potentially due the requirement of NFAT pathway in LPS mediated B cell proliferation [194]. We also investigated the expression of IRF4 protein in the primary B cells expressing M2 or M2stop in the presence or absence of CsA. Consistent with our observation in the inducible cell line (Figure 4A), primary B cells that were treated with CsA had up to a two-fold decrease in IRF4 expression on days 4 and 5 post-transduction (Figure 6C).

We further examined the levels of NFAT proteins from these primary B cells that received M2 (or M2stop) expressing retroviruses in the presence or absence of CsA. As expected,

only M2 expressing cells that did not receive CsA treatment expressed NFATc1, whereas M2stop expressing cells (with or without CsA), and M2 expressing cells that received CsA did not express any detectable levels of NFATc1 (Figure 7D). This is consistent with data from Bhattacharya et al [194], where the authors show that NFATc1 is induced only upon 48hours of LPS treatment. Since we stimulate the cells with LPS only overnight (12-16 hours) before retroviral transduction, we did not observe any basal NFATc1 levels in M2stop expressing cells. Furthermore, none of the cells expressed any detectable NFATc2 – indicating that this member of the NFAT family of proteins is not expressed in splenic B cells from mice. As a positive control for these immunoblots, 293T cells overexpressing both NFATc1 and NFATc2 were used (Figure 7D, lane 10). This data unequivocally shows that M2 expression alone can directly up-regulate NFAT expression in primary murine B cells, implicating a direct role for NFAT in M2-mediated functions.

M2 expression in primary B cells leads to changes in surface phenotype that closely mirror that of an activated, pre-plasma memory B cell phenotype ($CD19^{+}$, $B220^{low}$, $CD138^{low}$, $sIgD^{-}$) [58]. Therefore, we analyzed whether CsA treatment had any effect on M2-mediated differentiation of B cells. Predictably, addition of CsA perturbed the differentiation of M2 expressing cells into a pre-plasma cell type. As shown in Figure 7E, M2 expressing cultures that received CsA were similar to M2stop expressing cells with respect to their expression of activation markers and plasma cell differentiation markers. Namely, $MHC\text{-}IA^{b}$ downregulation and upregulation of CD25 were inhibited by CsA addition (compare black vs blue histograms in Figure 7E). B220 levels in M2 expressing cells that received CsA were similar to that of M2stop expressing cells, whereas M2 expressing cells without any CsA had strikingly down-regulated B220 levels. As noted in our previous work [58], CD138 levels were only modestly up-regulated, indicating that the cells have not fully differentiated into a plasma cell phenotype. However, M2 expressing cells without CsA addition were trending towards up-regulating CD138 expression

compared to M2 expressing cells that received CsA or M2stop expressing cells (with and without CsA) (Figure 7E). In contrast, sIgD and CD23 expression were strongly affected by addition of CsA to both the M2 and M2stop expressing cultures. M2 expressing cells that did not receive CsA treatment had completely down-regulated both sIgD and CD23, whereas CsA addition resulted in a considerable number of cells that still expressed sIgD and CD23 (compare black open histograms vs blue open histograms). While M2stop cultures were already severely affected in their ability to down-regulate both sIgD and CD23, CsA addition further affected this phenotype (compare grey shaded histograms vs red open histograms). This is partly due to the fact that LPS drives B cells to a plasmablast phenotype and addition of CsA in these cultures affects LPS driven B cell activation and differentiation as well. Consistent with our report, in humans, CD23 levels are down-regulated in plasma cells in an IRF4 dependent fashion [145,195]. Taken together, these data convincingly support a model where M2 activates the NFAT pathway to increase NFATc1 levels leading to increased expression of IRF4, resulting in differentiation of M2 expressing cells into a pre-plasmablast phenotype accompanied by a significant increase in IL-10 secretion.

IRF4 plays a critical role in both the establishment of MHV68 latency and virus reactivation

To gain an understanding of the role of IRF4 in MHV68 infection within the context of the infected host, we utilized IRF4 conditional knockout mice ($IRF4^{fl/fl}$ mice) in which exons 1 and 2 of the IRF4 locus are flanked by loxP sites [29]. Expression of Cre-recombinase in these mice results in the deletion of sequences flanking the loxP sites, thereby leading to deletion of IRF4 specifically in Cre-recombinase expressing cells. We have previously developed and characterized a recombinant MHV68 virus that expresses a Cre-recombinase cassette in a neutral locus of the MHV68 genome, between ORF27 and ORF29b [166]. Infection of C57BL/6 mice with this virus behaves similarly to infection with MHV68-WT virus with respect to acute

replication and establishment of latency [166]. In order to study the role of IRF4 in MHV68 infected cells, we infected IRF4$^{fl/fl}$ mice intranasally with 1000 PFU of either MHV68-Cre or MHV68-WT (wild type) virus. On day 16 post-infection, splenocytes were analyzed for establishment of latency and reactivation from latency by limiting dilution PCR and limiting dilution ex-vivo reactivation analyses respectively. As shown in Figure 8A, deletion of IRF4 in MHV68-Cre infected cells leads to a 60-fold decrease in establishment of latency in the spleen (1 in 4710 splenocytes contain latent viral genomes) compared to infection with a MHV68-WT virus (1 in 77 splenocytes harbor latent genomes), indicating a critical role for IRF4 for establishment of MHV68 latency in the spleen. Consistent with this observation, *Ochiai et al* [144] have demonstrated that mice with conditional deletion of IRF4 in CD19 expressing B cells, fail to develop germinal centers. Furthermore, they showed that this defect was intrinsic to IRF4-/- B cells by performing mixed bone marrow chimera studies with IRF4+/+ and IRF4-/- progenitors. Thus, they concluded that IRF4 plays a vital and essential role in germinal center formation and differentiation. Therefore, it is not surprising that deletion of IRF4 in MHV68 infected cells leads to a latency defect since germinal center B cells are the major latency reservoir for MHV68 infected cells. Strikingly, the efficiency of virus reactivation from latency was severely compromised in mice infected with MHV68-Cre virus (1 in 526,017 splenocytes capable of reactivating virus) compared to mice infected with MHV68-WT virus (1 in 3540 splenocytes capable of reactivating virus) (Figure 8B). This 150-fold reduction in viral reactivation capacity in cells infected with the MHV68-Cre virus is reminiscent of a defect in reactivation that we consistently observe in mice infected with the M2 null virus [21,162]. Thus in the absence of IRF4 from infected cells, the kinetics of viral latency and reactivation resemble that of a M2 null virus, persuasively arguing for a critical role for IRF4 in M2 mediated functions *in vivo* as well.

We have previously shown that in C57BL6/J mice infected with a M2 null virus there is a significant decrease in the percentage of infected cells exhibiting a plasma cell phenotype ($B220^{low}CD138^{hi}$) [60]. To extend our observation that M2 induces IRF4 expression, which is required for plasma cell differentiation, we have taken advantage of the development of a recombinant MHV68 that allows tracking of infected cells *in vivo*. This approach utilizes a transgenic MHV68 virus that expresses an eYFP-H2B fusion protein (MHV68-H2bYFP) [180]. Using the λRed mediated galK recombineering [167,179], we generated a new M2 null virus on the MHV68-H2bYFP backbone (M2stop.HY). As a control, we also created a genetically repaired marker rescue virus (M2MR.HY). We have extensively characterized the M2MR.HY and M2stop.HY viruses and have confirmed that they behave like the M2WT-MHV68 and M2stop-MHV68 viruses, respectively (data not shown) [21,58,60]. To address whether there is a defect in IRF4 expression *in vivo* in MHV68 infected B cells in the absence of M2 expression, we infected C57BL6/J mice with 1000PFU of either M2stop.HY or M2MR.HY viruses. On day 14 post-infection, splenocytes were harvested and analyzed for IRF4 levels by intracellular staining coupled with flow cytometry. As a control for YFP expression, we used WT-MHV68 (without an eYFP-H2b expression cassette) virus infected splenocytes. We also used WT-MHV68 infected cells to stain with an isotype control for IRF4 intracellular staining. We analyzed splenocytes from individual mice infected with either the M2stop.HY or M2MR.HY viruses for expression of IRF4 in infected cells (live cells/YFP+/IRF4+). Notably, M2stop.HY infected animals have a significant defect in the frequency of infected cells that express IRF4 compared to M2MR.HY infected animals; only ca. 8% of YFP+ cells in M2stop.HY infected animals express IRF4 compared to ca. 28% in M2MR.HY infected animals (Figure 9). Consistent with our previous finding that M2stop infected mice have a defect in virus infection in plasma cells, we now show that this defect is likely due to a significant defect in the frequency of virus infected B cells expressing IRF4.

DISCUSSION

Plasma cell differentiation-driven virus reactivation is a common theme in gammaherpesviruses biology [60,156,159,160]. In contrast to MHV68 where we have previously shown that the viral M2 antigen can promote plasma cell differentiation [60], for both EBV and KSHV there is no information regarding how plasma cell differentiation of latently infected B cells is regulated. Although there are no obvious homologs of the MHV68 M2 gene in the human gammaherpesviruses, it seems reasonable to speculate that EBV and KSHV encode viral gene products that are capable of promoting plasma differentiation – ensuring that virus reactivation occurs at both the appropriate time and anatomical site(s) (e.g., mucosal surfaces). Here, we describe the signaling pathway that ensues upon expression of M2. Expression of M2 in primary murine B cells results in secretion of IL-10, a cytokine associated with plasma cell differentiation in humans [176] and in mice [127]. We therefore hypothesized that identifying the mechanism underlying M2-driven IL-10 production will provide clues about pathways required for plasma cell differentiation driven virus reactivation. As a first step, we created an inducible cell line expressing M2 in a tightly regulated temporal manner. As described in (Figure 1C), this cell line makes IL-10 only when M2 expression is induced by doxycycline treatment, thereby providing us a means to study M2 mediated IL-10 production in a systematic fashion.

M2 activates the NFAT pathway (Figure 2, panels A & C), but does not appear to activate the NFκB, AP-1 or the ISRE pathways (Figure 2D-2F). The NFAT pathway, along with NFκB pathway, represents one of the primary pathways utilized by lymphocytes to transduce several signals required for proliferation, survival, maintenance and differentiation. Although it is surprising that M2 did not significantly activate the NFκB pathway (Figure 2D), this is potentially due to the fact that this cell line has high basal NFkB activity - likely necessary for survival and growth of this cell line. Notably, we have carried out a time-course analysis following induction

of M2 expression to confirm that the absence of NFkB activation is not a time-sensitive phenotype (data not shown). The inability of M2 to activate the AP-1 and ISRE pathways (Figure 2, panels E & F) suggests that M2 does not induce a generalized signaling cascade as in the case of BCR activation, but rather selectively activates the NFAT pathway to facilitate its signals.

M2 contains two tyrosines, Tyr^{120} and Tyr^{129} that are differentially required for the formation of a trimolecular complex consisting of Vav, Fyn and M2 [57]. It also contains nine PxxP motifs, some of which are capable of binding SH3 containing proteins [61,162], and shown to be important *in vivo.* Interestingly, a mutant virus with both Tyr^{120} and Tyr^{129} mutated to phenylalanine has a defect in reactivation from latency, fitting our hypothesis that the interaction of the tyrosines with Src family kinases is crucial for the signals driven by M2. Consistently, M2 inducible cell lines with mutations of either tyrosine 120 or 129 to phenylalanine fail to activate the NFAT pathway and fail to up-regulate IRF4 expression (Figure 5). Therefore, M2 seems to function predominantly as a scaffolding protein that forms multiprotein complexes mimicking or perpetuating signals from the BCR. Consistent with this hypothesis, published studies suggest that M2 forms a microsignalosome complex similar to that observed upon BCR crosslinking [61].

Interestingly, recent studies have shown mice lacking Stromal Interaction Molecules 1 and 2 (STIM1 and STIM2 - the ER Ca^{2+} sensor required for sensing depletion of ER Ca^{2+} stores) are defective in BCR induced SOC (Store Operated Calcium) influx, proliferation and NFAT activation. Also, these mice have a striking defect in IL-10 production, indicating that extracellular calcium flux mediated IL-10 production requires NFAT activity [71]. Their finding is the first report linking B cell derived IL-10 to NFAT activation, although they characterized these IL-10 producing B cells as B_{regs} – a subset of B cells that play an important role in controlling autoimmune responses. While, several other reports have identified a regulatory role

for B cell derived IL-10 in mice [122-125,127,128,196], we have not characterized whether M2 expressing B cells are phenotypically similar to B_{reg} cells described in these studies and whether these cells possess any regulatory capacity, namely limiting autoimmunity, implicated in these studies.

This study is the first description of a specific role for IRF4 in B cell derived IL-10. *Maseda et al* [127] have shown using IL-10 reporter mice that B_{reg} cells that transcribe IL-10 have increased transcripts of the plasma cell associated factors Blimp-1 and IRF4. However, there was no evidence suggesting that IRF4 was responsible for driving the B_{reg} cells to transcribe IL-10. Here, we show that IRF4 expression is sufficient to induce IL-10 in culture supernatants of DS10 and M12 cell lines, which do not normally express IRF4 or IL-10 (Figure 6, panels A & B). Concomitant with this finding, IRF4 activates an IL-10 promoter construct containing an enhancer element (Figure 6C). Strikingly, M2 synergizes with IRF4 to activate the promoter, as well as, IL-10 secretion (Figure 6A-C). Interestingly, since IRF4 by itself is a weak DNA binding protein, IRF4 synergizes with NFAT family members in activating the promoters of IL-4 and IL-10 in T cells [153,154]. Therefore, we expected IRF4 to synergize with NFAT family members to activate the IL-10 promoter in B cells, but failed to observe any such synergy with NFATc1 (data not shown). Nevertheless, since M2 synergizes with IRF4 to activate the IL-10 promoter and because M2 expression results in an increase in NFATc1 levels (Figure 3D), it is likely that the synergy with M2 is indeed mediated by NFATc1. While it is formally possible that M2 could possess a transcription factor-like function, it seems unlikely since there is no evidence so far suggesting a direct role for M2 in transcriptional regulation. Supporting this idea is the fact that M2 does not localize to the nucleus in B cells [54], although it does so in other cell types.

IRF4 is a lymphocyte-specific member of the interferon regulatory factor (IRF) family of proteins, well known for its role in plasma cell development and isotype switching in B cells, as

well as transcriptional regulation of B cell molecules, namely Igκ light chain enhancer, CD23,CD20 and MHC-I (reviewed in [148] and [147]). IRF4 is also involved in the regulation of several T-cell derived cytokines, especially those involved in T_h2 development and in T_h17 differentiation [150,151,173,175]. Along with Blimp-1, it is required for the differentiation and effector function of T_{reg} cells, displaying a multifactorial role in T cell differentiation and regulation [59,141,150,152,172,175]. Moreover, the role of IRF4 in development of T_h2 lineage is in part due to its role in regulation of the IL-10 promoter and IL-4 promoter [153,154,172,174]. Therefore, while IRF4 is extensively studied in T cell lineage commitment owing to its ability to regulate transcription of several cytokines, our report is the first characterization of IRF4 in modulation of B cell specific cytokines. This opens the possibility to explore whether B cell derived cytokines utilize similar mechanisms of regulation as observed in T cells.

Since LPS treatment drives plasmablast differentiation by up-regulating IRF4, Blimp-1, XBP-1, CD138 (syndecan-1) and immunoglobulin secretion, it is difficult to completely abolish IRF4 levels in our experiments using retrovirally transduced primary B cells [e.g., analyses of M2 expression in the presence or absence of CsA (Figure 7E)]. Retroviral transduction requires cell division and hence we transiently expose primary murine B cells to LPS overnight, prior to transduction with the MSCV vectors encoding M2 or M2stop. Therefore, CsA treatment potentially only reduces the levels of IRF4 that is newly synthesized following M2 expression versus that made in response to LPS stimulation. Consistently, this is reflected in IL-10 levels - in cultures that express M2 in the presence of CsA, the IL-10 levels are not decreased to basal levels as seen with M2stop expressing cultures (with or without CsA) (compare light blue bars to red bars in Figure 7B), indicating that a significant portion of IL-10 being made on days 4 and 5 post-transduction is heavily dependent on sufficient IRF4 expression by these cells. In this aspect, the data with M2 inducible B cell lines is robust since CsA is added at the time of addition of doxycycline and hence any IRF4 that is made is potentially through a NFAT-independent

pathway (Figure 4A) (likely via the NFκB pathway). Of note, the LMP1 oncogene of EBV induces IRF4 expression in human B cells and is required for the proliferation of these cells [197]. While the authors did not look at IL-10 levels, several independent reports describe the association of LMP1 expression with increased IL-10 levels [78,198-200]. Together, these data indicate that LMP1, somewhat similarly to M2, can induce IRF4 as well as IL-10.

Of particular interest is the *in vivo* data obtained using $IRF4^{fl/fl}$mice (Figure 8). Since the system we utilized knocks out IRF4 only in infected cells, it is to be noted that IRF4 expression is intact in other cells that are uninfected which may be sufficient to elicit a modest germinal center response. However, this defect in latency does not explain the striking defect observed in reactivation from latency upon infection with a MHV68-Cre virus, thereby attributing a specific reactivation defect in addition to the latency defect. This piece of data further tightly links plasma cell differentiation to reactivation as observed with the M2 null virus [60]. Based on observations from *Ochiai et al* [144], it would be interesting to study the course of virus infection in mice with IRF4 deleted in B cells specifically by crossing the $IRF4^{fl/fl}$ with CD19-Cre mice which express the Cre-recombinase from the CD19 promoter, thereby eliminating IRF4 specifically in B cells. Since these mice have a defect in germinal center response, we would speculate that infection of these mice with MHV68 will cause a significant defect in establishment of latency, as well as reactivation from latency.

Interestingly, the NFAT pathway has been implicated, both directly and indirectly, in EBV and KSHV infection. Indeed, induction of a calcium flux by PMA and ionomycin is a standard treatment for initiation of the viral lytic cycle. In addition, induction of the lytic cycle of EBV by surface immunoglobulin crosslinking can be blocked by CsA and FK506 [201], which acts to inhibit Ca^{2+} dependent transcription of the lytic switch gene BZLF-1 (Zta). This CsA sensitivity was mediated by calcineurin and NFATc2 in synergy with TPA and/or the EBV

induced $Ca^{2+/}$calmodulin dependent kinase type IV/Gr [202]. In KSHV, ionomycin is a known inducer of Rta (the conserved immediate-early gene sufficient to drive reactivation) – it has been published that in the PEL cell line, BCBL-1, and DMVEC (immortalized human dermal microvascular endothelial cells) calcium mobilization can reactivate latent KSHV [203]. Furthermore, KSHV encodes K1, an oncogenic protein capable of transforming rodent fibroblasts, that contains a variant ITAM motif at its C-terminal cytoplasmic tail that can initiate calcium flux in B cells and subsequent increase in cellular tyrosine phosphorylation leading to activation of NFAT and AP-1 [83-85,165]. Additionally, NFAT and AP-1 activation was associated with an increase in production of IL-10 and monocyte-derived cytokine (MDC) in BJAB cells [85]. However, unlike M2, K1 overexpression is insufficient to drive KSHV reactivation from PEL cells [204]. Taken together, despite discernible homology to any known cellular or viral protein, MHV68 M2 shares functional similarities with signaling molecules encoded by EBV and KSHV.

In conclusion, we propose a model in which interaction of M2 with Vav, Src and/or PLCγ2 initiates a cascade of events that result in activation of the NFAT pathway. This in turn leads to increased levels of IRF4 protein, which activates IL-10 promoter elements resulting in increased IL-10 expression (Figure 10). Notably, M2 induction of IRF4 expression likely involves the activation of another pathway(s) in addition to the NFAT pathway, since CsA treatment does not completely block M2 induction of IRF4 expression (Figure 4A and 7C) or IL-10 production (Figure 4C and 7B). Of specific interest is the role of NFAT and IRF4 in gammaherpesvirus biology. Since immunocompromised patients receiving CsA and FK506 are at high risk for lymphoproliferative disorders associated with EBV and KSHV, further insights into these pathways may eventually aid in the development of novel strategies for better controlling virus reactivation and expansion of latently infected cells in such settings.

FIGURES

Figure 1

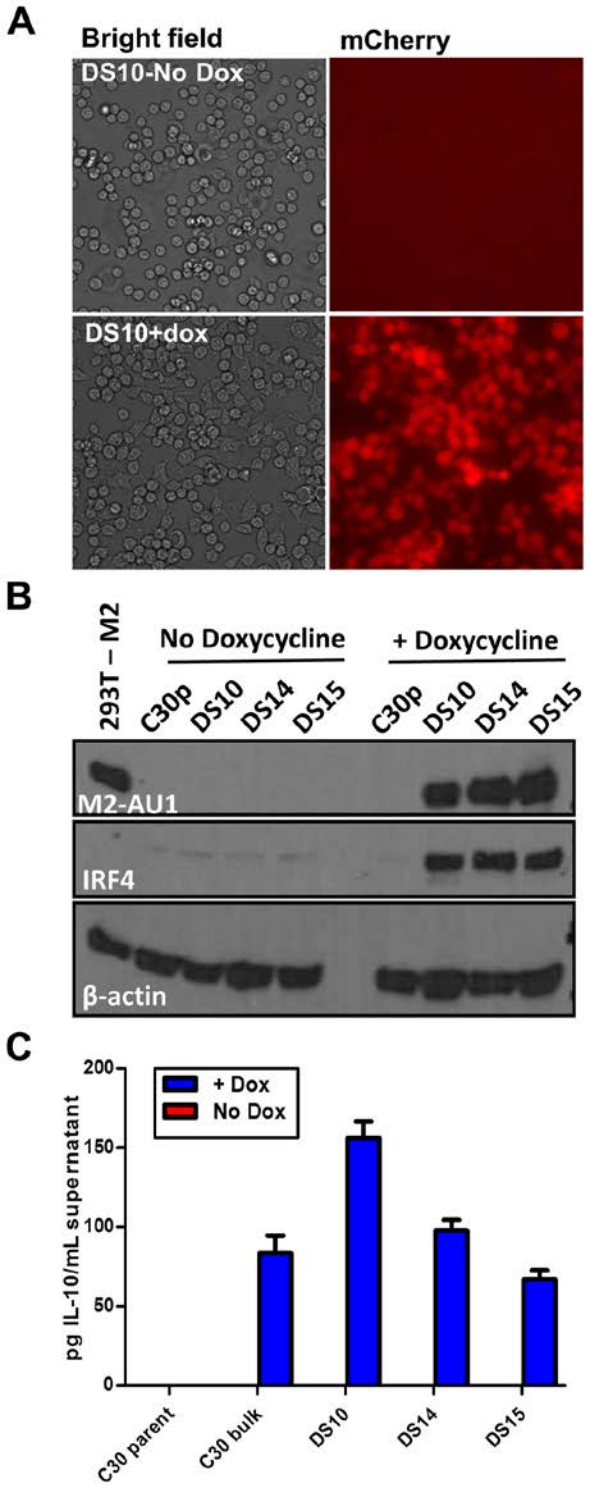

Figure 2

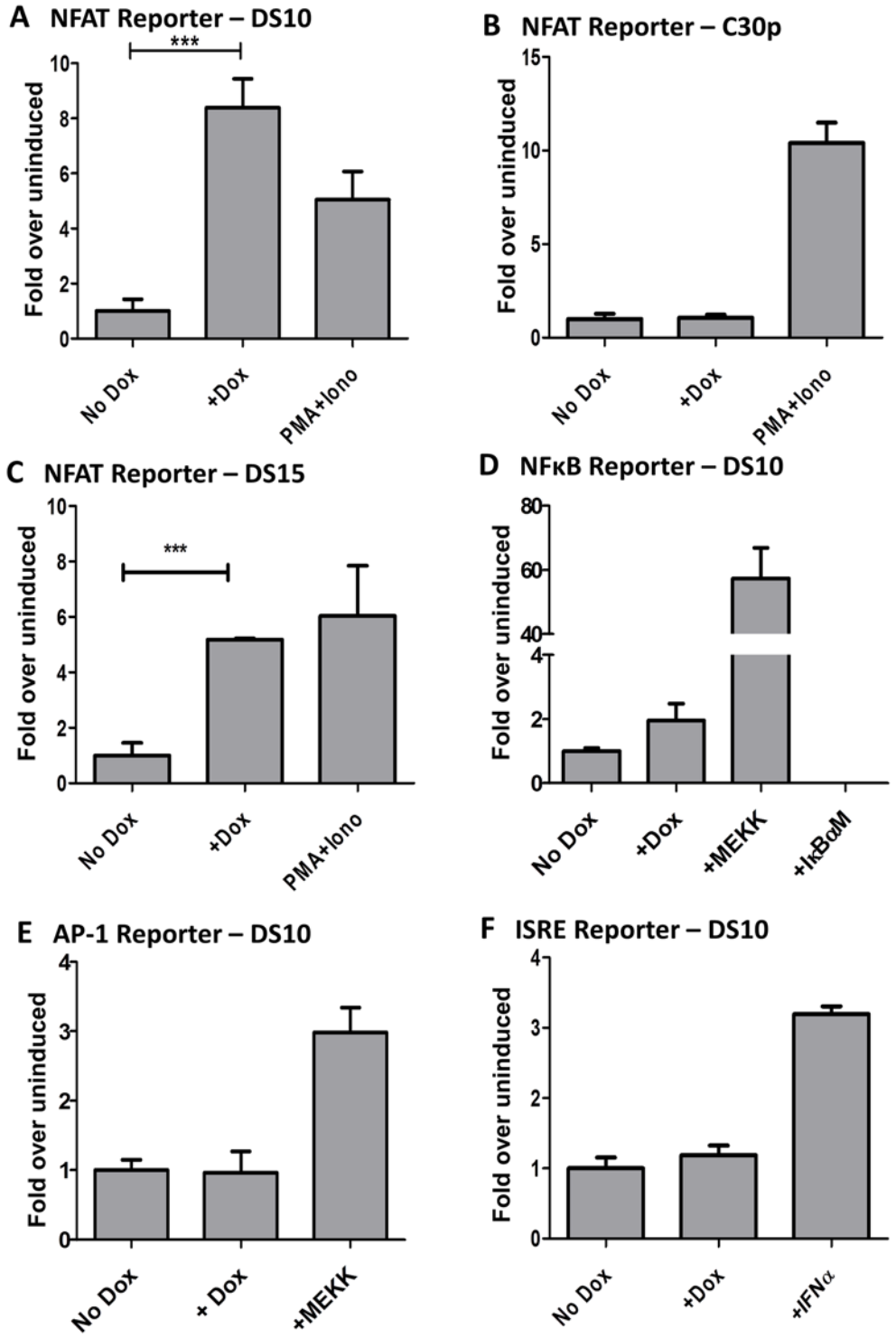
A NFAT Reporter – DS10
***
Fold over uninduced
No Dox
+Dox
PMA+Iono
B NFAT Reporter – C30p
Fold over uninduced
No Dox
+Dox
PMA+Iono
C NFAT Reporter – DS15
***
Fold over uninduced
No Dox
+Dox
PMA+Iono
D NFκB Reporter – DS10
Fold over uninduced
No Dox
+Dox
+MEKK
+IκBαM
E AP-1 Reporter – DS10
Fold over uninduced
No Dox
+ Dox
+MEKK
F ISRE Reporter – DS10
Fold over uninduced
No Dox
+Dox
+IFNα

Figure 3

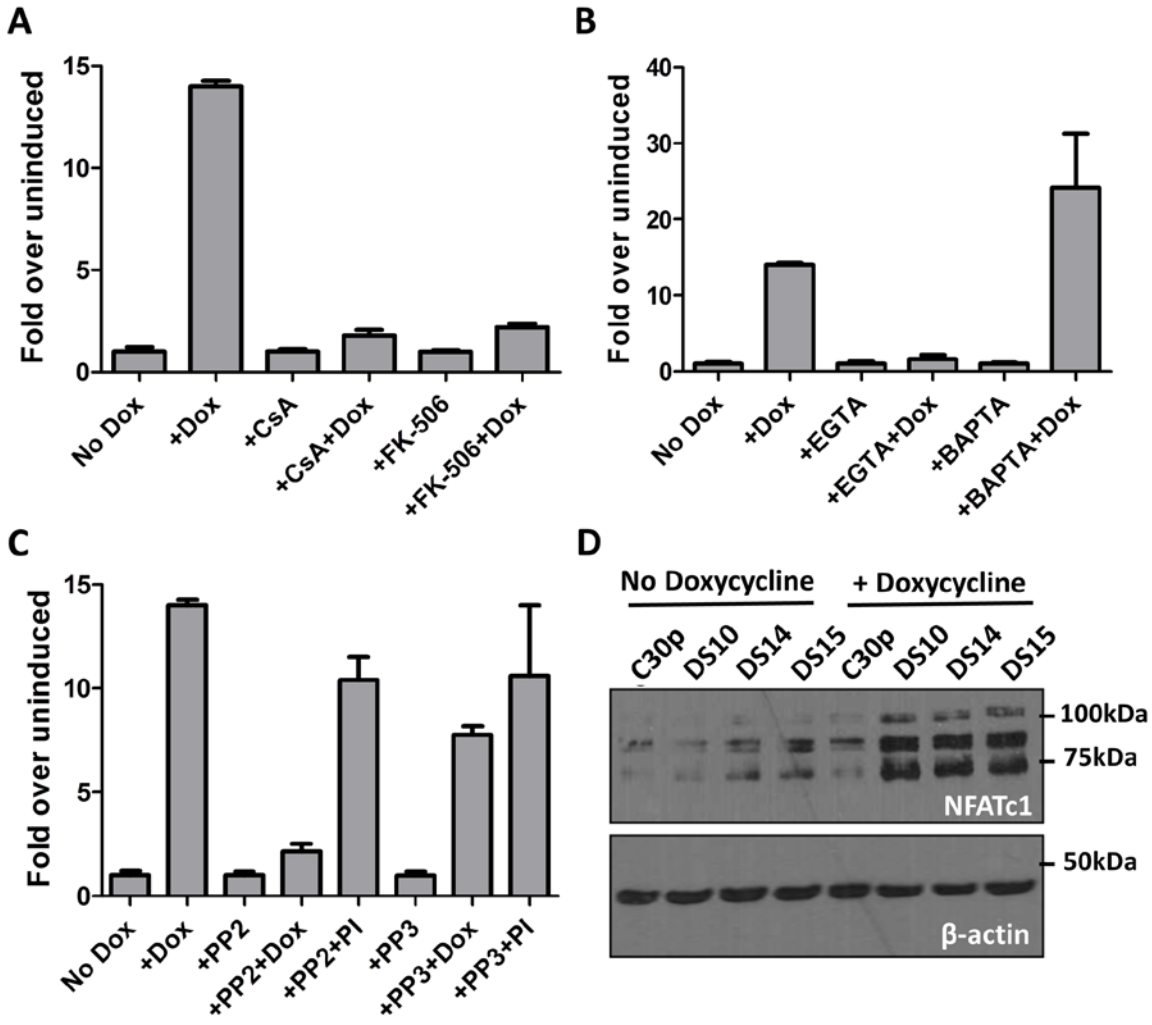
A
Fold over uninduced
15
10
5
0
No Dox
+Dox
+CsA
+CsA+Dox
+FK-506
+FK-506+Dox
B
Fold over uninduced
40
30
20
10
0
No Dox
+Dox
+EGTA
+EGTA+Dox
+BAPTA
+BAPTA+Dox
C
Fold over uninduced
15
10
5
0
No Dox
+Dox
+PP2
+PP2+Dox
+PP2+PI
+PP3
+PP3+Dox
+PP3+PI
D
No Doxycycline
+ Doxycycline
C30p
DS10
DS14
DS15
C30p
DS10
DS14
DS15
100kDa
75kDa
NFATc1
50kDa
β-actin

Figure 4

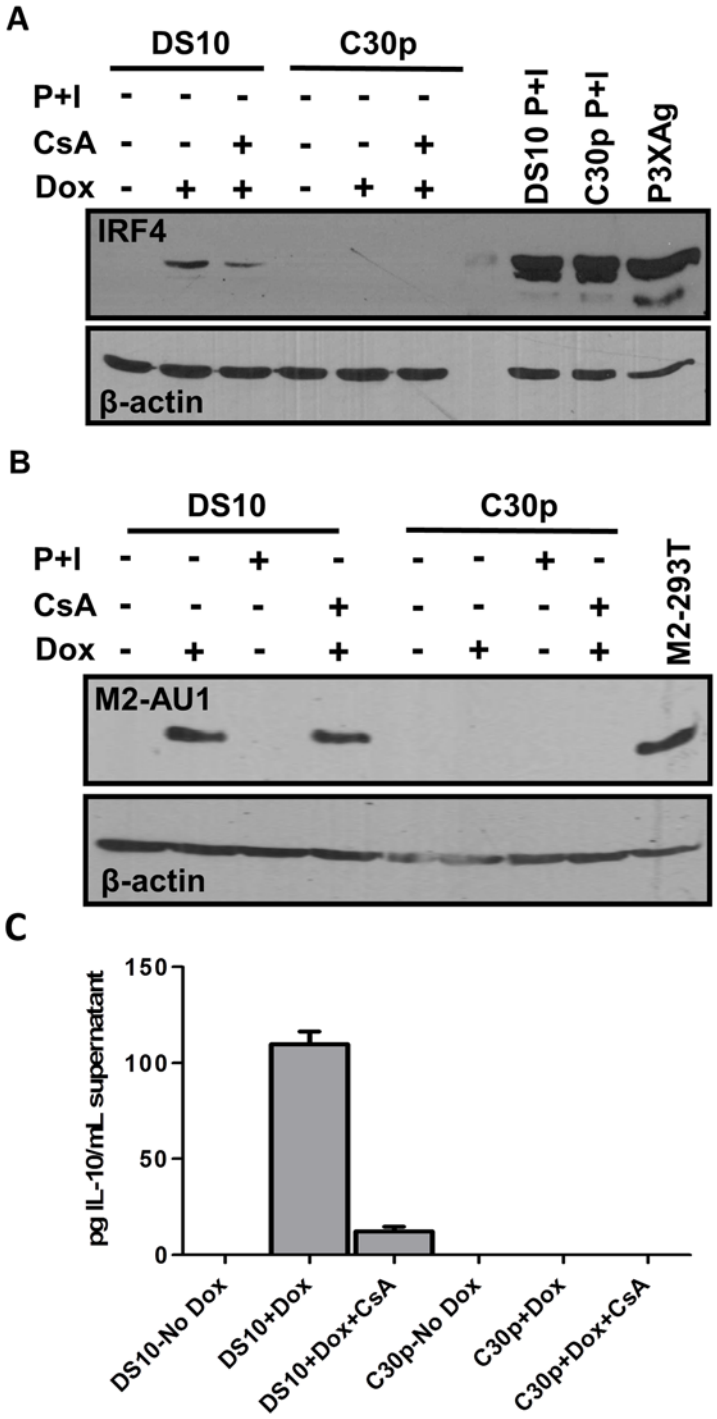
A
DS10
C30p
P+I - - - - - -
CsA - - + - - +
Dox - + + - + +
DS10 P+I
C30p P+I
P3XAg
IRF4
β-actin
B
DS10
C30p
P+I - - + - - - + -
CsA - - - + - - - +
Dox - + - + - + - +
M2-293T
M2-AU1
β-actin
C
pg IL-10/mL supernatant
150
100
50
0
DS10-No Dox
DS10+Dox
DS10+Dox+CsA
C30p-No Dox
C30p+Dox
C30p+Dox+CsA

Figure 5

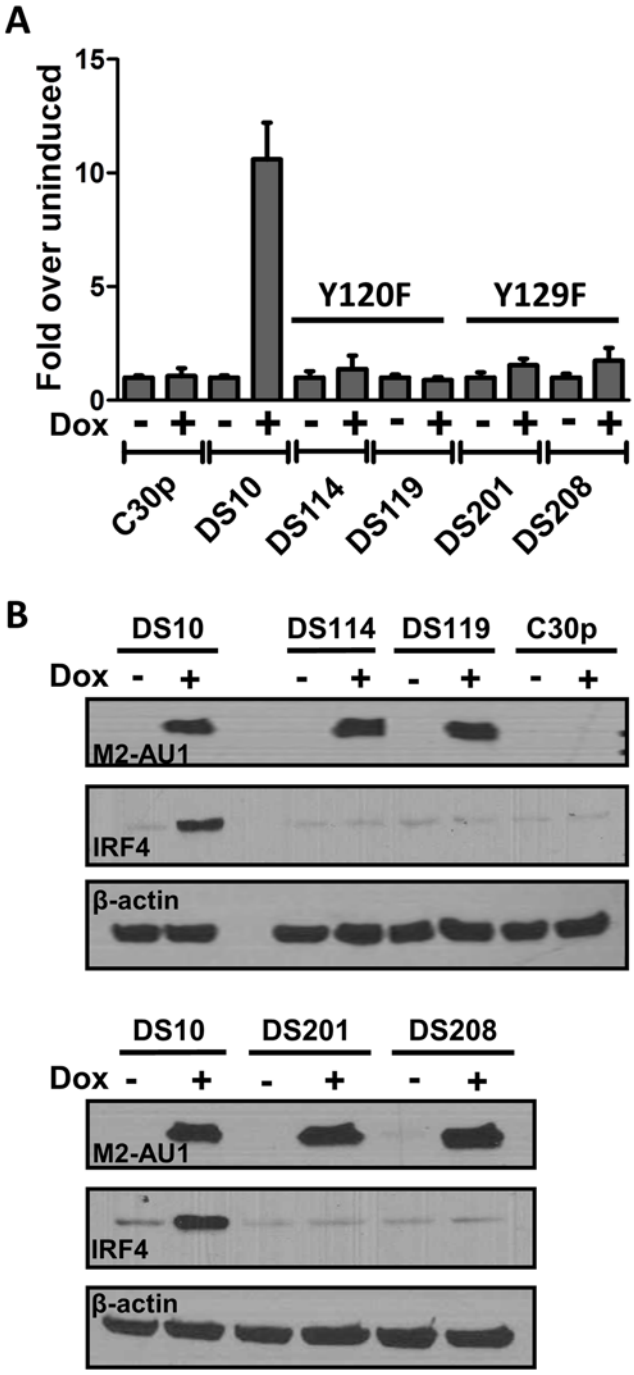
A
Fold over uninduced
15
10
5
0
Y120F
Y129F
Dox - + - + - + - + - + - +
C30p
DS10
DS114
DS119
DS201
DS208
B
DS10
DS114
DS119
C30p
Dox - + - + - + - +
M2-AU1
IRF4
β-actin
DS10
DS201
DS208
Dox - + - + - +
M2-AU1
IRF4
β-actin

Figure 6

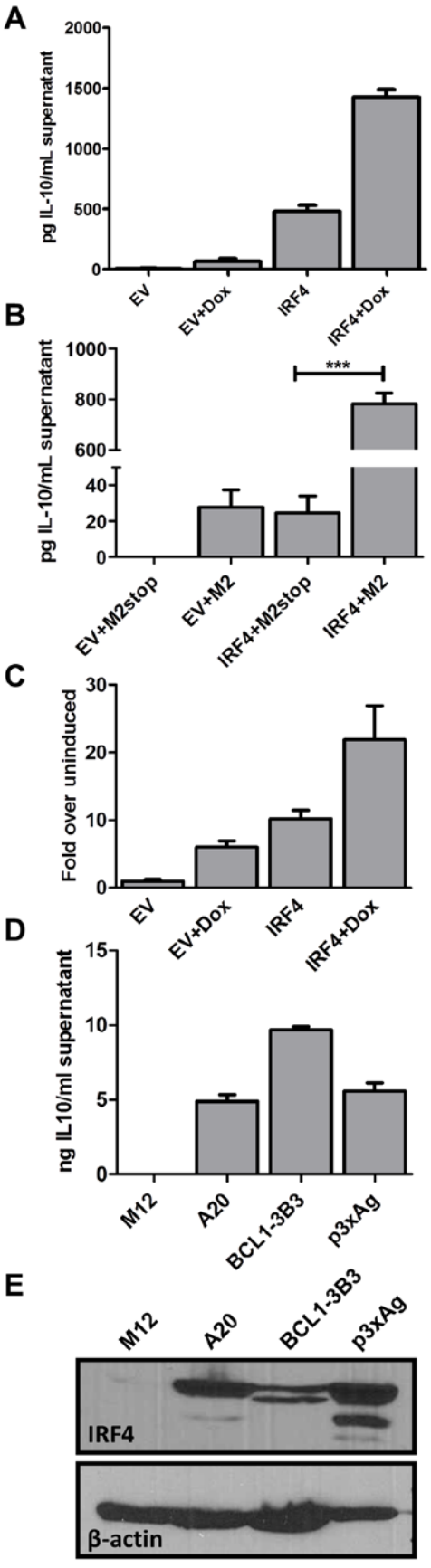
A
pg IL-10/mL supernatant
2000
1500
1000
500
0
EV
EV+Dox
IRF4
IRF4+Dox
B
pg IL-10/mL supernatant
1000
800
600
40
20
0
***
EV+M2stop
EV+M2
IRF4+M2stop
IRF4+M2
C
Fold over uninduced
30
20
10
0
EV
EV+Dox
IRF4
IRF4+Dox
D
ng IL10/ml supernatant
15
10
5
0
M12
A20
BCL1-3B3
p3xAg
E
M12
A20
BCL1-3B3
p3xAg
IRF4
β-actin

Figure 7

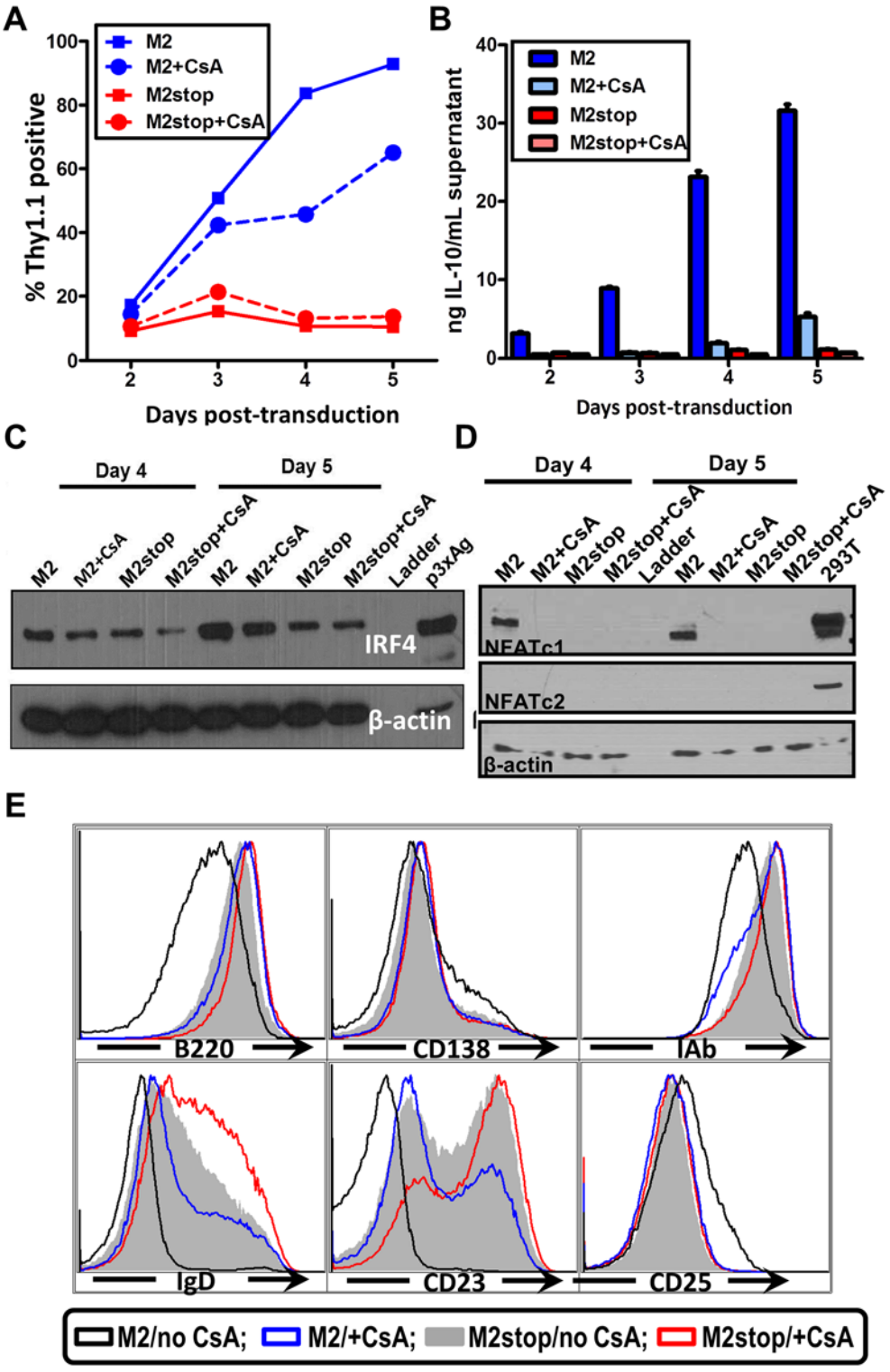
A
% Thy1.1 positive
M2
M2+CsA
M2stop
M2stop+CsA
Days post-transduction
B
ng IL-10/mL supernatant
M2
M2+CsA
M2stop
M2stop+CsA
Days post-transduction
C
Day 4
Day 5
M2
M2+CsA
M2stop
M2stop+CsA
Ladder
p3xAg
IRF4
β-actin
D
Day 4
Day 5
M2
M2+CsA
M2stop
M2stop+CsA
Ladder
293T
NFATc1
NFATc2
β-actin
E
B220
CD138
IAb
IgD
CD23
CD25
M2/no CsA; M2/+CsA; M2stop/no CsA; M2stop/+CsA

Figure 8

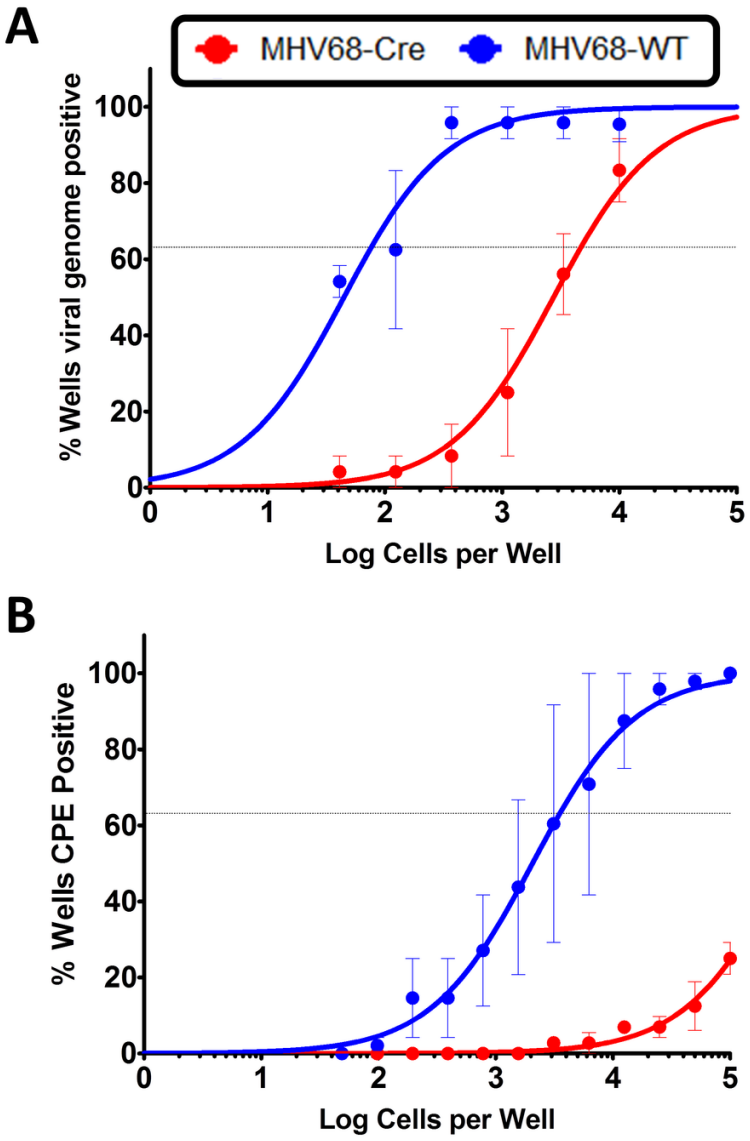
A
MHV68-Cre
MHV68-WT
% Wells viral genome positive
100
80
60
40
20
0
0
1
2
3
4
5
Log Cells per Well
B
% Wells CPE Positive
100
80
60
40
20
0
0
1
2
3
4
5
Log Cells per Well

Figure 9

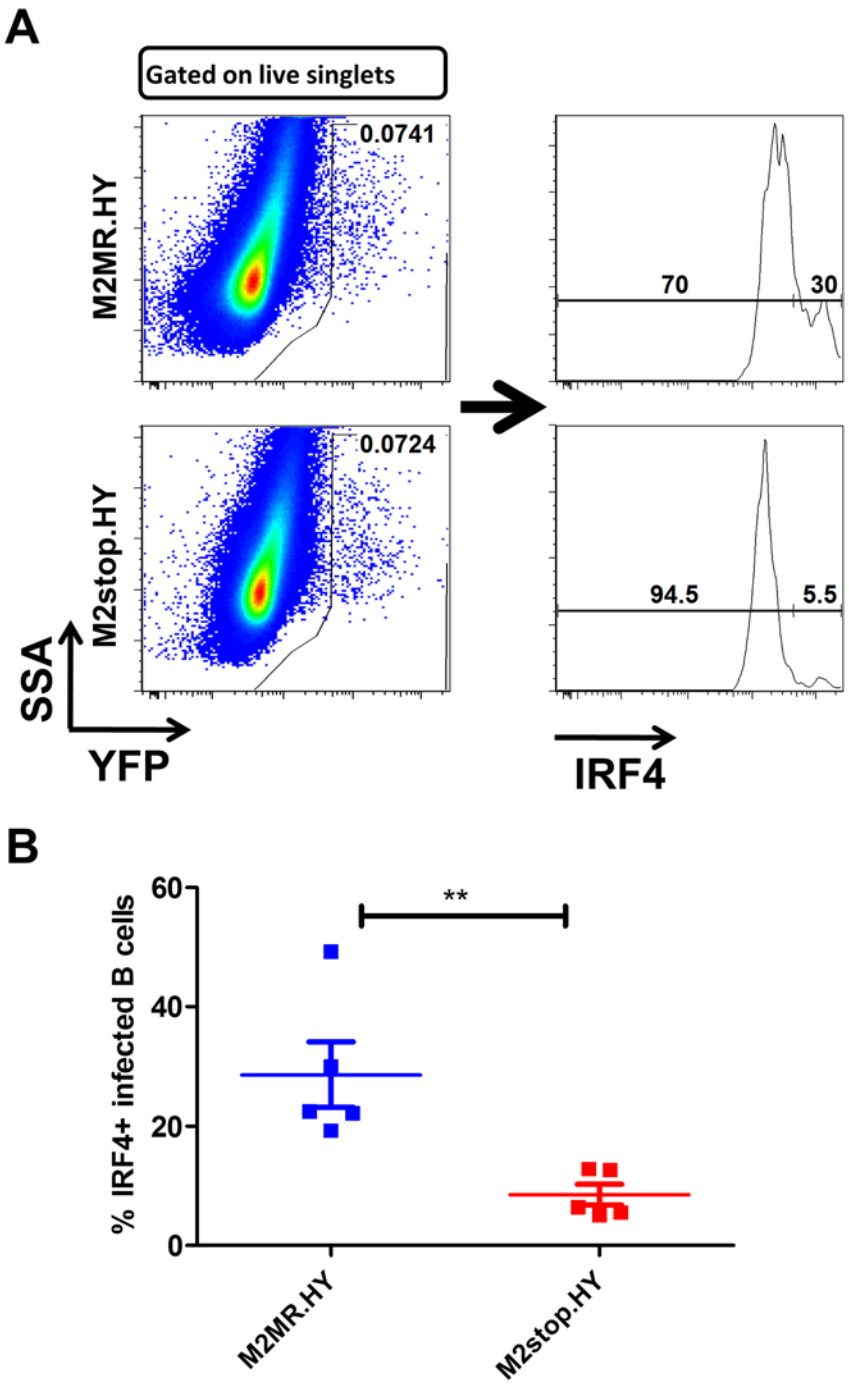
A
Gated on live singlets
M2MR.HY
0.0741
70
30
M2stop.HY
0.0724
94.5
5.5
SSA
YFP
IRF4
B
% IRF4+ infected B cells
60
40
20
0
**
M2MR.HY
M2stop.HY

Figure 10

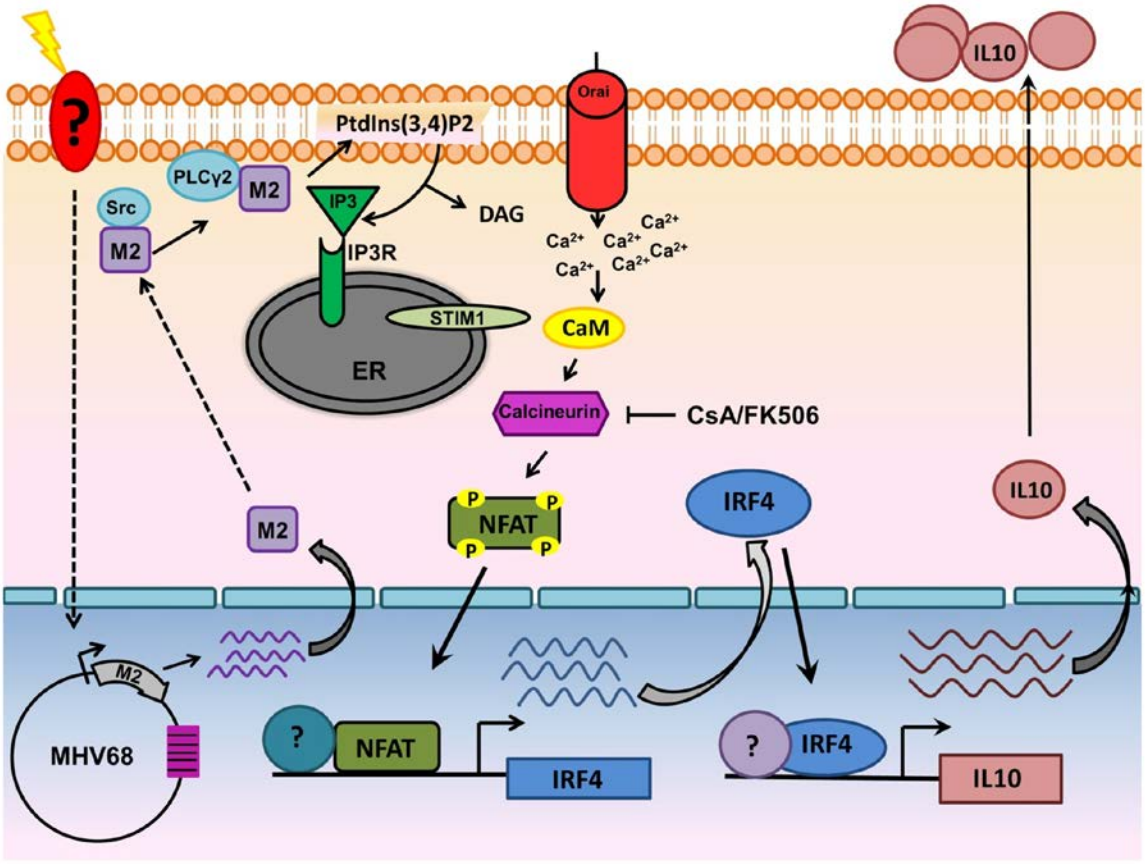
IL10
Orai
?
PtdIns(3,4)P2
PLCγ2
M2
IP3
DAG
Src
M2
IP3R
Ca2+
Ca2+
Ca2+
Ca2+
Ca2+
Ca2+
STIM1
CaM
ER
Calcineurin
CsA/FK506
IL10
M2
NFAT
IRF4
M2
MHV68
?
NFAT
IRF4
?
IRF4
IL10

Supplementary Figure 1

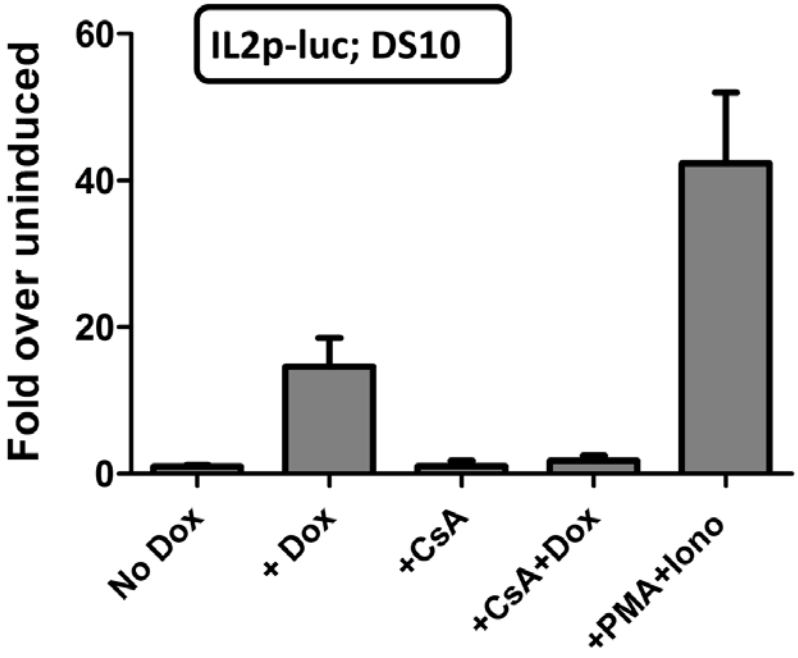

Supplementary Figure 2

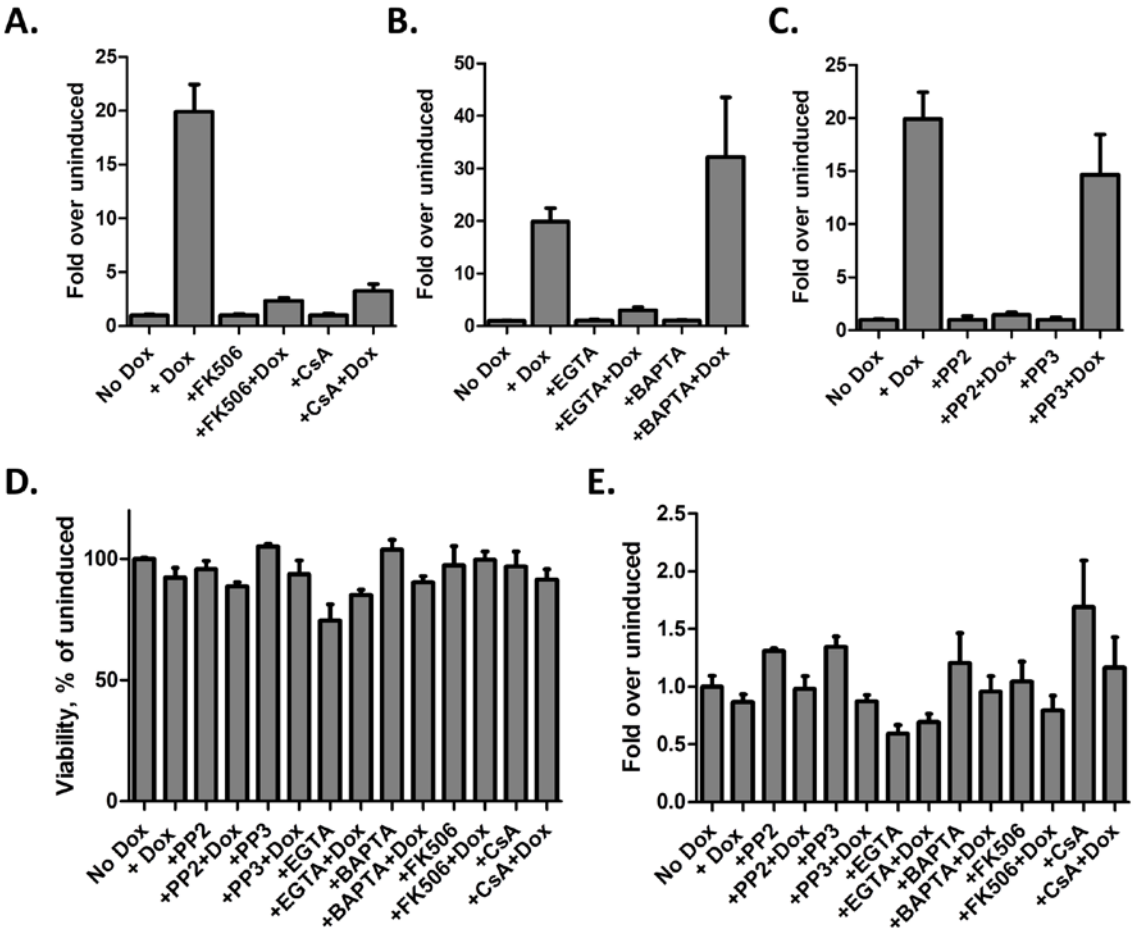

Supplementary Figure 3

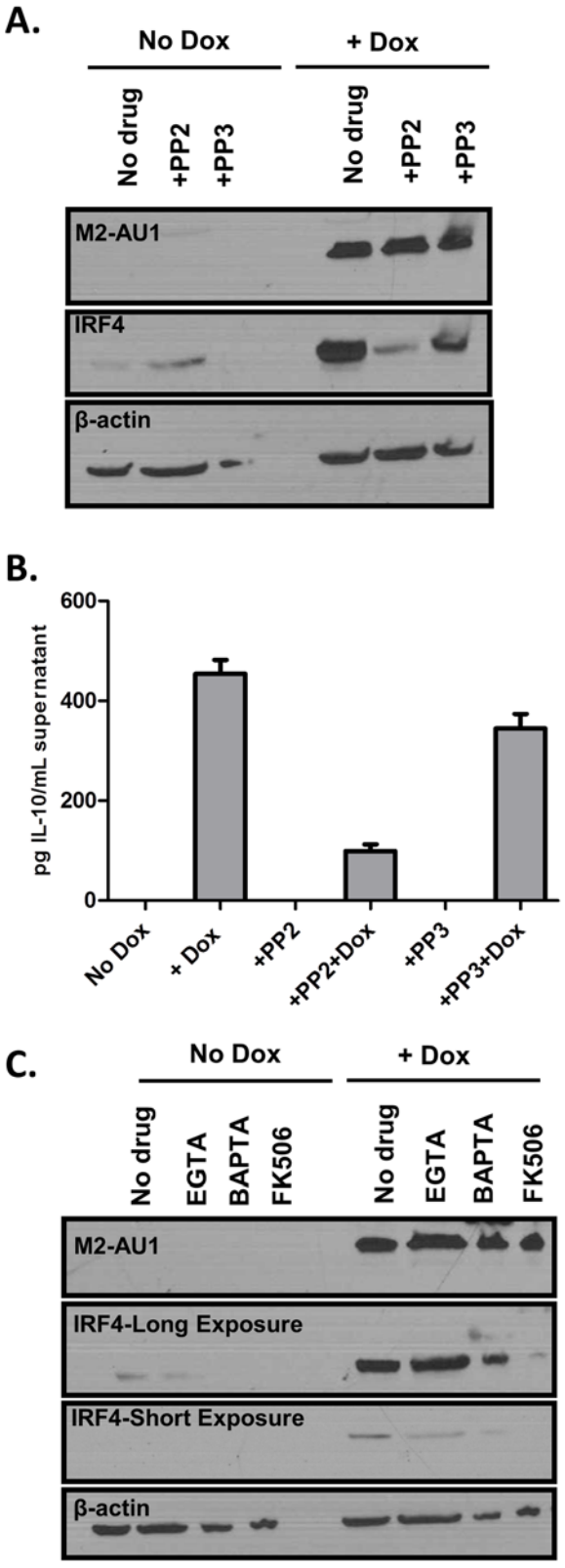

Supplementary Figure 4

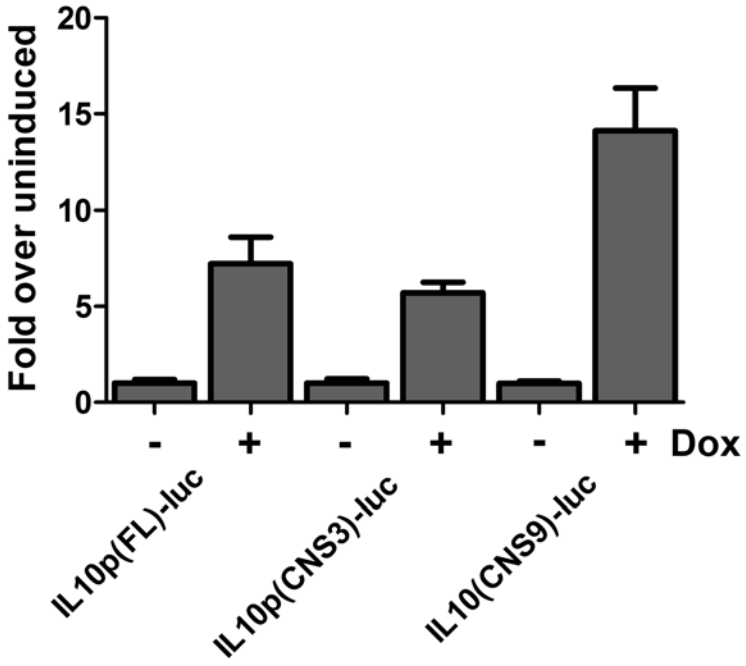

FIGURE LEGENDS

Figure 1. An inducible system to study M2 mediated signaling events. Doxycycline inducible M2 expressing cell lines were generated using the M12 murine B lymphoma cell line. C30p is the parental cell line stably carrying the TetON regulator plasmid, which is used as a negative control. C30bulk refers to the bulk inducible cells prior to limiting dilution analysis. DS10, DS14 and DS15 are individual clones of M2 inducible cell lines. (A) Representative bright-field and mCherry fluorescence images of the same field of DS10 cells that were either left uninduced (top panel) or treated with doxycycline for 48 hours (bottom panel). (B) The indicated cell lines were either left uninduced or induced with doxycycline for 48 hours. Whole cell lysates were harvested and 40μg protein was resolved by SDS-PAGE followed by immunoblotting for M2, IRF4 and β-actin using antibodies described in Materials and Methods. (C) Supernatants from $2x10^6$ cells that were either doxycycline induced for 24 hours, or left uninduced, were analyzed for IL-10 secretion by ELISA. Data shown is a representative figure from multiple experiments showing similar results.

Figure 2. M2 activates the NFAT pathway, but not other major signaling pathways such as NFkB, ISRE, or AP-1. $3 x10^6$ cells were nucleofected with 10μg of the indicated reporter plasmids using the Amaxa solution L or Ingenio (Mirus) electroporation solution as per manufacturer's protocol. After transfection, the cells were divided into two reactions - one half was left untreated and the other half received doxycycline for 48 hours prior to quantitating luciferase activity. Each condition was performed in triplicate wells. Reporter plasmids used are part of the PathDetect cis-reporting system from Agilent technologies. (A-C) Analysis of M2-inducible NFAT activity in DS10, C30p and DS15 cell lines. The pNFAT-luc reporter was nucleofected as described above. PMA (60ng/mL) and Ionomycin (1 μg /mL) treatment for 6 hours served as a positive control. (D) Analysis of M2 inducible NF-kB activity in the DS10 cell line. pNFκB-luc reporter was nucleofected as described above. pFC-MEKK plasmid and

pIκBαM plasmid served as the positive and negative controls respectively. (E) pAP-1 reporter plasmid was used as described above. pFC-MEKK plasmid served as a positive control. (F) pISRE-luc reporter plasmid was used as described above. IFNα treatment for 6 hours served as a positive control. For all analyses, luciferase activity is represented as fold over uninduced ± SEM.

Figure 3. M2 activation of the NFAT pathway is CsA and FK506 sensitive and requires extracellular calcium flux. (A, B and C) Impact of inhibitors on M2-induced NFAT activity. The NFAT reporter assay was performed as in Figure 2A.Doxycycline was added for 48 hours. CsA (500ng/mL), FK506(1μM), EGTA(2.5mM), BAPTA-AM(5μM), PP2 (10μM) and PP3 (10μM) were added 24 hours post-nucleofection and the lysates were assayed for luciferase activity at 48h post-nucleofection. Data are represented as fold over respective uninduced conditions, setting the uninduced samples in each drug treatment to 1. (D) The indicated cell lines were either left uninduced or induced with doxycycline for 48 hours. Whole cell lysates were harvested and 60μg protein was resolved by SDS-PAGE followed by immunoblotting for NFATc1 using antibodies mentioned in materials and methods. β-actin was used as a loading control.

Figure 4. M2 induction of IRF4 by M2 is partially dependent on NFAT pathway. (A) DS10 and C30p cells were either left uninduced or induced with or without CsA for 48 hours in the culture media. Whole cell lysates were harvested at 48h post induction and $5x10^5$ cell equivalents were analyzed for levels of IRF4 protein by immunoblotting. PMA and Ionomycin treatment for 6 hours served as a positive control for IRF4 induction. P3X63Ag8 cell lysates served as a stimuli independent positive control. (B) Duplicate gel run using whole cell lysates from (A) to verify expression of M2 using antibody for AU1 tag. (C) Supernatants from cells in Figure 4A were analyzed for IL-10 levels by ELISA.

Figure 5. Tyrosines 120 and 129 of M2 are indispensable for M2 mediated NFAT activation and IRF4 expression. (A) $3x10^6$ of the indicated cell types were nucleofected with 10μg of the NFAT reporter plasmid s using Ingenio electroporation solution as described in Figure 2A. After transfection, the cells were divided into two reactions - one half was left untreated and the other half received doxycycline for 48 hours prior to quantitating luciferase activity. Each condition was performed in triplicate. Luciferase activity is represented as fold over uninduced ± SEM. (B) Whole cell lysates from the indicated cell lines were analyzed for expression of M2, IRF4 and β-actin as described in Figure1B.

Figure 6. IRF4 expression in B cells leads to IL-10 secretion and M2 synergizes with IRF4 to enhance IL-10 levels. (A) $3x10^6$ DS10 cells were transfected with 10μg of either an empty vector (pMSCV-IRES-GFP, designated pMIG-EV) or an IRF4 expression vector (pMSCV-IRF4-IRES-GFP, designated pMIG-IRF4) and the reaction was divided into two wells-one well received doxycycline treatment for 48hours and the other well was left uninduced. Each reaction was performed in triplicates. Supernatants were collected at 48hours post induction with doxycycline and IL-10 levels were measured by ELISA (B) $1x10^6$ M12 cells per well were nucleofected with an expression vector containing M2 or M2stop, together with either pMIG-EV or pMIG-IRF4.Supernatants were harvested 48hours after nucleofection and analyzed for IL-10 levels by ELISA. (C) DS10 cells were nucleofected as in (A) above with either pMIG-EV or pMIG-IRF4 along with 2.5 μg of IL-10pCNS9-luc reporter construct. Each reaction was divided into two reactions as above and luciferase activity was measured 48hours post doxycycline induction. (D and E) The indicated cell types (A20, BCL1-3B3, P3xAg and M12) were plated at a density of 2.5 $x10^5$ cells in each well of a 6-well plate. Supernatants and whole cell lysates were harvested at 48 hours and analyzed for IL-10 levels by ELISA (D) and IRF4 expression by immunoblotting (E).

Figure 7. Inhibition of NFAT pathway in primary murine B cells leads to reduced IRF4 expression and IL-10 levels correlating with changes in B cell surface phenotype. (A-E) Primary murine B cells were isolated as indicated in materials and methods, transduced with retroviruses expressing either M2 or M2stop. At the time of transduction, half of the cells received 500ng/mL CsA and the other half was left untreated. (A) The cells were analyzed for Thy1.1 expression by flow cytometry on days 2 to 5 post-transduction. Cells were first gated on live cells and then gated on Thy1.1 and plotted as frequency of cells that were positive for Thy1.1. (B) Supernatants were collected from the cells used in (A) and analyzed for IL-10 levels by ELISA. (C and D) Whole cell lysates from cells in replicate wells as in (A) were harvested for analyzed for IRF4, NFATc1, NFATc2 and β-actin expression by immunoblotting. 10 μg protein was loaded per well. (E) Gated live cells from the indicated conditions were analyzed for their expression of the surface markers B220, CD138, MHC-IA^{b}, IgD, CD23 and CD25. Representative histograms are from day 4 post-transduction depicting one of triplicate samples per condition.

Figure 8. IRF4 is required for establishment of MHV68 latency as well as for reactivation from latency. IRF4$^{fl/fl}$ mice were infected with 1000 PFU of either MHV68-Cre or MHV68-WT virus intranasally. On day 16 post infection, splenocytes were analyzed by limiting dilution analyses to determine (A) the frequency of virus capable of establishing latency and (B) the frequency of virus capable of reactivating from latency.

Figure 9. M2stop infected mice exhibit a decreased frequency of infected B cells expressing IRF4. C57BL6/J mice were infected intraperitoneally with 1000PFU of the indicated viruses and splenocytes were analyzed on day 14 post infection. (A) Representative flow plots illustrating the gating strategy. Splenocytes were gated to remove doublets following gating on the live cell population using a live/dead stain (Materials and Methods). (B) Frequency of live, singlet YFP+

cells that were IRF4 positive between M2stop.HY and M2MR.HY viruses. Data shown is from individual mice with five mice per virus group.

Figure 10. Model of M2 mediated IL-10. Upon BCR engagement, multiple protein kinases including Src family kinases (Lyn,Fyn,Src,Blk,Yes), Syk, Btk get activated leading to the activation of PLCγ2.Activated PLCγ2 catalyzes the hydrolysis of phosphatidylinositol-4,5-biphosphate [(PtdIns(4,5)P2] to DAG and IP3. Binding of IP3 to its receptor on the ER membrane leads to release of ER Ca^{2+} stores. However, this increase in Ca^{2+} is only transient and following depletion of ER Ca^{2+} stores, an influx of extracellular Ca^{2+} occurs (termed as SOCE-Store Operated Calcium Entry). This prolonged and sustained increase in Ca^{2+} leads to activation of the Calcineurin-NFAT pathway. In the case of M2, *Miranda et al* have shown that M2 can interact with Fyn and PLCγ2. Our model suggests that interaction of M2 with proximal membrane signaling molecules such as Src kinase and/or PLCγ2 potentially mimics events that occur upon BCR engagement resulting in the Ca^{2+} mediated activation of the NFAT pathway. Induction of IRF4 by M2 is dependent, at least partially by the activation of NFAT pathway. IRF4 can activate regulatory elements in the IL-10 promoter locus (termed CNS-Conserved Noncoding Sequences) in T cells and in our case, in B cells as well. These series of events leads to eventual increase in the levels of IL-10 observed upon induction of M2.

Supplementary Figure 1. M2 expression activates the IL2promoter. $3x10^6$ DS10 cells were nucleofected with 10μg of the IL2-promoter-luc plasmid using Ingenio solution as described in Figure 2A. After transfection, the cells were divided into two reactions - one half was left untreated and the other half received doxycycline for 48 hours prior to quantitating luciferase activity. Each condition was performed in triplicate wells. Luciferase activity is represented as fold over uninduced ± SEM. In reactions with CsA addition, CsA was added at 24 hours post-nucleofection. Treatment with PMA and Ionomycin served as a positive control.

Supplementary Figure 2. Addition of drugs to DS10 cells does not have a significant effect on cell viability. (A-C) DS10 cells were used to perform a NFAT-reporter assay as in Figure 3A-3C. (D) Cells from panel A-C were counted using trypan blue exclusion to determine the effect of the drugs on the viability of the cells. Viability was plotted as a percentage of uninduced, setting uninduced samples to a 100%. (E) Live cell numbers were plotted as fold over uninduced, setting the uninduced samples to 1. Data is representative of an average of counts from three replicate wells per condition.

Supplementary Figure 3. Effect of drugs on levels of M2 and IRF4 expression. (A and C) Replicate wells of DS10 cells were treated with drugs as in supplementary figure 2A-2C. Whole cell lysates were harvested and 40μg of protein was analyzed by western blotting for levels of M2 expression (using an AU1 antibody) and IRF4 expression. (B) Supernatants from supplementary figure 3A were analyzed for IL10 levels by ELISA. Data is representative of duplicate wells per condition.

Supplementary Figure 4. IL10p-CNS9-luc has the maximal activity upon M2 expression. IL-10pFL-luc, IL10pCNS-3-luc and IL10pCNS-9-luc plasmids (described in Materials and Methods) were nucleofected into DS10 cells as described in Figure 6C. Luciferase activity is plotted as fold over uninduced controls.

CHAPTER III

INTRODUCTION

Gammaherpesviruses, members of the *Herpesviridae* family are lymphotropic viruses that are characterized by their ability to establish latency in lymphocytes, particularly in B cells. The human viruses of this family, Epstein-Barr Virus (EBV) and Kaposi's Sarcoma associated Herpesvirus (KSHV) are associated with a range of lymphoproliferative diseases and lymphomas in immunocompromised situations (reviewed in [13]). EBV, a member of the lymphocryptovirus genus, is found in all cases of endemic Burkitt's lyphoma, and is associated with other lymphoid cancers such as Hodgkin's Lymphoma and post-transplant lymphomas, as well as carcinomas such as gastric carcinoma and nasopharyngeal carcinoma (reviewed in [184]). KSHV, a member of the more common rhadinovirus genus, is the etiologic agent of majority of AIDS-related KS, and is associated with Primary Effusion Lymphoma (PEL) and Multicentric Castleman's disease (reviewed in[205]). However, strict species tropism of this family of viruses greatly hampers detailed studies of pathogenesis and host defense in an *in vivo* setting. Much of the *in vivo* studies have been accumulated from limited utilization of either small-animal models or primate models.

Murine gammaherpesvirus 68 (MHV68) infection of inbred strains of mice provides a powerful and well-characterized rodent model for studying gammaherpesvirus infections. Infection of mice with MHV68 results in a productive acute replication phase in the lung and spleen which is cleared 2-3 weeks post-infection (reviewed in [13]). Latency is established primarily in splenic B cells -particularly in naïve, germinal center B cells and memory B cell subsets, as well as macrophages, dendritic cells and lung epithelial cells, as is the case for EBV [32,34,35]. Long-term latency is predominantly established in memory B cells [33]. Recently we have shown that similar to EBV and KSHV, plasma cells represent the major reactivation reservoir for MHV68 as well [60], strongly linking the conserved strategies utilized by this virus

family. Moreover, it was shown that a MHV68 gene product called M2 plays a pivotal role in driving differentiation of infected B cells to plasma cells [60].

Sequence analysis and characterization of the MHV68 genome initially identified M2 as a latency associated gene product that bears no homology to any known cellular or viral protein [23,51]. M2 is crucial for both establishment and reactivation from latency, in a route-and dose-specific manner, but dispensable for acute viral replication in lungs of mice [20,21]. M2 contains several SH3 binding PxxP motifs and two closely-spaced tyrosines (Y120 and Y129), and we have shown the functional importance of some of these residues *in vivo* [206]. Although MHV68 M2 does not bear sequence homology to any known gene product, the organization of the functional domains in M2 closely resembles domains present in the cytoplasmic N- terminal domain of EBV LMP2A. Furthermore, M2 possesses functional and positional homology to EBV LMP-1 by inducing IL-10 in the culture supernatants and by modulating B cell signaling [78]. M2 also activates the NFAT pathway, similar to that of K1 of KSHV which mimics constitutive ITAM mediated BCR signaling to activate the NFAT pathway [83,190]. M2 induces IL10 expression in primary murine B cells [58] and we have recently shown that this induction occurs via a NFAT dependent pathway involving IRF4 induction [190]. Depending on the cell type, IL10 activates the JAK-STAT pathway *via* activation of JAK1 (associated with the IL10 receptor α chain) and/or TYK2 (associated with the IL10 receptor β chain) and induces the activation of STAT1, STAT3, and, in some cases, STAT5 [20,187,207-209].

In vitro studies have shown that Y120 residue and a C-terminal PxxP motif of M2 are involved in the formation of a complex comprising of M2, Vav1 and Fyn [56]. Additionally, it was shown that Y120 of M2 is constitutively phosphorylated in a B cell line and a mutant virus with Y120 and Y129 mutated to phenylalanine exhibits M2 null phenotype in latency establishment *in vivo* [57]. It was also recently shown that M2 interacts with several cellular proteins *via* Y120 and/or Y129 residues. While Y120 was predominantly associated with Vav1, p85α subunit of PI3K and NCK1,

Y129 found to interact with PLCγ2, p85α subunit of PI3K and SHP2 [61]. However, requirement of these individual tyrosine residues in some essential functions of M2, namely establishment of latency, reactivation from latency coupled with plasma cell differentiation, and IL-10 production is unknown. In an earlier study, we have shown that both of these tyrosines are required independently for activation of the NFAT pathway and IRF4 induction [190]. In this study, we aimed to further characterize the roles of Y120 and Y129 in key functions of M2, both *in vitro* and *in vivo*.

MATERIALS AND METHODS

Ethics statement. This study was carried out in strict accordance with the recommendations in the Guide for the Care and Use of Laboratory Animals of the National Institutes of Health. The protocol was approved by the Emory University Institutional Animal Care and Use Committee and in accordance with established guidelines and policies at Emory University School of Medicine (Protocol Number: YER-2002245-031416GN).

Mice and infections. Female C57BL6/J mice aged 6-8 weeks were purchased from Jackson labs (Bar Harbor,ME) and infections were done at 9-12 weeks of age. Mice were housed and maintained at the Whitehead vivarium according to Emory University and IACUC (International Animal Care and Use Committee) guidelines. Mice were anesthetized using isoflourane before infecting with 1000 PFU of the respective viruses via either intranasal or intraperitoneal infection. For flow cytometry analyses, individual mice were analyzed and for the latency and reactivation analyses, pooled splenocytes from 3-5 mice per group were used.

Plasmids. The Y120F and Y129F mutations were created by overlapping PCR using the following primers: Y120F – (5’ GAAGAAAACATCTTCGAAACTGCTAAC 3’) and (5’GT TAGCAGTTTCGAAGATGTTTTCTTC 3’); Y129F – (5’ AGTGAACCAGTCTTCATCCAG CCAATC 3’) and (5’GATTGGCTGGATGAAGACTGGTTCACT 3’).The overlapping PCR products were then cloned into pCR-BLUNT (Invitrogen), sequenced and positive clones were then cloned into pMSCV-IRES-Thy1.1 vector as described in [58], using Bgl II restriction sites.

Construction of mutant viruses. M2stop.HY and M2MR.HY viruses are described previously [190].The Y120F.HY and Y129F.HY viruses were created in a similar manner. Briefly, the MHV68-H2bYFP BAC described in [180] was used as a backbone to create a M2/galK intermediate BAC where the M2 ORF was replaced with a galK cassette. The M2/galK

intermediate was made by amplifying the galK gene from pGalK using the following primers – gK-M2-FP (5′ tggagggggtttcaacaggcactagtctgatgaggtttcgttttcaggtaTCAGC ACTGTCCTGCTCCTT-3′) and gK-M2-RP (5′-tccaggcgtgtttaaagaaaaagttatgttctgcgtt agcaccttcactgCCTGTTGACAATTAATCATCGGCA-3′). These primers contain 50 bp homology arms that flank the M2 ORF. The resulting PCR product was transformed into the SW102/H2bYFP cells and screened by positive selection on minimal media containing galactose as the carbon source. Following confirmation of the M2/galK intermediate by restriction digest, the galK region was swapped out and replaced with either M2 or M2stop containing PCR products amplified from pMIT-Y120F or pMIT-Y129F plasmids using the same homology arms used for generating the M2/galK intermediate: M2-FP (5′-tggagggggtttcaacaggcactagtctgatgaggtt tcgttttcaggtaATGGCCCCAACACCCCCACA-3′) and M2-RP (5′- tccaggcgtgtttaaagaaaaa gttatgttctgcgttagcaccttcactgTTATATATAGCGATAGGTATCCTCCTCG – 3′). After confirming the presence of required mutation by sequencing, the PCR products were electroporated into the M2/galK intermediate and recombinants were selected on minimal plates containing glycerol and 2-deoxy-D-galactose. Potential colonies were screened by colony PCR and confirmed by sequencing prior to final confirmation by Southern blotting (data not shown).

Flow cytometry. Flow cytometry on primary murine B cells were performed as described previously [58]. Briefly, cells were resuspended in about 100uL of FACS buffer (PBS with 2% FCS + 1mM EDTA). Fc block was done prior to staining with fluorophores to block FcγIII/II receptors by adding Rat monoclonal anti CD16/32 (eBioscience) for 10 minutes. The cells were washed once with FACS buffer prior to staining with an antibody cocktail. Antibodies used for surface staining of primary B cells include Thy1.1-APC (eBioscience) and CD19-FITC. For staining splenocytes from infected mice, a similar protocol was used. Antibodies in the cocktail for infected cells include GL7-Ax660/APC (eBioscience), CD95-PECy7, CD138-PE, CD3, CD4, CD8-PerCP (BD Pharmingen), B220-Pacific Blue (Southern Biotech) described in [180]. CD3,

CD4 and CD8 were used in the same fluorophore to eliminate T-cells. This mix is referred to in the text as dump gate.

B cell isolation. Murine primary B cells were isolated by immunomagnetic negative selection using the EasySep Mouse B Cell Enrichment Kit (Stem Cell Technologies) as per manufacturer's instructions. The purity of B cell isolation was routinely analyzed and found to be ≥95% as determined by staining for CD19 by flow cytometry. The cells were plated at 1×10^6 cells/mL of a 24 well plate overnight with cRPMI containing 20-25 µg/mL LPS (Sigma) prior to retroviral transduction.

Retroviral transduction. Retroviruses were prepared as described in [58]. Briefly, BOSC23 (ATCC) producer cells were plated at a density of 1.5×10^6cells per 60 mM or $3x10^6$ cells per 100mM collagen coated dish (BD biosciences) overnight. After 18–24 hours of plating, the cells were transfected with 5 µg(for 60mM) or 10ug(for 100mM dish) of either pMIT-M2, pMIT-M2stop, pMIT-Y120F or pMIT-Y129F plasmids. Supernatants were harvested at 72 hours and used immediately or frozen at −80°C until ready for use. On the day of transduction, the retroviruses were centrifuged at 2000rpm for 10 minutes to remove any cellular debris and supplemented with 5 µg/mL of polybrene. 750 µL of the media was removed from the B cells and replaced with 1 mL of the retrovirus containing polybrene. The cells were spin infected for 2500 rpm for one hour at 30°C. Post-transduction, 750 µL of the supernatant was removed from each well and 1 mL of fresh media was added back. Triplicate wells per condition were analyzed by flow cytometry at days 2–5 post-transduction.

Limiting Dilution analysis for latency and ex-vivo reactivation. Determination of frequency of latently infected splenocytes was done by performing a limiting dilution, single-copy sensitive nested PCR assay, as previously described [31,35]. Briefly, frozen splenocytes were thawed,

counted and washed in isotonic buffer prior to plating in serial three-fold dilutions onto a background of 10^4 uninfected 3T12 cells in 96-well plates. Following a proteinase K mediated digestion step to lyse the cells, the samples were subject to two rounds of nested PCR. Twelve PCRs were performed for each dilution for a total of six dilutions starting with 10^4 cells. Each PCR plate contained control reactions that contained 0, 0.1,1, or 10 copies of plasmid DNA in a background of uninfected cells. Products were analyzed on a 2% agarose gel. Determination ofthe frequency of splenocytes capable of reactivating virus from latency was done by using a limiting dilution ex-vivo reactivation assay, as previously described [31,35]. Briefly, single cell suspensions of splenocytes from infected mice were plated in a two-fold serial dilution fashion (starting with 10^5 splenocytes per well) on to MEF monolayers in 96-well tissue culture plates. Twenty-four wells were plated per dilution and 12 dilutions were plated per sample. Wells were scored microscopically for cytopathic effect (CPE) at 14–21 days post-explant. Preformed infectious virus was detected by plating parallel samples of mechanically disrupted cells onto MEF monolayers alongside intact cells. We did not observe a significant amount of preformed infectious virus in any of the assays described (data not shown).

RESULTS

Tyrosines 120 and 129 of M2 are required for IL10 production and expansion of primary murine B cells.

In vitro analyses of M2 functions have shown that Y120 of M2 is the predominant residue required for formation of a trimolecular complex of M2 with the Src kinase Fyn and Vav. It was also shown that Y120 is constitutively phosphorylated upon expression in a B cell line as well as a non-hematopoietic cell line [56]. However, in our recent studies on the signaling of M2, both Y120 and Y129 were singly required for activation of the NFAT pathway by M2. Both Y120 and Y129 were also required for induction of the plasma cell associated transcription factor, IRF4 [190]. Since M2 induction of IRF4 leads to IL-10 induction in B cells, we wanted to further study the roles of the individual tyrosines of M2 in IL-10 production in a more physiological context, namely primary murine B cells. We made retroviral constructs in which each of the tyrosines at positions 120 and 129 of M2 was mutated to a phenylalanine. B cells were isolated from primary murine splenocytes and transduced with the retroviruses Y120F and Y129F. The expression of an IRES-Thy1.1 cassette downstream of M2 expression served as a surrogate marker to monitor M2 expression. As shown in Figure 1A, M2 expressing cells expanded in culture over time, consistent with our previous results [58]. However, expression of either Y120F or Y129F mutant form of M2 abolished M2 mediated expansion of Thy1.1 expressing cells, with both the mutants expressing levels of Thy1.1 similar to that of M2stop, a negative control retrovirus that expresses a translational stop codon at amino acid 13 of the M2 ORF. In addition, as shown in Figure 1B, supernatants from B cells transduced with a wild-type M2 retrovirus produced significant amounts of IL-10, compared to M2stop, as observed in our previous analyses [58]. On the other hand, neither Y120F nor Y129F induced IL-10 as observed upon M2 expression (Figure 1B). Furthermore, we also tested the lack of IL-10 induction in M2 inducible cell lines described in [190] that contain Y120F or Y129F mutations. Consistent with

the data in primary B cells, as shown in Figure 1C, IL-10 production was absent upon doxycycline induction of two independent clonal inducible cell lines containing either Y120F or Y129F mutations. These data indicate that although Y120 is the predominant tyrosine required for interactions with Src kinases and Vav, Y129 is also required for efficient function of M2, namely IL-10 production and expansion of primary B cells.

M2 induced IL-10 primarily signals through pSTAT3, but not pSTAT1 or pSTAT5.

Several studies have shown that IL-10 induces a positive feedback signaling by acting through the IL-10R which signals primarily through activation of STAT3, as well as STAT1 or STAT5 in some cell types (reviewed in [109], [187,209]). In order to understand whether M2 induced IL-10 signals using a similar pathway, we measured activation of STAT3 by evaluating the levels of phosphorylated STAT3 by flow cytometry. Primary B cells were transduced with retroviruses expressing either M2 or M2stop and the levels of pSTAT3 were measured by phosphoflow. As shown in Figure 2A, on days 2 and 3 post transduction, M2 transduced cells had higher levels of pSTAT3 compared to M2stop transduced cells. As expected, negative control B cells from IL-10 knockout mice that were transduced with either M2 or M2stop expressing retroviruses failed to up-regulate pSTAT3 (Figure 2A and 2B). Since IL-10 can signal via pSTAT1 and pSTAT5 in some cell types, we also looked at pSTAT1 and pSTAT5 levels upon M2 expression. As shown in Figure 2C and 2D, M2 transduced B cells failed to up-regulate pSTAT1 or pSTAT5, respectively. In contrast, positive controls in each experiment, namely, IFNγ and GM-CSF induced pSTAT1 (Figure 2C and 2E) and pSTAT5 (Figure 2D and 2F), respectively, compared to unstimulated samples. It is to be noted that pSTAT5 is predominantly activated in T cells in response to IL-2 [189] and in myeloid cells in response to GM-CSF [188]. Therefore, we observed only a modest increase in the GM-CSF positive control sample compared to unstimulated B cells. Additionally, pSTAT1 and pSTAT5 levels are moderately higher in both

M2 as well as M2stop transduced samples (Figure 2E and 2F) compared to unstimulated samples indicating that LPS stimulation can activate some levels of pSTAT1 and pSTAT5 in murine B cells. In order to make the B cells proliferate to be conducive to retroviral transduction, we stimulate them overnight with LPS.

Based on our results from Figure 1A and 1B which suggest a lack of B cell proliferation and IL-10 production upon expression of Y120F or Y129F mutant retroviruses, we wanted to verify whether the pSTAT3 levels induced by wild-type M2 was altered in Y120F and Y129F mutants. As shown in Figure 3A and Figure 3B, both Y120F and Y129F mutant retroviruses fail to induce pSTAT3 levels similar to that of wild-type M2. This is consistent with our idea that the pSTAT3 levels we observe upon M2 expression are a result of M2-mediated IL-10 feeding back upon the IL-10R to activate pSTAT3, rather than M2 itself activating STAT3 to increase pSTAT3 levels. In addition, when we block the IL-10 signaling with an antibody against the IL-10R, we fail to see increase in pSTAT3 levels (data not shown). Together, these results indicate that M2 mediated IL-10 signals predominantly through pSTAT3 and that M2 requires Y120 as well as Y129 for IL-10 production in primary murine B cells.

Y129 but not Y120 of M2 is required for an efficient establishment of latency and reactivation from latency in vivo.

Given the requirement of both Y120 and Y129 in M2 mediated functions *in vitro* in primary B cells, we wanted to further characterize the requirement of each of these tyrosines *in vivo* in the pathogenesis of MHV68 infection, namely in establishment of latency and reactivation from latency. Furthermore, *Miranda et al* have shown that a double mutant virus with both tyrosines Y120 and Y129 mutated to phenylalanine have a severe latency phenotype similar to that of an M2 null virus, indicating that at least one or both the tyrosines are required for M2 mediated functions *in vivo* [57]. To identify the requirement of each of the tyrosines, we made

mutant viruses in which either Y120 or Y129 was mutated to phenylalanine, designated Y120F.HY and Y129.HY, respectively. We used the λRed recombineering system utilizing galK selection method described by *Warming et al* [167] to make the mutant viruses. To this end, we utilized a MHV68-H2bYFP transgenic virus expressing a EYFP cassette fused to the histone H2B open reading frame to allow us to monitor infected cells by flow cytometry and immunofluorescence. This virus has been extensively characterized and behaves similarly to the wild-type MHV68 virus [180]. The mutations in the tyrosine mutant viruses were confirmed by PCR of the M2 region derived from BAC-purified DNA as well as from DNA obtained from latently infected splenocytes. To further confirm the absence of unwanted mutations or insertions within the region of homologous recombination, we performed Southern blotting analyses combined with RFLP analyses (data not shown). We have previously described a M2null virus, and a marker rescue virus termed M2stop.HY and M2MR.HY, respectively. These viruses were also created using the MHV68-H2bYFP background and behave similarly to their non-transgenic counterparts [190].

Previous studies have shown that the requirement of M2 in the establishment of latency is dependent on the dose and route of infection [21]. Low dose intranasal (IN) inoculation with 100 PFU of M2stop virus resulted in a severe latency defect which was overcome by a higher dose of inoculation at $4x10^5$ PFU or with a intraperitoneal (IP) inoculation with 100 PFU [20,21]. Since the transgenic H2BYFP viruses have been characterized primarily with a 1000PFU IN or IP, we chose to look at the requirements of the Y120F and Y129F mutant viruses at 1000PFU, via either IP or IN route. Since the kinetics of IP infection are faster than that observed with an IN infection, we analyzed days 14-15 post-infection compared to days 16-18 post infection for IN infections. As depicted in Figure 4A, infection of mice with M2stop.HY virus via the IN route showed a ~9 fold defect in establishment of latency compared to M2MR.HY (1 in 2339 cells carrying viral genome in M2stop.HY infected cells compared to 1 in 259 cells in M2MR.HY infected cells).

Surprisingly, infection with Y120F.HY showed only a moderate defect (about ~3 fold defect) in latency compared to M2MR.HY infection, suggesting that Y120 is largely dispensable for establishment of latency. On the other hand, infection with the Y129F.HY virus showed frequencies of viral genome positive cells similar to that of M2stop.HY (1 in 5533 cells), indicating that Y129 is required for efficient establishment of latency (Figure 4A). Consistent with the latency phenotypes, the frequencies of splenocytes reactivating virus are similar for M2MR.HY and Y120F.HY infected mice (1 in 10447 and 1 in 13366). In contrast, M2stop.HY and Y129F.HY infected mice have a severe defect in reactivation with ~24-fold lower compared to either M2MR.HY or Y120F.HY infected mice (Figure 4B) [21]. As expected, infection of mice *via* the IP route partially rescued the latency defect observed with M2stop.HY and Y129F.HY in the IN route, with a modest 3-5 fold defect compared to M2MR.HY and Y120F.HY, respectively (1 in 137 cells for M2MR.HY, 1 in 488 cells for M2Stop.HY, 1 in 178 cells for Y120F.HY and 1 in 597 cells for Y129F.HY) (Figure 4C). Similar to the results from the IN infection, we observed that upon IP infection, the Y120F.HY infected mice possess frequencies of reactivating cells within a two-fold range of difference compared to that of M2MR.HY infected mice (1 in 6729 cells in Y120F.HY vs 1 in 11614 cells in M2MR.HY) (Figure 4D). As we have previously observed with the M2stop.HY virus, IP infection partially rescued the severe reactivation defect [20] observed with the IN infection with only a 3-5 fold defect in reactivation compared to M2MR (Figure 4D). Y129F.HY infected mice also have frequencies of reactivation that were identical to that of M2stop.HY infected mice in IP infection as observed in the IN infection (Figure 4D). Of note, we did not observe a significant amount of preformed infectious virus in any of the assays described (data not shown). Taken together, these data show that despite an absolute requirement for both Y120 and Y129 in M2-mediated functions *in vitro*, only Y129 is required for M2-mediated functions *in vivo*. This is corroborated by the data from *Miranda et al* which shows that a double mutant virus with mutations in both tyrosines exhibits an M2stop

phenotype. Our data shows that Y120 is largely dispensable for an efficient establishment of latency as well as reactivation from latency.

Y129, but not Y120, of M2 is required for efficient access of infected B cells to the plasma cell reservoir.

Previously, we have shown that M2 is required for plasma cell differentiation of infected cells and that plasma cells are the major reactivation reservoir upon infection [60]. Using a transgenic virus that can mark infected cells by eYFP expression, it was shown that upon infection with a M2 null virus (M2stop.YFP), there was a significant decrease in the frequency of infected cells with a plasma cell phenotype. Since the viruses used in the current study express an H2bYFP cassette, we can identify the frequencies of infected cells by monitoring YFP expression by flow cytometry on infected splenocytes. We infected mice *via* either IP or IN route to determine the frequencies of infected B cells and B cell sub-populations by flow cytometry. As depicted in Figure 5A, on days 16-18 post infection *via* IN route, M2MR.HY, M2stop.HY and Y120F.HY had similar frequencies of YFP+ B cells (doublet-discriminated/$CD3^{-}CD4^{-}CD8^{-}$/ $B220^{+}$) whereas Y129F.HY infected mice had a smaller percentage of infected B cells. It was surprising that the Y129F.HY infection seemed to have a significant defect in frequencies of infected cells compared to M2stop.HY. We believe that this could be due to the fact that the Y129F is perhaps a deleterious mutation which results in a less functional M2 protein compared to M2stop.HY virus in which there is no M2 protein being made (it is to be noted that the Y129F.HY mutant did not have any defects in their growth phenotype and grew to similar titers as that of M2MR.HY and M2stop.HY). Furthermore, we found that there were similar frequencies of YFP+ B cells in the M2stop.HY infected mice compared to that of M2MR.HY infected mice despite a log defect in latency establishment. We believe that this is due to the high mouse-to-mouse variability we observe with the YFP marking of infected cells (as observed here in Figure 5A and 5B and in

[60,180,210]. Interestingly, we did observe a significant decrease in the YFP+ B cell fraction upon infection with the M2stop.HY compared to M2MR.HY(0.05% in M2stop.HY compared to 0.24% in M2MR.HY) *via* IP inoculation. Despite variable numbers of overall YFP+ B cells in the different viruses, there were no differences in the total number of germinal center(GC) B cells ($CD3^-CD4^-CD8^-/B220^+$,$GL7^+CD95^+$) and plasma cells ($CD3^-CD4^-CD8^-/B220^{lo}CD138^{hi}$) upon infection *via* either IN or IP route (Figures 5C – 5F). Notably, in our earlier analyses of infections with M2stop.YFP virus, we noticed a decreased number of total GC cells upon M2stop.YFP infection at a dose of 100PFU administered *via* IN route [60]. Thus our data in Figure 5C indicates that the defect in eliciting a strong germinal center response at 100PFU IN can be overcome by infecting with a 1000PFU. It is to be noted that in both IN or IP inoculations, we have some rare occasions where we fail to observe a considerable number of YFP+ cells to perform further analysis of infected GC cells or plasma cells. We believe this is due to an inefficient infection as a result of the mice coughing up the inoculum in an IN infection or due to inefficient trafficking. For this reason, we have excluded mice with very low YFP+ cells from the analysis of infected GC cells and plasma cells. Since we have consistently seen greater than 70% of the YFP+ cells to be in the GC population, we excluded mice which had a very low YFP+ frequency of less than $5x10^{-3}$ B cells infected and contain less than 50% YFP+ cells in the GC. The number of mice excluded in each group are as follows: 3/14 and 3/16 mice in M2MR.HY infected group in IN and IP respectively, 1/10 and 2/16 mice in M2stop.HY infected group in IN and IP respectively, 4/15 and 1/16 mice in Y120F.HY infected group in IN and IP respectively, 2/10 and 1/16 mice in Y129F.HY infected group in IN and IP respectively. Of note, these mice were included in the analysis of total YFP+ B cells and can be seen as the data points that lie on or very close to the x-axis (Figure 5A and 5B).

Based on the results from Figure 4, we expected that the Y129F.HY virus infected cells will also have a defect in plasma cell differentiation similar to a M2 null virus. To further

characterize the requirement of the individual tyrosine residues in their ability to efficiently infect GC cells and plasma cells, we analyzed YFP+ cells with either a GC or plasma cell phenotype. Upon IN infection of mice with the M2MR.HY, M2stop.HY, Y120F.HY or Y129F.HY viruses, the frequency of YFP+ cells with a GC phenotype (Figure 6A) were similar between the different groups. This trend changed upon IP infection, in which case there was a significant decrease in the frequency of YFP+ cells with a GC phenotype in M2stop.HY, Y120F.HY and Y129F.HY infected cells compared with the M2MR.HY infected cells (Figure 6B). Despite this difference, majority of the virus infected cells possessed a GC phenotype in all the cases (Figure 6A and 6B). In contrast to the above data, there was a striking difference in the frequency of YFP+ cells with a plasma cell phenotype in M2stop.HY virus infected cells compared to the M2MR.HY infected cells upon either IP or IN infections (Figure 6C and 6D) - ~7% of M2MR.HY infected cells *vs* 1.4% in M2stop.HY infected cells via IN route and ~10% of M2MR.HY infected cells *vs* 2.8% in M2stop.HY infected cells *via* IP route. In addition, infection with the Y120F.HY virus had a ~2-fold decrease in the fraction of infected cells with plasma cell phenotype indicating that the Y120 residue may be partly required for the infected cells to differentiate into plasma cells. Consistent with our above results, the Y129F.HY virus was similar to that of the M2stop.HY virus in its ability to form infected cells with a plasma cell phenotype (Figure 6C and 6D). Taken together, our data strongly demonstrates that majority of M2 mediated functions *in vivo* are mediated *via* its Y129 residue.

DISCUSSION

From prior studies on the functions of M2, it is hypothesized that M2 primarily functions as a molecular scaffold acting to relay signals that mimic those involved in BCR crosslinking [55-57,61,162,190,211]. M2 contains nine PxxP motifs capable of binding cellular proteins with SH3 domains as well as two tyrosines capable of binding SH2 domain containing proteins, owing to which several interacting partners for M2 have been identified. However, the importance of these interactions in a functional outcome during an *in vivo* infection setting still remains unclear. Identifying specific domains in the proteins that interact with M2 is crucial to gaining a better physiological perspective of how MHV68 utilizes M2 to hijack the host cell signaling machinery to its own benefit. As a first step towards this, we sought to identify the requirement of tyrosines Y120 and Y129 in functions mediated by M2.

In this study, we have identified Y129 as the critical tyrosine residue important for the function of the MHV68 gene M2, *in vivo*. Surprisingly, mutation of Y120 to phenylalanine had very little effect on the functions of M2 – only a 3 fold in latency (in the IN route) (Figure 4A) and a moderate defect in the differentiation of infected B cells to become plasma cells (Figure 6C). This strongly indicates that Y120 is mostly dispensable or only partially required for M2 mediated functions *in vivo*. However, in our *in vitro* studies, Y120 was required for M2 induction of the NFAT pathway, IRF4 [190] and IL-10 levels (Figure 1B). Notably, Y120 is constitutively phosphorylated in a B cell line and has shown to be the key interacting residue of M2 with Vav1, Fyn and NCK1 [57,61]. This could mean that either - 1) in an *in vivo* setting, either a host factor or a viral factor outside of M2 compensates for the loss of Y120 whereas that factor is absent in our *in vitro* setting, or 2) perhaps constitutive phosphorylation on Y120 is required for “tonic” signaling in B cells expressing M2, which is required for their normal functions and survival. On the other hand, Y129 phosphorylation is possibly tightly regulated and active only upon antigen

dependent signaling and therefore plays a vital role in functions of M2 *in vivo*. If the latter is true, the discrepancy with the requirement of Y120 *in vitro* maybe due to absence of potential overlapping effector signaling molecules required by both the tyrosines in the *in vitro* settings, but substituted for or compensated by other factors in the *in vivo* setting. Indeed, *Pires de Miranda* have shown that in a latently infected B cell line, S11, Y129 is required for the interaction of M2 with PLCγ2 [61], an activator of calcium signaling required for activation of the NFAT pathway. Consistently, we have shown that the NFAT pathway is partially required for induction of IRF4, a key player in plasma cell differentiation [190]. It is therefore worthwhile to speculate that the phosphorylation status of M2 strongly dictates the outcome of M2 mediated functions.

Additionally, we also made mutations of Y120 and Y129 to aspartic acids in an effort to mimic constitutive phosphorylation. However, in the primary B cell assays, we found similar results as those observed with the Y→F mutations (data not shown). This might mean that either constitutive phosphorylation is deleterious to the function of the protein rendering it unstable or that the mutations fail to mimic phosphorylation effectively. We did not pursue the Y→D mutations further since the focus of the study aimed at understanding the requirement of a particular tyrosine in M2 mediated function(s), rather than the effect of phosphorylation of M2 itself. It is also formally possible that the disconnect we observe with Y120 *in vitro vs in vivo* is due to the fact that most of the *in vitro* studies are done in B cell lines which are transformed, or in primary B cells that are stimulated with LPS. In these conditions, the status of the signal transduction pathways is deregulated and/or different from that occurring during an infection. This necessitates the requirement of an *in vivo* infection model such as above, for studying gammaherpesvirus biology and strongly argues for a setting where *in vitro* findings are presented with complementing *in vivo* results.

FIGURES

Figure 1

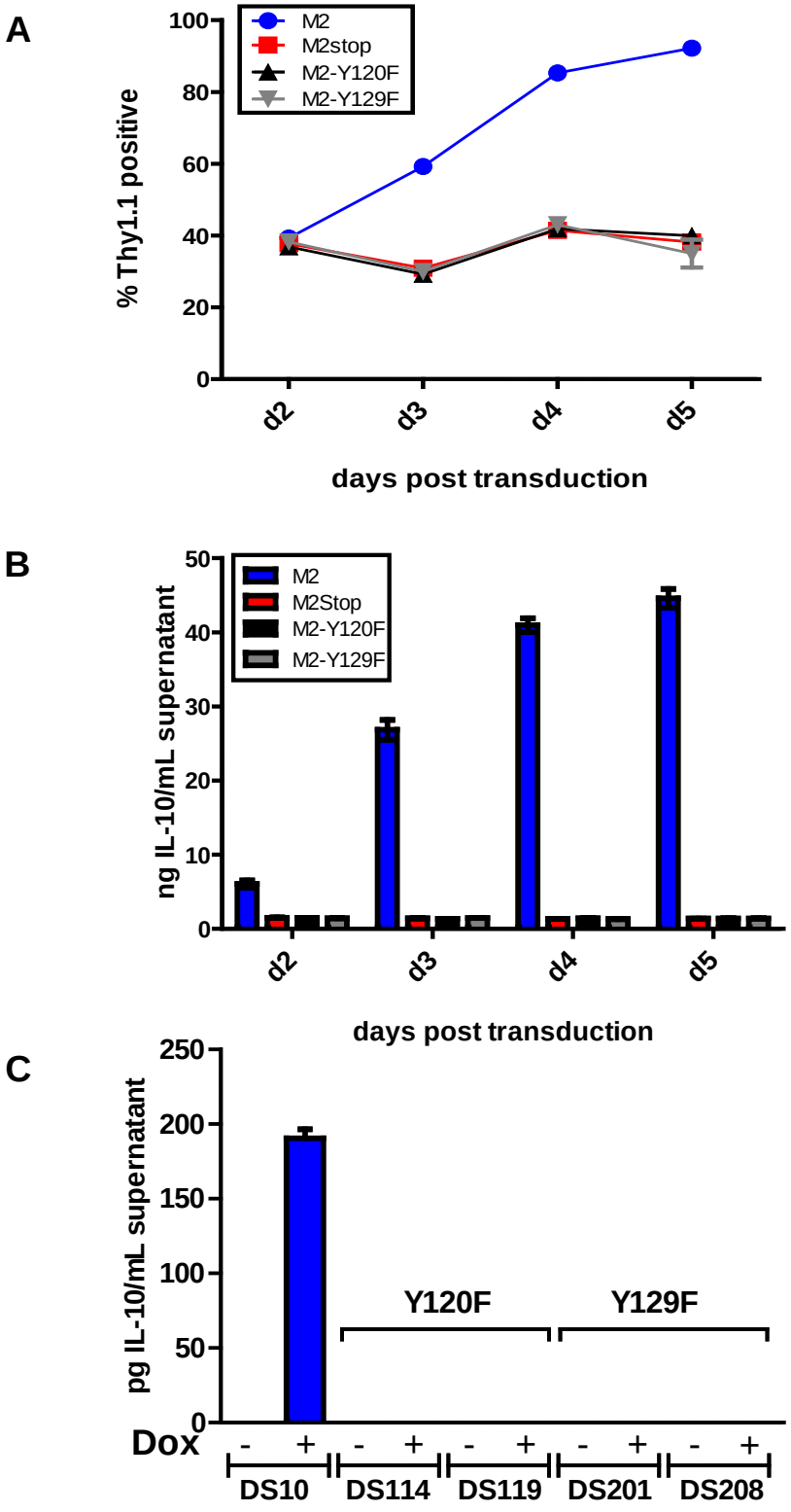

Figure 2

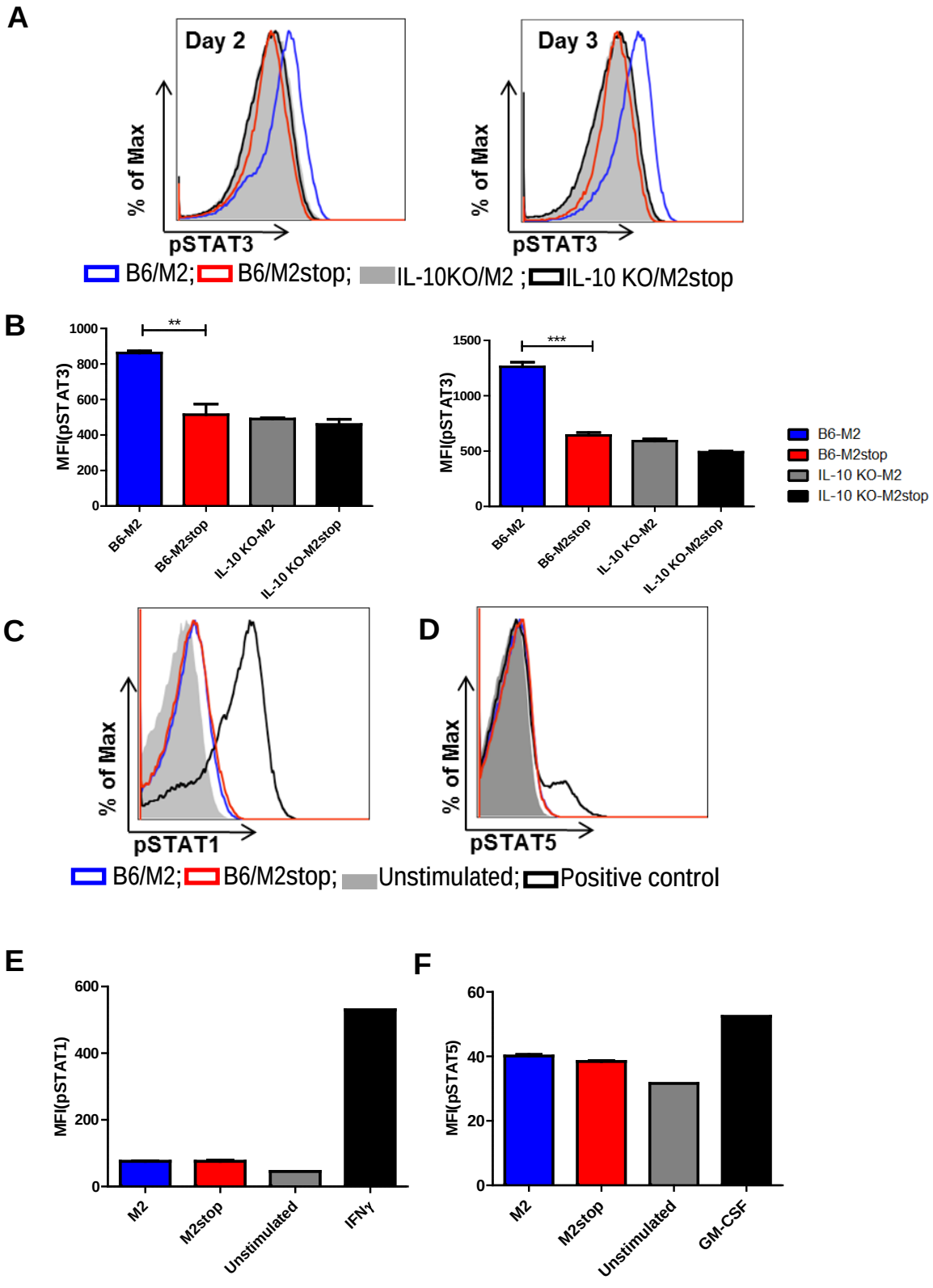
A
Day 2
Day 3
% of Max
pSTAT3
B6/M2; B6/M2stop; IL-10KO/M2 ; IL-10 KO/M2stop
B
MFI(pSTAT3)
**
***
B6-M2
B6-M2stop
IL-10 KO-M2
IL-10 KO-M2stop
C
D
pSTAT1
pSTAT5
B6/M2; B6/M2stop; Unstimulated; Positive control
E
F
MFI(pSTAT1)
MFI(pSTAT5)
M2
M2stop
Unstimulated
IFNγ
GM-CSF

Figure 3

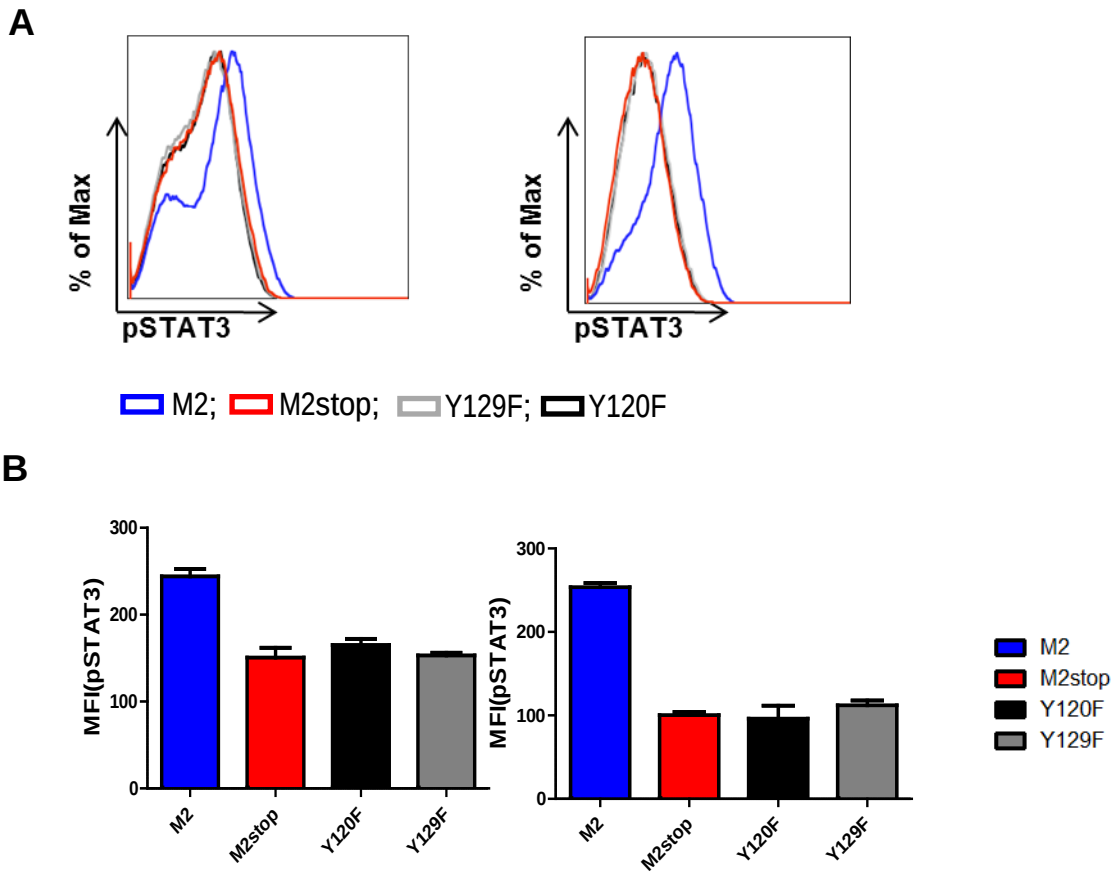
A
% of Max
pSTAT3
% of Max
pSTAT3
M2; M2stop; Y129F; Y120F
B
MFI(pSTAT3)
300
200
100
0
M2
M2stop
Y120F
Y129F
MFI(pSTAT3)
300
200
100
0
M2
M2stop
Y120F
Y129F
M2
M2stop
Y120F
Y129F

Figure 4.

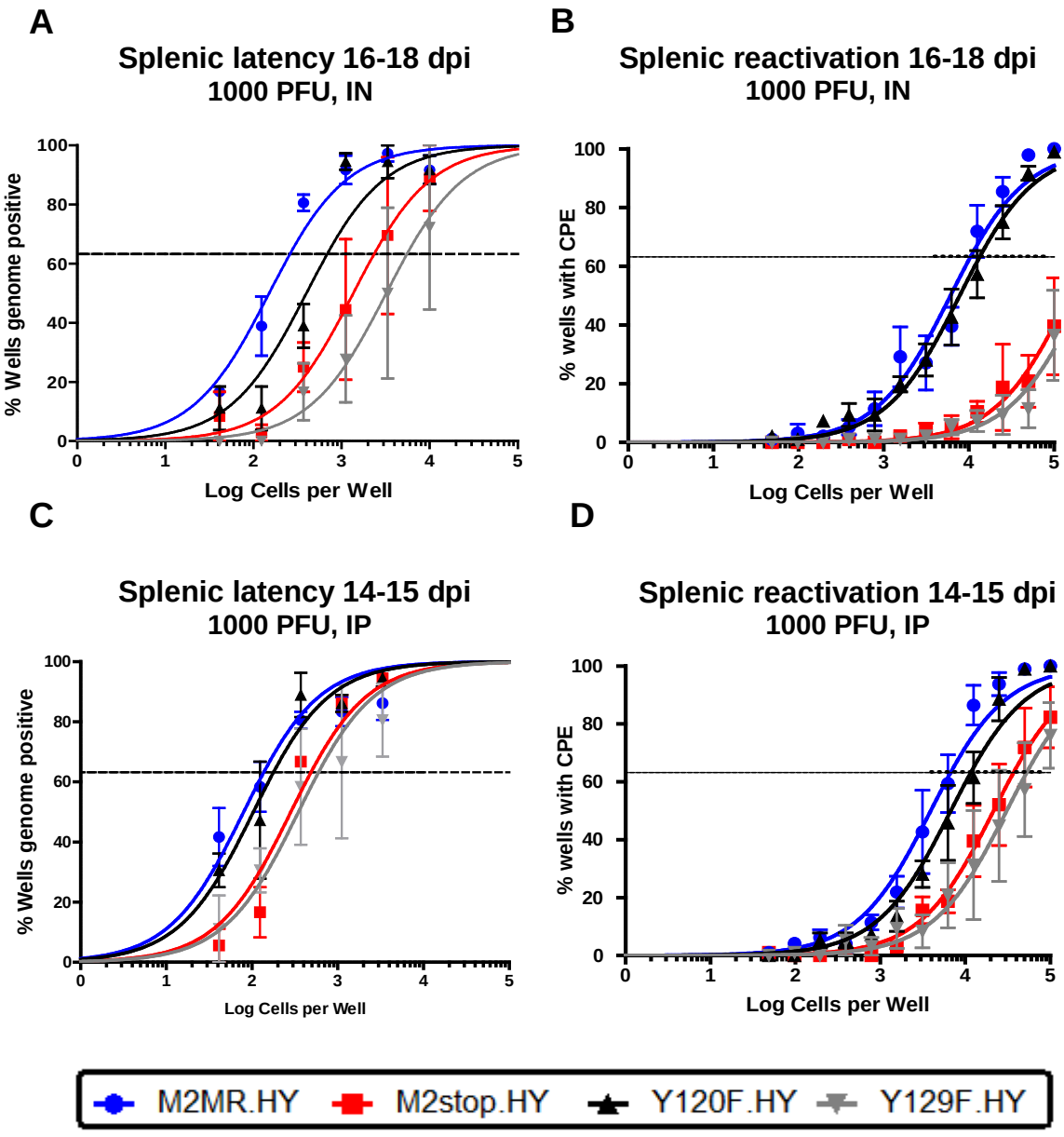
A
Splenic latency 16-18 dpi
1000 PFU, IN
% Wells genome positive
Log Cells per Well
B
Splenic reactivation 16-18 dpi
1000 PFU, IN
% wells with CPE
Log Cells per Well
C
Splenic latency 14-15 dpi
1000 PFU, IP
% Wells genome positive
Log Cells per Well
D
Splenic reactivation 14-15 dpi
1000 PFU, IP
% wells with CPE
Log Cells per Well
M2MR.HY
M2stop.HY
Y120F.HY
Y129F.HY

Figure 5

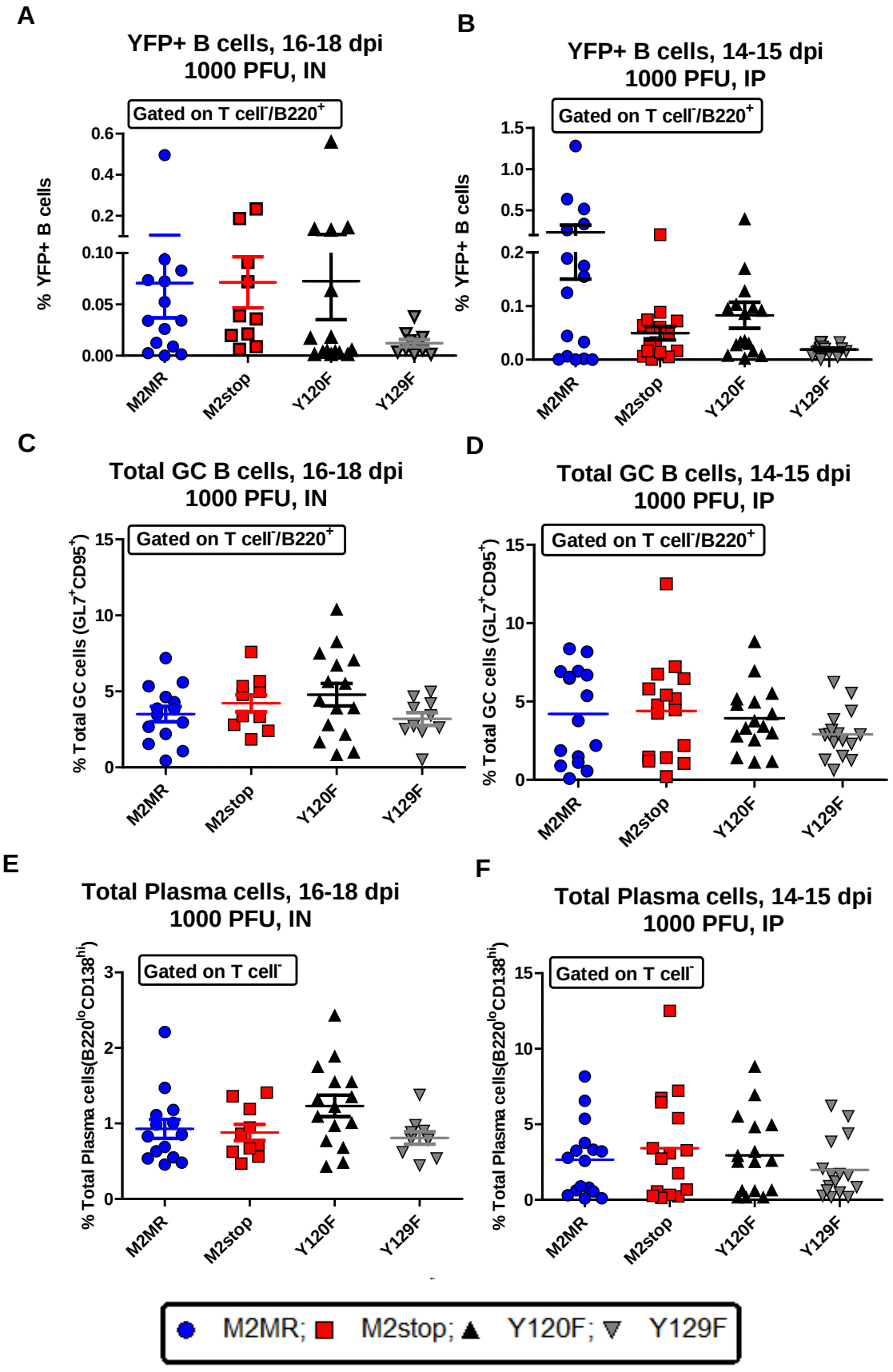
A
YFP+ B cells, 16-18 dpi
1000 PFU, IN
Gated on T cell-/B220+
% YFP+ B cells
M2MR
M2stop
Y120F
Y129F
B
YFP+ B cells, 14-15 dpi
1000 PFU, IP
Gated on T cell-/B220+
% YFP+ B cells
C
Total GC B cells, 16-18 dpi
1000 PFU, IN
Gated on T cell-/B220+
% Total GC cells (GL7+CD95+)
D
Total GC B cells, 14-15 dpi
1000 PFU, IP
Gated on T cell-/B220+
% Total GC cells (GL7+CD95+)
E
Total Plasma cells, 16-18 dpi
1000 PFU, IN
Gated on T cell-
% Total Plasma cells(B220loCD138hi)
F
Total Plasma cells, 14-15 dpi
1000 PFU, IP
Gated on T cell-
% Total Plasma cells(B220loCD138hi)
M2MR; M2stop; Y120F; Y129F

Figure 6

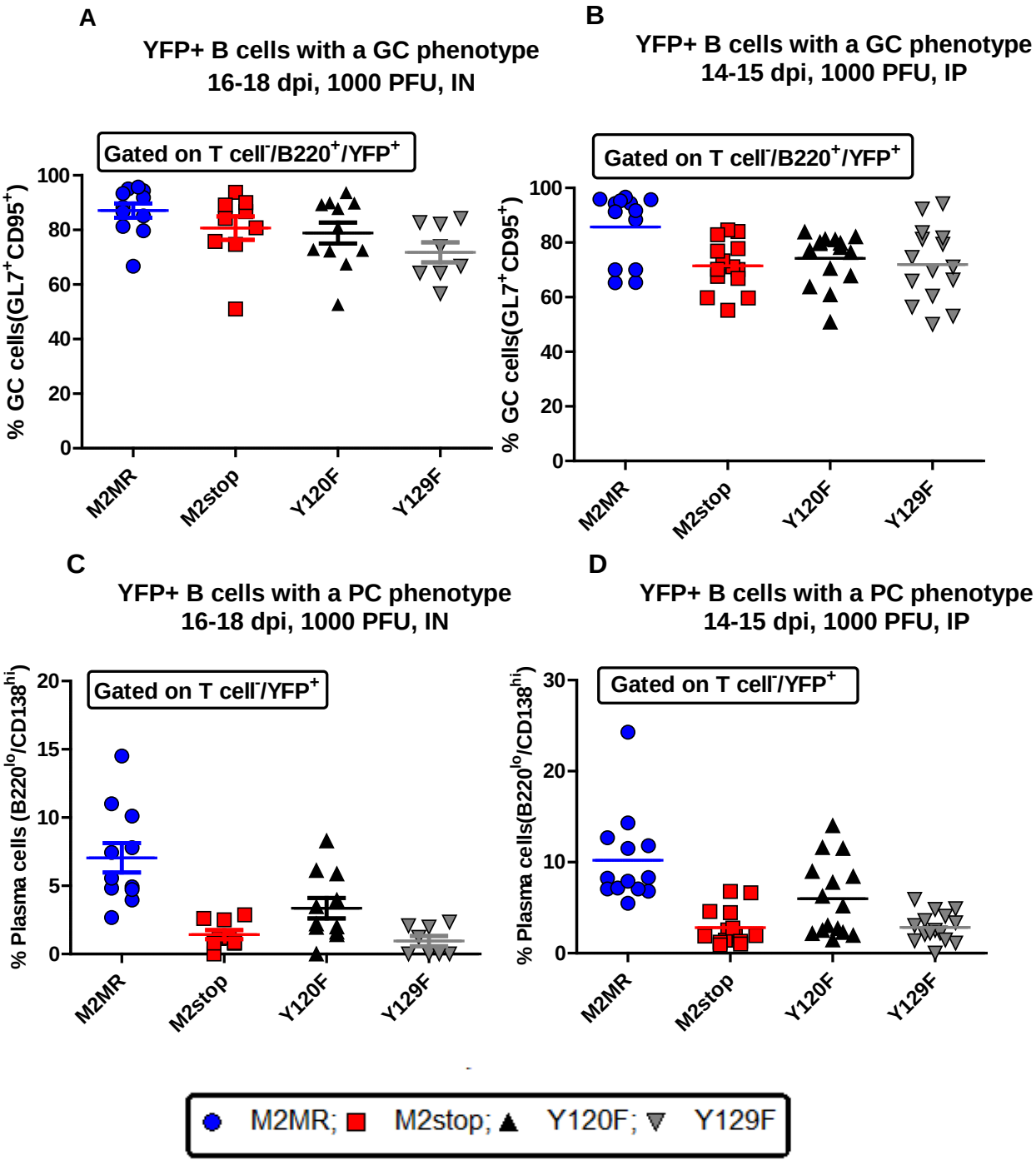
A
YFP+ B cells with a GC phenotype
16-18 dpi, 1000 PFU, IN
Gated on T cell-/B220+/YFP+
% GC cells(GL7+CD95+)
M2MR
M2stop
Y120F
Y129F
B
YFP+ B cells with a GC phenotype
14-15 dpi, 1000 PFU, IP
Gated on T cell-/B220+/YFP+
% GC cells(GL7+CD95+)
C
YFP+ B cells with a PC phenotype
16-18 dpi, 1000 PFU, IN
Gated on T cell-/YFP+
% Plasma cells (B220lo/CD138hi)
D
YFP+ B cells with a PC phenotype
14-15 dpi, 1000 PFU, IP
Gated on T cell-/YFP+
% Plasma cells(B220lo/CD138hi)
M2MR; M2stop; Y120F; Y129F

FIGURE LEGENDS

Figure 1. Y120 and Y129 of M2 are required for expansion of primary murine B cells and for IL-10 production. (A and B) Primary murine B cells were transduced with retroviral vectors encoding Y120F or Y129F mutations of M2, wild type M2 or M2stop as a negative control. On days 2-5 post transduction, the cells were analyzed by (A) flow cytometry to monitor Thy1.1 expression, and (B) the supernatants from cells in (A) were analyzed for IL-10 secretion by ELISA. (C) 1-2x10^6 cells each of the Y120F or Y129F inducible cell lines described in materials and methods were induced with doxycycline for 48 hours and supernatants were harvested for measurement of IL-10 secretion by ELISA. Data shown represents one experiment with at least three replicates. Each experiment was done at least twice with at least three independent replicates per experiment.

Figure 2. M2 induced IL-10 signals through positive feedback involving STAT3, but not STAT1 or STAT5. (A-F) Primary B cells from either wild type C57BL6 (B6) mice or IL10-/- mice (as indicated) were transduced with retroviral vectors encoding either M2 or M2stop. On days 2 and 3 post transduction, the cells were analyzed by phosphoflow as described in materials and methods. (A) B cells from B6 or IL10 -/- mice transduced as mentioned above were analyzed for pSTAT3 levels after gating on live cells by forward and side scatter characteristics. Representative histograms of pSTAT3 levels, one each on day 2 and day 3 are shown. (B) Mean Fluorescent Intensities (MFIs) of pSTAT3 fluorescence from average of three independent replicates are shown for each condition shown in A. (C-D) B cells from B6 mice transduced as mentioned above were analyzed for pSTAT1 or pSTAT5 levels, respectively. Positive control for pSTAT1 induction is IFNγ treatment of cells at 100ng/mL for 15 minutes and positive control for pSTAT5 induction is treatment of cells with GM-CSF at 100ng/mL for 15 minutes. Representative histogram from day 2 post-transduction for each condition is shown. (E-F) Mean Fluorescent Intensities (MFIs) of pSTAT1 or pSTAT5 fluorescence from average of three

independent replicates are shown for each condition shown in C and D. The experiments were done at least three times with three replicates in each experiment.

Figure 3. Y120F and Y129F do not induce pSTAT3 levels. (A-B) Primary B cells from wild type C57BL6 (B6) mice were transduced with retroviral vectors encoding either Y120F, Y129F, wild type M2 or M2stop. On days 2 and 3 post transduction, the cells were analyzed by phosphoflow as described in materials and methods. (A) B cells from B6 mice transduced as mentioned above were analyzed for pSTAT3 levels after gating on live cells by forward and side scatter characteristics. Representative histograms of pSTAT3 levels, one each on day 2 and day 3 are shown. (B) Mean Fluorescent Intensities (MFIs) of pSTAT3 fluorescence from average of three independent replicates are shown for each condition shown in A.

Figure 4. M2 requires Y129, but not Y120, for efficient establishment of latency and reactivation from latency in splenic B cells. (A-D) C57BL6 mice were infected with 1000PFU of the indicated virus either intranasally (A-B) or intraperitoneally (C-D) and splenocytes were harvested at indicated time points. (A and C) The frequency of splenocytes harboring viral genomes were estimated by a limiting dilution, nested PCR assay as described in materials and methods. (B and D) The frequency of splenocytes reactivating virus in a limiting dilution *ex vivo* assay were analyzed on days 14-21 post plating, as described in materials and methods. For IN experiments (A and B), mice were harvested on 16-18 dpi and for the IP experiments (C and D) mice were harvested on 14-15 dpi. For the *ex-vivo* reactivation assay (B and D), intact cells were serially diluted and plated on a MEF monolayer alongside mechanically disrupted cells (as a measure of preformed infectious virus present), as described in materials and methods. The level of preformed infectious virus was below the limit of detection in the above experiments and is therefore not shown in the figures. Results shown in panels A and C are from 3 individual experiments with 3-5 mice per group. Results shown in panels B and D are from 4 individual experiments with 3-5 mice per group.

Figure 5. Infections with Y120F or Y129F mutant viruses do not have an effect on the total number of germinal center B cells or plasma cells. (A-F) C57BL6 mice were infected with 1000PFU of the indicated virus either intranasally (A, C and E) or intraperitoneally (B, D and F) and splenocytes were harvested at indicated time points. Splenocytes were stained for flow cytometry as described in materials and methods. (A and B) Mice were harvested at the indicated time points after either IN (A) or IP (B) inoculation. Splenocytes were analyzed for expression of YFP positive B cells after gating out doublet cells, followed by gating on T cell$^-$ (a mix containing CD3, CD4 and CD8 antibodies to gate out T cells) and B220$^+$ cells. Data shown represents the frequency of T cell$^-$/B220$^+$/YFP$^+$ cells. (C -F) Splenocytes were stained as above for determining the frequency of total number of cells with a germinal center phenotype, defined as T cell$^-$/B220$^+$/CD95$^+$GL7$^+$ cells in panel C and D or, total number of cells with plasma cell phenotype, defined as T cell$^-$/B220^{lo}CD138^{hi} cells in panel E and F. Each data point refers to an individual mouse and the plots depict total mice from 3-4 experiments with 3-5 mice per group per experiment.

Figure 6. Y129, but not Y120, of M2 is required for differentiation of infected B cells to plasma cells. (A-D) C57BL6 mice were infected with 1000PFU of the indicated virus either intranasally (A and C) or intraperitoneally (B and D) and splenocytes were harvested at indicated time points. Splenocytes were stained for flow cytometry as described in materials and methods. (A and B) Mice were harvested at the indicated time points after either IN (A) or IP (B) inoculation. YFP positive cells with a germinal center phenotype were analyzed as follows- doublet discriminated cells were gated on T cell$^-$ (a mix containing CD3, CD4 and CD8 antibodies to gate out T cells)/B220$^+$/YFP+/CD95$^+$GL7$^+$. Data shown represents the frequency of T cell$^-$/B220$^+$/YFP$^+$ cells that are CD95$^+$GL7$^+$, representing the infected cells with a germinal center phenotype.(C and D) Mice were harvested at the indicated time points after either IN (C) or IP (D) inoculation. YFP positive cells with a plasma cell phenotype were analyzed as follows-

doublet discriminated cells were gated on T cell$^-$ (a mix containing CD3, CD4 and CD8 antibodies to gate out T cells)/YFP+/B220^{lo}CD138^{hi}. Data shown represents the frequency of Tcell$^-$/YFP$^+$ cells that are B220^{lo}CD138^{hi} representing the infected cells with a plasma cell phenotype. Each data point refers to an individual mouse and the plots depict total mice from 3-4 experiments with 3-5 mice per group per experiment.

CHAPTER IV

INTRODUCTION

Gammaherpesviruses belong to the *Herpesviridae* family of viruses and are characterized by their ability to establish a lifelong infection in their hosts. Due to their narrow host tropism, research on the human members of the family is limited to studies in tissue culture models. The human members of this family, namely Epstein Barr virus (EBV) and Kaposi's Sarcoma-Associated herpesvirus (KSHV), have been implicated in several types of lymphoid disorders, thereby warranting an animal model to enable detailed studies on pathogenesis and host-pathogen interactions. Murine gammaherpesvirus68 represents a small-animal model for studying various aspects of gammaherpesvirus biology. Previous studies have highlighted that several genes are conserved between the different members of the family, both functionally and by their location in the genome (reviewed in [212]). Additionally, each member of the family also possesses genes that are specific to that particular member with no sequence homology to other family members. One such gene of MHV68, M2 was identified in a screen of latency associated genes [51] and later shown to be important for establishment of latency, as well as reactivation from latency [20,21,44,213]. Previous studies on M2 have revealed that it acts as a modulator of B cell signaling by inducing the activity of NFAT pathway leading to Interferon Regulatory Factor 4 (IRF4) expression and IL-10 production [58,190]. Consistently, M2 is also required for differentiation of a latently infected cell to become plasma cells, the major reactivation compartment for MHV68 [60].

Suppressor of cytokine signaling (SOCS) proteins and cytokine-inducible SRC homology 2(SH2)-domain-containing proteins (CISs/CISHs) are a family of eight proteins(CIS and SOCS1-SOCS7) that act as negative feedback regulators of cytokine signaling and suppressors of inflammation. They contain a central SH2 domain involved in substrate binding by recognition of

cognate phosphotyrosine motifs, a variable amino-terminal domain and a C-terminal SOCS box domain involved in the ubiquitination of several substrate proteins leading to their degradation (reviewed in [197]). In human monocytes and polymorphonuclear neutrophils (PMNs), IL10 induces the expression of SOCS3 leading to inhibition of IFNγ induced STAT1 activation [199]. *Ding et* al [78,95] showed that SOCS1 and SOCS3, but not SOCS2, are able to partially inhibit IL10-mediated STAT3 activation and proliferative responses. Several viruses such as Influenza A virus, HBV and RSV have known to induce SOCS proteins to inhibit interferon signaling [214-224]. SOCS1 and SOCS3 are the well-studied members of the family and their mechanism of action has been identified in some cases, whereas, the functions and role of SOCS2 have only recently been appreciated. Indeed, it was shown that the major transactivator protein of HIV, Tat, induces SOCS2, leading to deregulation of IFNγ signaling [214].

In this study, we aimed to characterize the gene expression profile of M2 expression in B cells. We also included in our analysis controls that would let us analyze M2-induced IL-10 dependent and IL-10 independent changes. We focus on the IL-10 independent genes in this report, and characterize the role of one such gene, SOCS2.

MATERIALS AND METHODS

Cell lines. M12 and DS10 cells were grown in complete RPMI-1640 (cRPMI) supplemented with 10% FCS, 100 U/mL penicillin, 100 mg/mL streptomycin, 2 mM L-glutamine and 50 mM β-mercaptoethanol. Primary murine B cells were cultured in complete RPMI-1640 along with 10 mM non-essential amino acids, 1 mM sodium pyruvate and 10 mM HEPES. 293T cells were maintained in complete DMEM (Dulbecco's Modified Eagle Medium) medium supplemented with 10% FCS, 100 U/mL penicillin, 100 mg/mL streptomycin and 2 mM L-glutamine. Cells were routinely counted using trypan blue exclusion method.

RNA preparation and Microarray analysis. Primary murine B cells were transduced with pMIT-M2 and pMIT-M2Stop as described in *Rangaswamy et al* [190]. At 3 days post-transduction, total RNA was isolated using Trizol as per manufacturer's instructions and sent to the Emory Biomarker Profiling core at the Winship Cancer Institute. For microarray analyses, RNA was prepared from three independent transductions to generate at least three biological replicates. Quality Control of the RNA was done by analyzing the samples on an Agilent Total RNA Nano Series II Bioanalyzer. RNA Expression was profiled using the Illumina beadchip. The gene expression data was analyzed by SAM (significance Analysis of Microarrays) and GSEA (Gene Set Enrichment Analysis). Pathway analysis was done using Ingenuity Pathway Analysis (IPA). Further functional clustering and gene ontology was done using the publicly available Database for Annotation, Visualization and Integrated Discovery (DAVID).

cDNA preparation and quantitative RT-PCR. RNA was harvested from the primary murine B cells by lysing in TRIzol (Invitrogen) according to the manufacturer's instructions. Three micrograms of RNA was treated with DNase I (Invitrogen), and 3 μg of DNase-treated RNA was reverse transcribed using Superscript II reverse transcriptase (RT) (Invitrogen) according to the

manufacturer's instructions. Minus-RT controls were performed in parallel. 1 uL of the resulting cDNA was subject to either a standard PCR using the following primers: SOCS2, (5'GGA AGT ATG ACT GTT AAT GAA GCC 3'), and (5'CCC AGA TCG TAC CGG TAC ATT 3'); and *GAPDH*, 5′-CCTGCACCACCAACTGCTTAG-3′ and 5′-GTGGATGCAGGGATGATGTTC-5′; The same cDNA was also subject to a quantitative real time PCR (qRT-PCR) using iQ Supermix (Bio-Rad) with the same primers described above. The qRT-PCR was performed in a Becton-Dickinson iCycler and analyzed using Bio-Rad iCycler software. Cycling conditions were as follows: 95°C for 5 min and then 40 cycles at 95°C for 30 s, 55°C for 30 s, and 72°C for 30 s. Data were analyzed using the $\Delta\Delta C_T$ method, where $\Delta\Delta C_T = [C_T(\text{gene}) - C_T(GAPDH)]_{M2} - [C_T(\text{gene}) - C_T(GAPDH)]_{M2stop}$. The data are presented as the evaluation of $2^{-\Delta\Delta}CT$ for each sample, representing the change (*n*-fold) in transcript level of each gene in the treated samples, normalized to the level for GAPDH and relative to the normalized level for that gene in the untreated control [225].

Plasmids and reporter constructs. pGAS-luc reporter plasmid was obtained from (Agilent technologies) as part of the PathDetect Signal Transduction Pathway cis-reporting systems. It contains 4× repeats of a GAS enhancer element sequence upstream of a luciferase reporter gene. pMSCV-M2-IRES-Thy1.1(pMIT-M2) and pMSCV-M2stop-IRES-Thy1.1(pMIT-M2stop) are described [58]. pEF-FLAG/SOCS2 plasmid was a kind gift of Dr.Douglas Hilton (The Walter and Eliza Hall Institute of Medical Research, Australia). pEBG-M2AU1-GST was constructed by PCR amplification of the M2 ORF from pMIT-M2 vector using primers that contain the AU1 tag and inserting the PCR product into pEBG-EV, described by *Liang et al* [53]. Primers used were: M2 (5' GGCGGATTCATGGCCCCAACACCCCCACAAG 3') and (5'GCGGCCGCTTATATATAGC GATAGGTATCCTCCTCG 3').

Immunofluoresecence analysis. DS10 cells were cytospun at 6000 cells per slide. Cells were fixed with 4% formaldehyde in PBS, washed with PBS, permeabilized with 1% Triton in PBS,

and blocked with 0.1% Triton X-100 (TX100) in PBS containing 5% bovine serum albumin (blocking buffer). Primary antibodies used include mouse anti-AU1 (1:200) (Covance) and rabbit anti-SOCS2 (1:100) (Abcam). Primary antibodies were diluted in blocking buffer and incubated at room temperature for 1 hour on a rocking platform. The slides were then washed in PBS for 30 minutes followed by incubation with secondary antibodies for 1 hour at room temperature. Secondary antibodies used include chicken anti-mouse Alexa 647 at 1:1000 and goat anti-rabbit Alexa 568 at 1:1000 (Molecular Probes, Invitrogen). The cells were washed three times in PBS prior to mounting with Prolong antifade reagent with DAPI (Invitrogen). Images were collected on a Zeiss Axiovert 200 M fluorescent scope using Axiovision imaging software.

Co-immunoprecipitations. For co-immunoprecipitation experiments, 293T cells were co-transfected with the indicated plasmids in 10cm dishes using the TransIT-293 reagent (Mirus Bio LLC).Forty-eight hours post transfection, lysates were prepared by lysing in1.1 mL of lysis buffer containing 50 mM Tris-HCl,150 mM NaCl,1 mM EDTA and 0.1% TritonX-100 supplemented with Complete mini-EDTA-free protease inhibitor tablet (Roche) and 1 mM NaF and 1 mM Na_3VO_4.and shearing with a 20G needle. After clearing by centrifugation at 4°C, 0.1 mL was saved for whole cell lysate analysis, and the remaining 1 mL lysate was incubated overnight at 4°C with anti-FLAG (M2) agarose beads (Sigma) to pull down FLAG tagged SOCS2 or with anti-AU1 sepharose beads (Covance) to pull down AU1 tagged M2. Beads were washed according to manufacturer's instructions, and then separated on 10% SDS-PAGE gel and transferred to nitrocellulose. Blots were probed with either mouse anti-AU1 (Covance) or rabbit anti-SOCS2 (Invitrogen). Secondary antibodies used were donkey anti-mouse or donkey anti-rabbit at 1:5000 (Jackson immunoresearch).

Transfections and reporter assays. $1–1.5\times10^6$ of the indicated cells were centrifuged, washed once with PBS and resuspended in 100 µL of Ingenio electroporation solution (MirusBio) or solution L (Lonza). Triplicate wells were used per condition. 5 µg reporter DNA prepared using

Qiagen endofree maxiprep kit was added to the electroporation mixture and nucleofected using Amaxa Nucleofector I system. Forty eight hours after transfection, the cells were pelleted by centrifugation, washed with PBS and lysed using Promega passive lysis buffer. Lysates were clarified, and luciferase activity was determined using luciferase reporter assay kits (Promega). Luciferase activity was measured using a Turner Designs 2000 luminometer.

Statistical analysis. Statistical data analysis was performed using GraphPad Prism software. Data shown represents one of at least triplicate experiments. Error bars represent standard error mean. Significance was determined by two-tailed, unpaired Student's t-test with a confidence level of 95%.

RESULTS

Gene Expression profile of M2 expression in B cells.

While the signaling mechanism(s) involved in the induction of IL-10 has been explored in detail, there are no reports on the analysis of global changes in gene expression upon M2 expression. As a first step towards this, we initiated a gene expression study by performing microarray analysis on primary murine B cells transduced with retroviruses encoding M2 or M2stop. To identify changes in gene expression that lead to M2 dependent functions described in *Siegel et al* [58], microarray analysis was performed in primary murine B cells. We have previously reported a retroviral transduction assay of primary murine B cells with retroviruses expressing M2 or M2stop (a negative control construct that contains a translational stop codon at amino acid 13 or M2 ORF). Using this assay, we have shown that M2 expression induces significant levels of IL-10 in culture supernatants [58,190]. Therefore, we used this system to look at changes in cellular gene expression upon M2 expression. On day 3 post-transduction, total RNA was isolated from the following four conditions: (1) C57/B6 WT B cells transduced with M2, (2) C57/B6 WT B cells transduced with M2stop, (3) IL10 -/- B cells transduced with M2 and (4) IL10 -/- B cells transduced with M2stop. The IL10-/- B cell transductions were used as controls to exclude any changes in gene expression resulting from endogenous IL-10 present in the cells. As shown in Figure 1, the numbers in the bars above the Venn diagram refer to the experimental condition as described above, while the numbers within the circles refer to the number of genes differentially regulated in each comparison. We used the following strategy to narrow down the list of genes that were differentially regulated - only the genes that were differentially regulated in the comparisons between conditions (1 vs 2) and (3 vs 4) were further evaluated53 genes were differentially regulated by M2 in both the WT and in IL10-/- B cells in an IL-10 independent manner.

SOCS2 is highly up regulated upon M2 expression in B cells.

The final 49 genes, which we termed as ‘core’ genes, were further analyzed by using Database of Annotation, Visualization and Integrated Discovery (DAVID) software to determine the functional annotations for this set of genes. Not surprisingly, as shown in Figure 2, most of these genes belonged to a functional cluster related to “cytokine activity” group and the top 2 up regulated genes were SOCS2 and CISH - both belonging to the SOCS (suppressors of cytokine signaling) family. The results from the microarray data were validated using quantitative RT-PCR to determine the fold change in the expression levels of murine SOCS2 transcripts. Total RNA was isolated from primary murine B cells transduced with retroviral vectors encoding either M2 or M2stop, and cDNA was generated. Since the microarray was done at one time point, namely day 3 post-transduction, we wanted to determine if there was a trend in the levels of SOCS2 with time post transduction. Therefore cDNA from days 2, 3 and 4 post-transduction were used to PCR murine SOCS2 transcripts. As shown in Figure 3A, there appears to be an increase in the levels of SOCS2 transcript levels (the amount of cDNA used as template in the PCR is kept constant in the different time points). To obtain quantitative levels of transcripts, the same cDNA from Figure 3A was subjected to quantitative RT-PCR(qRT-PCR) using primers for SOCS2 and cycle conditions in From the qRT-PCR results shown in Figure 3B, there is a significant increase in the levels of SOCS2 transcripts on days 3 and 4 compared day 2 post transduction. The glyceraldehyde-3-phosphate dehydrogenase (GAPDH) gene was used as a control in Figure 3A to validate that the RNA levels of a house-keeping gene remained constant at each time point. In Figure 3B, results are plotted as fold change in SOCS2 transcript level relative to GAPDH expression. Taken together, this data demonstrates that SOCS2 transcripts are up-regulated in primary murine B cells upon M2 expression, consistent with the results from the microarray analysis.

M2 interacts with and co-localizes with SOCS2.

SOCS2 belongs to the SOCS family of proteins involved in negatively regulating cytokine signaling that contain SH2 binding domains, which are high affinity binding sites for phosphorylated tyrosine residues. Interestingly, M2 contains two tyrosine residues at positions 120 and 129 which are

functionally important *in vivo* and have been shown to be phosphorylated constitutively in B cells [57,64]. Therefore we hypothesized that M2 could directly interact with the SOCS proteins *via* its phosphorylated tyrosines to modulate signaling pathways that are primarily (but not exclusively) IL-10 independent. To assess this possibility, we tested whether M2 interacts directly with SOCS2 using immunoprecipitation methods. AU1-tagged M2 was co-expressed with a FLAG-tagged SOCS2 (kindly provided by Dr.Doug Hilton, WeHI) in 293T cells. M2 was immunoprecipitated from total cell lysates using AU1 beads and bound SOCS2 was detected using anti-SOCS2 antibody (shown in Figure 4A). Using lysates from the same experiment, we immunoprecipitated SOCS2 by using FLAG beads, and immunoblotted for M2 using anti-AU1 antibody (Figure 4B). These results indicate that M2 interacts with SOCS2. Whole cell lysates were run alongside on these blots to confirm expression of both SOCS2 and AU1 in the respective blots. Given that M2 interacts with SOCS2, we further wanted to investigate whether M2 can co-localize with SOCS2 in B cells. To test this, we utilized an M2 inducible B cell line, DS10 that we have previously reported [190], that expresses M2 only upon induction with doxycycline. . We used this system to evaluate levels of SOCS2 expression upon M2 expression. As shown in Figure 4C, there was no M2 or SOCS2 expression in the absence of doxycycline induction. Upon doxycycline induction, we detected both M2 and SOCS2 in the B cells and they appear to co-localize in the cytoplasm outside of the nucleus.

SOCS2 expression inhibits IFNγ in B cells independent of IL-10.

The HIV gene product, Tat (transactivator protein), is a potent transactivator protein required in HIV replication [226]. In peripheral blood monocytes, Tat induced SOCS2 expression which resulted in inhibition of interferon γ (IFNγ) signaling [214]. It has previously been reported that LPS induction of SOCS3 in macrophages results in suppression of IFNγ signals via inhibition of STAT1 activation [227]. Given the requirements of SOCS family members in inhibition of interferon signaling in macrophages and monocytes, we wanted to test if this was true in B cells as well. To do this, we transfected the pGAS-luc reporter plasmid that contains 4X repeats of the interferon γ-activated

sequence (GAS) that drives luciferase expression. The B lymphoma cell line M12 was co-transfected with the pGAS-luc vector along with a SOCS2 expression plasmid. IFNγ added at 1000U/mL served as a positive control for reporter activity. As shown in Figure 5A, in the presence of IFNγ at 1000U/mL, there was a significant increase in the luciferase activity. However, upon SOCS2 expression, IFNγ mediated luciferase activity was inhibited to levels similar to that of the untreated controls. IL-10 has been shown to inhibit IFNγ production from T cells and macrophages [107,108,228]. Since SOCS proteins regulate a wide variety of cytokines and because M2 induces high levels of IL-10 [58], we wanted to make sure that the inhibition of IFNγ signaling (measured by GAS-reporter activity) was not IL-10 dependent. Therefore, we performed the GAS reporter assay in the presence of exogenous IL-10. To make sure the amount of IL-10 is not a factor, we included 10-fold ranges of IL-10 from (0.01 ng/mL up to 10ng/mL). As shown in Figure 5B, IL-10 did not affect GAS reporter activity at any of the concentrations added. It is to be noted that the highest concentration of IL-10 used, at 10ng/mL is almost 10 times physiological levels in the serum of humans or mice [229,230].Taken together, our data shows that SOCS2 can inhibit IFNγ signaling in B cells, in an IL-10 independent manner.

DISCUSSION

M2 induces the production of IL-10 in primary murine B cells, B cell lines and *in vivo* in serum from infected mice [58,190,231]. Additionally, M2 expression led to the increased levels of IL-2, MIP-1α, IL-6, and IgG, as well as differentiation to a pre-plasma memory B cell phenotype [58]. Therefore, M2 seems to manipulate other cellular pathways that ultimately synergize with IL-10 signaling, resulting in the observed increased proliferation, survival and differentiation of these B cells. Identifying the changes in cellular signaling in response to M2 induction requires an unbiased analysis of changes in the patterns of cellular gene, as well as mapping changes in post-translational modifications (e.g., phosphorylation) of cellular proteins involved in signal transduction. In this study we aimed to study changes in the gene expression profile of M2 expressing primary B cells. As shown in Figure 1, the number of genes differentially regulated between conditions 1 vs 2 (1321 genes) is striking compared to the number of genes differentially regulated between conditions 3 vs 4 (84 genes). This suggests that M2 mediated functions in the primary B cells are primarily IL-10 dependent and only a small subset of genes are IL-10 independent.

As depicted in Figure 4, the data showing M2 interaction with SOCS2 is of great interest. Since the tyrosine residues at positions 120 and 129 in M2 are targets for phosphorylation, it is highly likely that M2 interaction with SOCS2 likely occurs via interaction of a tyrosine(s) with the SH2 domains of SOCS2 - perhaps redirecting the functions of these cellular regulators to alter cytokine or other signaling pathways. Indeed, it has been previously shown that M2 expression down regulates the levels STAT2 (and in some cases, STAT1) - leading to inhibition of interferon signaling [53]. Further studies will be done to address the domain(s) in SOCS2 and M2 required for this interaction. Particularly, SOCS2 was shown to bind SOCS3 leading to its degradation via a proteasome dependent manner [232], raising a speculation that SOCS2 mediates degradation of other SOCS family members that are being recruited to inhibit cytokine signaling induced by M2.

This would offer new insights into the studies of cytokine signaling where multiple SOCS family members are being activated simultaneously in response to different signals.

Our finding that SOCS2 transcripts were highly up regulated in M2 expressing B cells, although counter intuitive to the fact that M2 leads to increase in a number of cytokines, namely IL-10, provides new insights into the role of SOCS proteins in B cells. To date, there are no reports on the role of SOCS2 in B cells, except one study where SOCS2 was induced in B cells upon treatment with 2,3,7,8-tetrachlorodibenzo-*p*-dioxin (TCDD), a xenobiotic compound, by activation of the SOCS2 promoter [233]. It has also been suggested that SOCS2 possesses dual roles in cytokine signaling, capable of inhibiting as well as enhancing cytokine production. Consistently mice that either overexpress SOCS2 or lack SOCS2 have a gigantism phenotype [232,234,235], due to deregulated signaling of the growth hormone. The finding that SOCS2 can inhibit IFNγ signaling in B cells coupled with the results that M2 can interact with SOCS2 suggests that perhaps the interaction with M2 and SOCS2 plays a role in IFNγ signaling. F. Our data suggests a model wherein, in the context of infection, M2 mediated SOCS2 acts to antagonize the effects of IFNγ produced by cell types such as macrophages, NK cells and T-cells, in an IL-10 independent manner (Figure 6). Consistently, IFNγ levels were elevated in a LPS treated *in vitro* culture of peritoneal macrophages from SOCS2-/- mice [236].

The studies of SOCS2 on IFNγ signaling are currently unclear. Song et al reported that in HeLa cells, SOCS1 and SOCS3 are capable of inhibiting IFN mediated STAT1 activation, as measured by pSTAT1 levels by western blotting. However, they failed to observe any effect of SOCS2 overexpression on activation of STAT1 [237]. It is possible that the discrepancy with our results is reflective of the cell type used (murine B cells vs human epithelial cells), and perhaps the read out of IFNγ signaling. It is to be noted that our results measure IFNγ signaling by the ability of SOCS2 to activate a GAS reporter construct whereas, in the other study, STAT1 activation was measured as an output of IFNγ signal. It is to be noted that type I interferons

namely, IFNα and β also act via STAT1 and hence measurement of STAT1 activation is not specific to IFNγ signal (reviewed in [238]). As such, it is important to consider the cross-talk which occurs between the interferon family members while drawing general conclusions on the roles of SOCS family members.

Our data is consistent with a report showing SOCS2 mediated inhibition of IFNγ signaling done in HEK293 cells using a 8XGAS-reporter construct[214]. Notably, both the systems, namely, using a GAS reporter activity as well as using STAT1 activation status are indirect measures of IFNγ signaling and requires further characterization. Therefore, to gain a deeper understanding of SOCS2 mediated inhibition of IFNγ signaling, additional experimental setups that include as the use of IFNγR-/- B cells or measuring downstream IFNγ gene targets such as IRF -1, is required[239]. Interestingly KSHV encodes several viral IRF molecules which target the cellular interferon pathways (reviewed in [240]) and one particular member, vIRF3 is shown to inhibit IFNγ activity to modulate MHC II expression [241].

In conclusion, this study gives a brief description of the changes in gene expression mediated by MHV68 M2 in primary murine B cells. We also demonstrate increased levels of a negative regulator of cytokine signaling, namely SOCS2 upon M2 expression, and that M2 can interact with SOCS2. We also define, for the first time, a role for SOCS2 in inhibition of IFNγ signaling in B cells. Further studies on the functional outcome of these interactions and signaling events will provide valuable insights into mechanisms of regulation of the interferon response to virus infections.

FIGURES

Figure 1

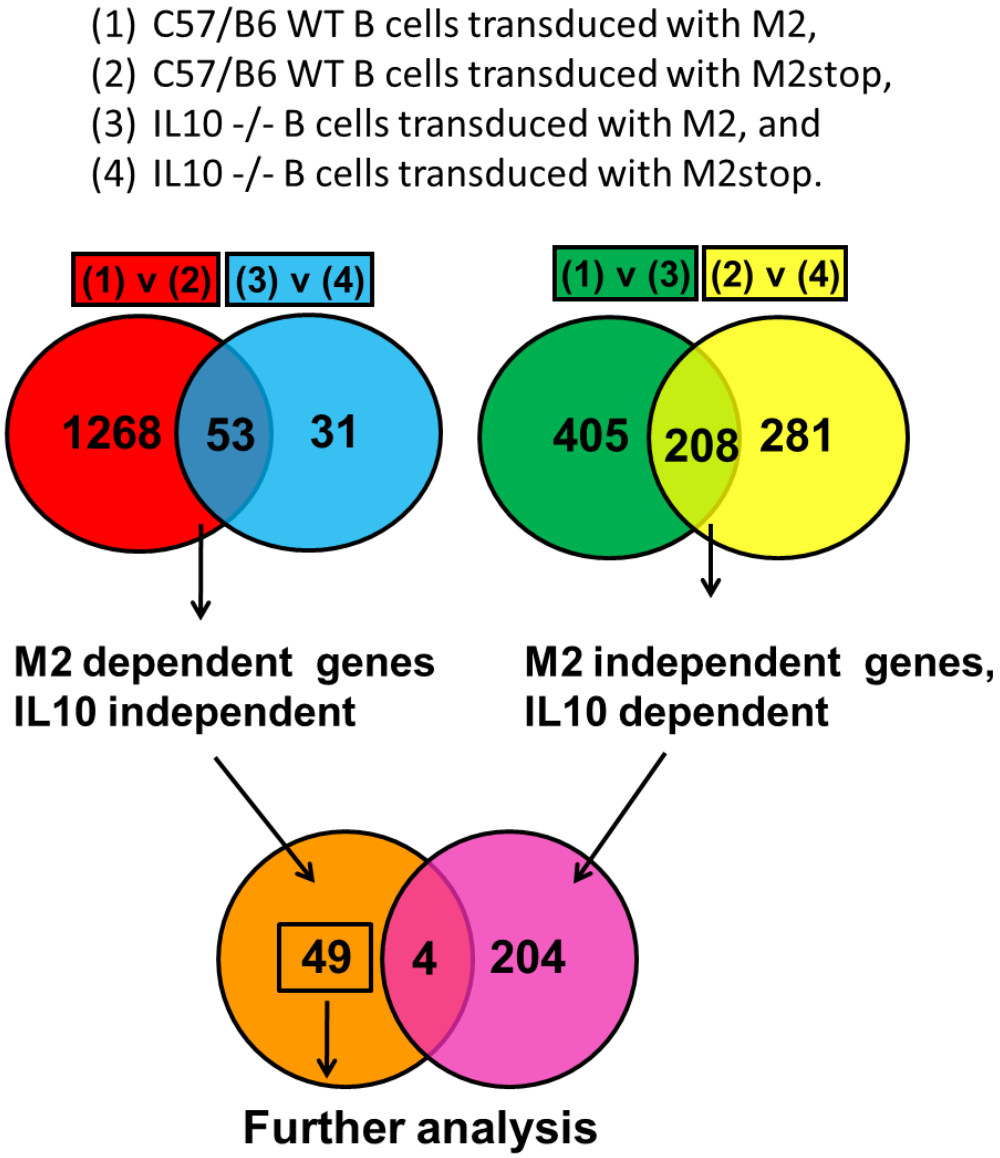

Figure 2

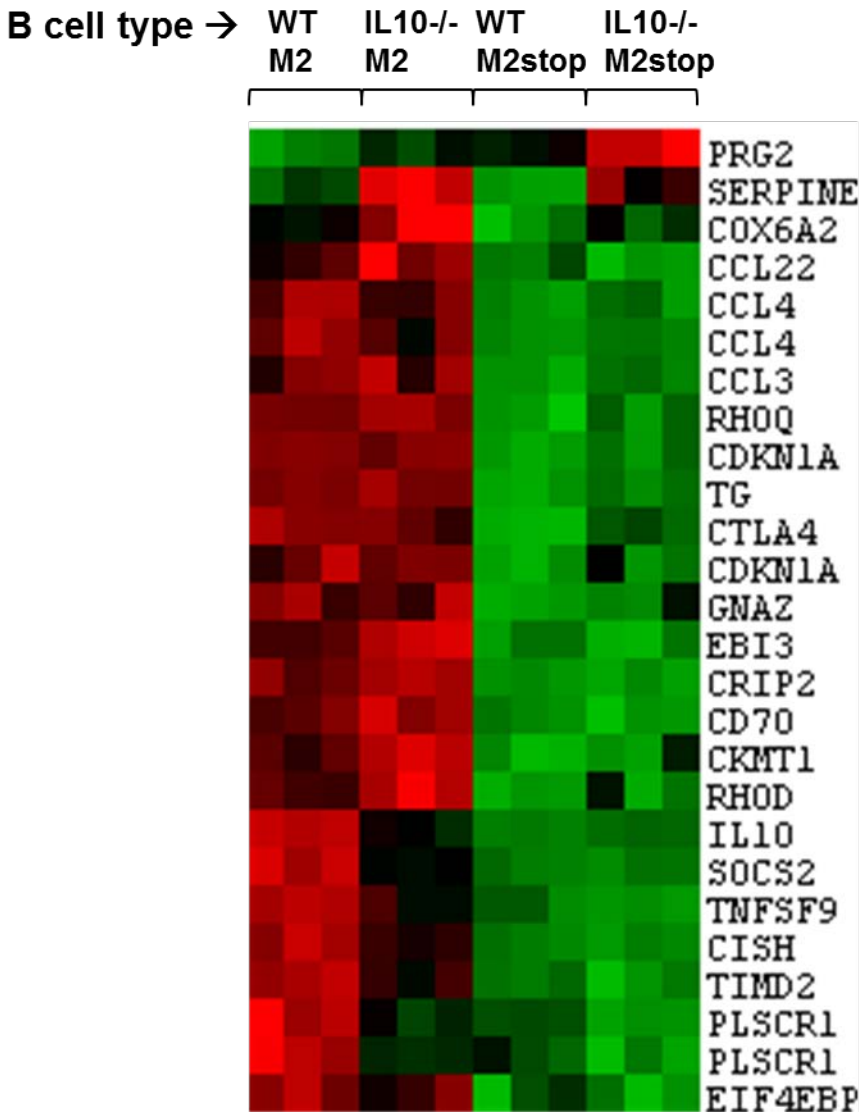
B cell type →
WT M2
IL10-/- M2
WT M2stop
IL10-/- M2stop
PRG2
SERPINE
COX6A2
CCL22
CCL4
CCL4
CCL3
RHOQ
CDKN1A
TG
CTLA4
CDKN1A
GNAZ
EBI3
CRIP2
CD70
CKMT1
RHOD
IL10
SOCS2
TNFSF9
CISH
TIMD2
PLSCR1
PLSCR1
EIF4EBP

Figure 3

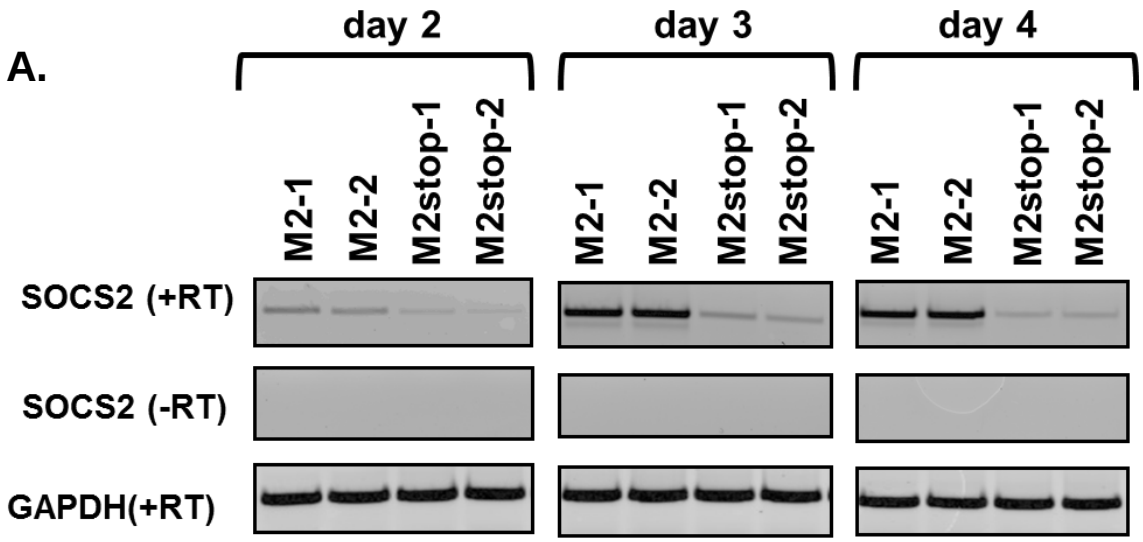
A.
day 2
day 3
day 4
M2-1
M2-2
M2stop-1
M2stop-2
SOCS2 (+RT)
SOCS2 (-RT)
GAPDH(+RT)

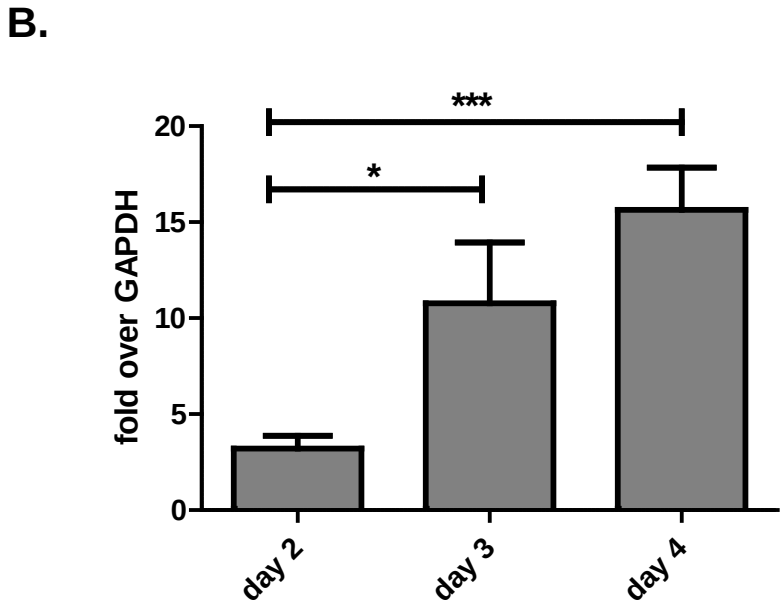
B.
***
*
20
15
10
5
0
fold over GAPDH
day 2
day 3
day 4

Figure 4

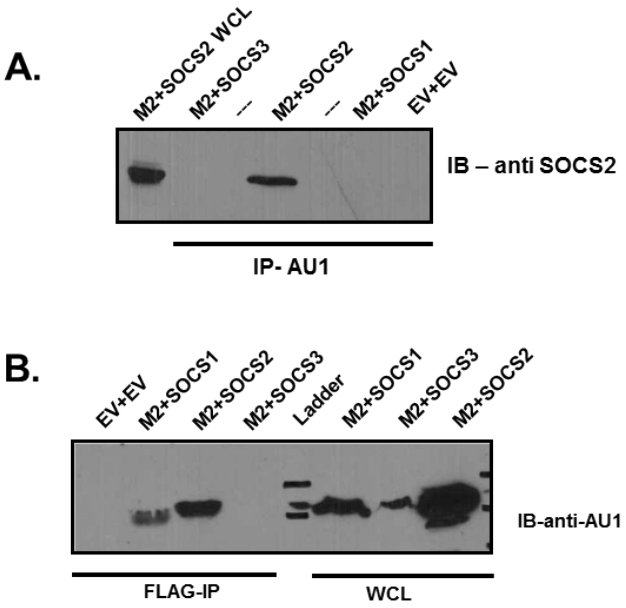
A.
M2+SOCS2 WCL
M2+SOCS3

M2+SOCS2

M2+SOCS1
EV+EV
IB – anti SOCS2
IP- AU1
B.
EV+EV
M2+SOCS1
M2+SOCS2
M2+SOCS3
Ladder
M2+SOCS1
M2+SOCS3
M2+SOCS2
IB-anti-AU1
FLAG-IP
WCL

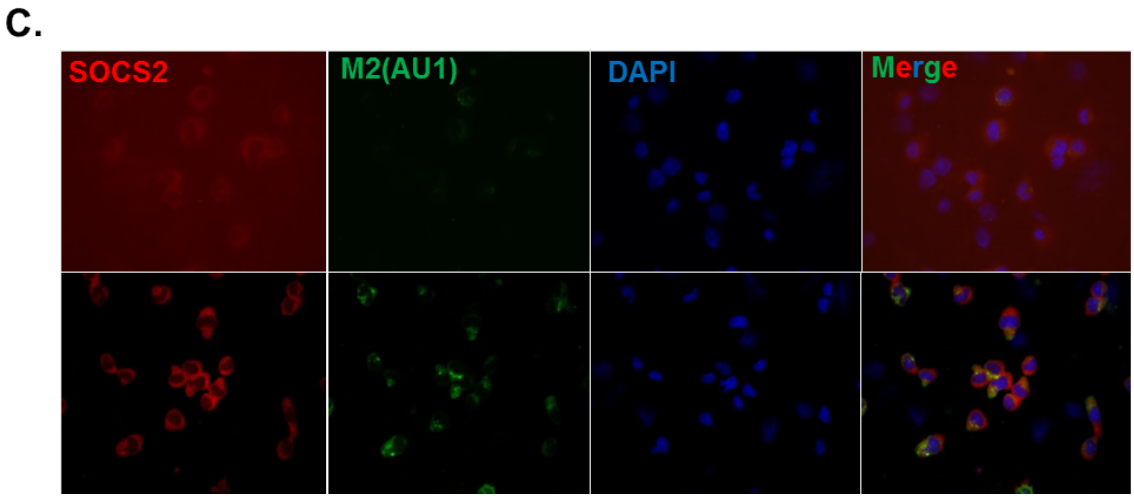
C.
SOCS2
M2(AU1)
DAPI
Merge

Figure 5

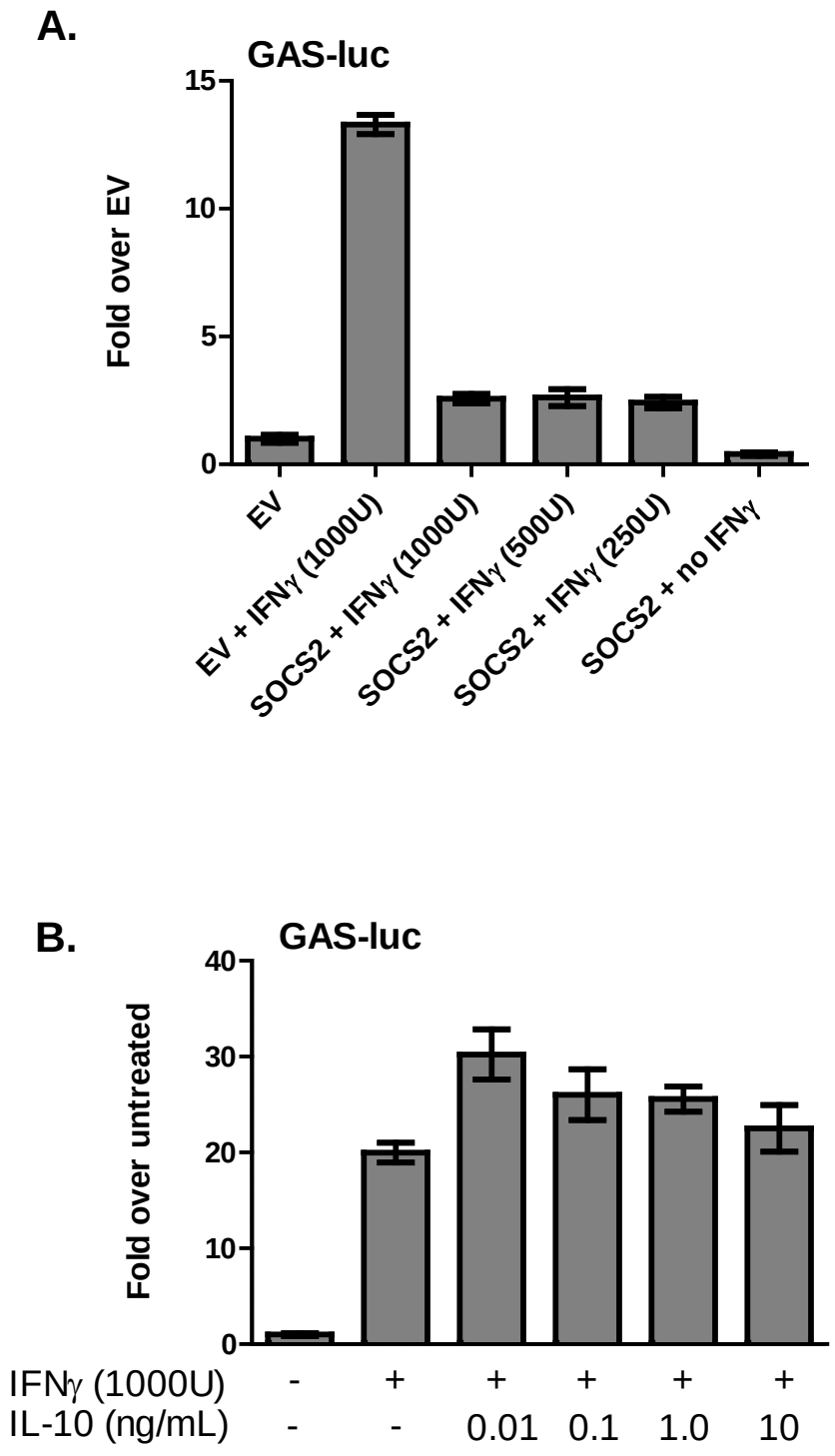
A.
GAS-luc
Fold over EV
15
10
5
0
EV
EV + IFNγ (1000U)
SOCS2 + IFNγ (1000U)
SOCS2 + IFNγ (500U)
SOCS2 + IFNγ (250U)
SOCS2 + no IFNγ
B.
GAS-luc
Fold over untreated
40
30
20
10
0
IFNγ (1000U) - + + + + +
IL-10 (ng/mL) - - 0.01 0.1 1.0 10

Figure 6

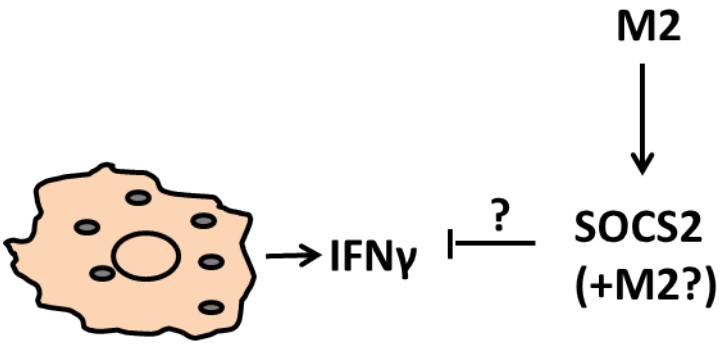

FIGURE LEGENDS

Figure 1. Venn Diagram analysis of differentially regulated genes. Summary of the microarray analyses of M2 expression in WT and IL10-/- cells. The venn diagram analysis was used to narrow down on genes that are IL-10 independent.

Figure 2. Genes that belong to the gene cluster 'cytokine activity'. The genes in Figure 1 were analyzed in DAVID software. Functional clustering of the top scoring genes in the cytokine activity group by DAVID is shown.

Figure3. SOCS2 is upregulated in M2 transduced cells. To confirm the microarray data, reverse transcriptase PCR and quantitative real time PCR were performed. (A and B) RNA from either pMIT-M2 or pMIT-M2stop transduced B cells were prepared by lysing in TRIzol. cDNA prepared was prepared using reverse transcriptase as described in materials and methods and subject to (A) standard PCR or (B) quantitative real time PCR.

Figure 4. M2 interacts with SOCS2. (A and B) 293T transfected with M2 and SOCS2 expression plasmids were immunoprecipated and immunoblotted for the indicated proteins. EV refers to an expression construct lacking either M2 or SOCS proteins. (C) DS10 cells that express M2 upon dox induction were either left untreated (top panel) or treated with 500ng/mL of Dox to induce M2 expression for 48 hours. Immunofluorescence was done as described in materials and methods. Images were collected at a magnification of 400X.

Figure 5. SOCS2 inhibits IFNγ activity in an IL-10 dependent manner. (A) M12 cells were transfected with pGAS luc reporter vector and a SOCS2 expression vector in the presence or absence of IFNγ. Luciferase data is represented as fold over empty vector. (B) M12 cells were transfected with pGAS luc reporter vector in the presence or absence of IFNγ and/or IL-10 at the indicated amounts. Luciferase data is represented as fold over untreated cells.

Figure 6. Model of SOCS2 function. M2 expression results in the expression of SOCS2, made in an IL-10 independent manner. SOCS2 acts to inhibit IFNγ signaling, potentially coming from sources other than B cells. In doing so, M2 is able to inhibit the anti-viral state thereby capable of establishing an efficient latency in the B cells.

CHAPTER V

SUMMARY, FUTURE DIRECTIONS AND CONCLUSIONS

Using the MHV68 mouse model of infection as a tool to study gammaherpesviruses has proven highly successful in the field of gammaherpesvirus biology. Sequence homology of several MHV68 genes with their counterparts in the human herpesviruses has revealed the functional roles of such genes in gammaherpesvirus biology. Perhaps this is best exemplified in the studies on the latency associated nuclear antigen (LANA). The *in vivo* role of the episomal maintenance protein mLANA has been widely studied in MHV68, whereas available data from kLANA (the ortholog in KSHV) relies on *in vitro* biology [45,179,225,242-247]. However, it is important to bear in mind those genes that are unique to each family member which may not possess sequence homology but elicit functions that are reminiscent of functions of unique or conserved genes in the human herpesviruses. In this dissertation, we have shown that one such unique gene of MHV68, M2, possesses functional similarities to signaling proteins in the human herpesviruses EBV and KSHV (described below).

Mechanism of M2 induction of IL-10

Previous studies on the functions of M2 in mediating IL-10 production [58] and in plasma cell differentiation leading to reactivation of MHV68 [60], left unresolved questions that could only be answered upon a careful investigation into the mechanisms of B cell signaling mediated by M2. Several biochemical studies have attempted to answer this, but thus far, a clear picture is yet to emerge. As a first step towards answering this question, we attempted to create a B cell line model that recapitulates some aspects of M2 functions, namely induction of IL-10 and IRF4 protein. We successfully did this by creating an inducible cell line system that expresses M2 in a tightly regulated manner using the tetON inducible cell systems. Employing this system, in

Chapter 2 of this thesis, we have described the molecular pathway involved in mediating IL-10 induction by M2.

We demonstrated that inducible M2 expression in a B cell line designated DS10, leads to activation of the NFAT pathway. Activation of the NFAT pathway was dependent upon Src kinase activity as well as extracellular calcium flux, as determined by utilizing chemical inhibitors that block Src kinases or extracellular calcium influx, respectively. We also show that M2 mediated activation of the NFAT pathway was inhibited by traditional pharmacological inhibitors of the pathway, namely cyclosporine and FK506. Furthermore, we showed that M2 induction of IRF4, a plasma cell associated transcription factor, is dependent, at least partially on the activation of the NFAT pathway. In this work, we also discovered a novel role for IRF4 in IL-10 production in B cells by demonstrating that IRF4 can activate cis-elements in the IL-10 gene locus to directly increase IL-10 promoter activity and subsequent increase in IL-10 levels. We show that M2 synergizes with IRF4 in mediating IL-10 promoter activity and IL-10 secretion. In primary murine B cells, inhibition of the NFAT pathway by addition of CsA resulted in decreased levels of IRF4, absence of NFAT protein expression and a significant decrease in IL-10 secretion accompanied by differences in plasmacytic B cell differentiation compared to cells without CsA. Finally, we show that Cre mediated deletion of IRF4 in $IRF4^{fl/fl}$ mice severely compromised establishment of latency as well as reactivation from latency, strongly emphasizing the importance of IRF4 in MHV68 pathogenesis *in vivo*. Conversely, infection of C57BL/6 mice with a M2 null virus resulted in a decreased expression of IRF4 in infected splenocytes, further highlighting the requirement of IRF4 in M2 mediated functions, particularly perhaps in reactivation [190].

The data described in Chapter 2, together with previously published *in vivo* and *in vitro*-derived roles of M2 [20,55,57,58,60,61,64,162,248] reveal that M2 acts as a multi-functional protein uniting various functional aspects of EBV and KSHV, namely LMP-1 induction of IRF4,

IL-10 and CD40 signaling [78,197-200] LMP2a modulation of BCR signaling [77,249-252], EBV encoded vIL-10[96,253] and KSHV K1 activation of the NFAT pathway[85,254]. Given that the signaling capacities of these human herpesviral proteins have extensively been studied, their similarity to M2 warrants some investigation into the roles of these proteins in the progression of disease, particularly in plasma cell differentiation leading to virus reactivation. One approach to pursue this would be to create chimeric viruses where the M2 ORF is replaced with either LMP-1, LMP-2a, vIL-10 or K1 and looking at the ability of these chimeric viruses in undergoing plasma cell differentiation and reactivation.

This study leads to several future questions. One primary line of investigation would be the analysis of M2 expression *in vivo*. While M2 is known to be present in latently infected splenocytes *in vivo* during infection, the particular B cell subset that expresses M2 is still unknown. We have previously characterized a recombinant eYFP expressing virus and an H2bYFP expressing virus, both capable of marking infected splenocytes *in vivo* [180,210]. The advantage of using the MHV68-H2bYFP is that we can identify infected splenocytes not only by flow cytometry, but also by staining spleen sections by immunofluorescence. Therefore, a virus that expresses the H2bYFP protein (or any other fluorescent protein) driven by the endogenous M2 promoter would readily allow is to track the cell populations that express M2. As an extension of this, a dually fluorescent virus, where a RFP (or mCherry) expression cassette drives M2 expression made in the background of the MHV68-H2bYFP virus would be even more useful in identifying the subpopulations within the YFP infected cells that are expressing M2. Indeed, this line of research is currently being pursued in our lab. This would greatly aid in identifying the exact timing and location of M2 expression in the viral lifecycle and further our understanding of the ability of the virus to evade host cell responses.

In Chapter 3 of this dissertation, we have identified Y129 residue of M2 as critical for M2 mediated functions, namely, IL-10 production and IRF4 induction *in vitro*, as well as plasma

cell differentiation and reactivation *in vivo*. This study strongly emphasizes on the utility of the MHV68 model to study *in vivo* pathogenesis using viral mutants, which is impossible to study in the human herpesviruses. Our study is also supportive of biochemical data from other investigators that suggest a model where M2 acts as a scaffolding protein [61] to form a signalosome-like structure comprising of PLCγ2, Src kinases and Vav, as observed upon BCR cross-linking (reviewed in [66]). Taken together, data from chapter 2 and 3 provide valuable insights into the functions of M2, both from the perspective of the host as well as the virus. We show the host factors required for mediating the functions of M2 and the residues in M2 that are critical for these functions. Further studies in this arena will address the requirements of other domains in M2 that are required for plasma cell differentiation and reactivation. We have previously reported a panel of M2 mutants and described their requirement in latency and reactivation [162], however, the requirement of these residues in plasma cell differentiation remains to be tested. It would be particularly useful to make the M2 mutant viruses in the background of the H2bYFP virus which will help to track the infected cell population [180] as well as image spleen sections by immunofluorescence (as described above).

M2 mediated plasma cell differentiation and reactivation from latency.

Another key question that arises from this project is whether IL-10 is involved in plasma cell differentiation. Currently, there are no conclusive reports on the ability of IL-10 to induce plasma cell differentiation in mice. In both humans and mice, a subset of B cells termed B regulatory cells (B_{regs} or B10 cells) have been shown to play a regulatory role by suppression of inflammatory responses in autoimmunity ([122-127] and reviewed in [128]). One study in mice showed that these cells have the capacity for plasma cell differentiation [127] by expression of IRF4 and Blimp-1. However, there are no reports on the ability of these cells to differentiate in humans. In humans B cells, there are some reports on IL-10 induction of plasma cell

differentiation [176], where *in vitro* treatment of a GC-like B cell line with IL-10 resulted in plasma cell differentiation. Our data strongly supports that IL-10 may perhaps be involved, at least in an indirect fashion, in plasma cell differentiation. Whether the B_{regs} are capable of plasma cell differentiation is a topic that is widely being pursued by several investigators. With respect to gammaherpesvirus biology, identifying potential roles of IL-10 in plasma cell differentiation will particularly be helpful in understanding the role of vIL-10 of EBV.

Based on our current understanding, we believe that M2 mediated plasma cell differentiation occurs *via* M2 induction of IRF4, the plasma cell associated transcription factor. However, we cannot rule out that other host or viral factors do not play a role in M2 induction of plasma cell differentiation and/or reactivation. Importantly, we have recently shown that IRF4 synergizes with the lytic transactivator, RTA, to activate the M1 promoter (O'Flaherty BM and Speck SH, manuscript in revision). Therefore, it will not be surprising if M2 perhaps, functions with or induces the expression of RTA. As a preliminary step to this, we have shown that M2 can activate the promoter of RTA in B cells (Rangaswamy US, Wakeman BM and Speck SH, unpublished data). Further studies will assess the cis-and trans- factors required for M2 mediated up regulation of RTA activity. Based on immunofluorescence data, there is no evidence of M2 localizing to the nucleus [53,61]. Therefore, we believe that M2 recruits other cis-elements that can translocate to the nucleus to mediate transcriptional activation of RTA. Interestingly, the zinc finger antiviral protein (ZAP) which serves to bind viral mRNA molecules and target them for degradation was shown to target M2 mRNA. Consistent with this, knockdown of ZAP resulted in increased reactivation concomitant with increased RTA as well as M2, indicating that perhaps M2 acts to increase RTA levels [169].

Complementary to the above studies, it is also likely that M2 can also regulate the expression of other plasma cell associated factors, namely Blimp-1 and XBP-1. Consistent with the role of plasma cells in mediating reactivation, we have already shown that MHV68 requires

Blimp-1 for virus specific antibody responses and for efficient latency and reactivation [211]. In our studies using IRF4$^{fl/fl}$ mice infection with a Cre expressing virus, it is possible that the Cre mediated deletion affected subsets other than B cells that MHV68 can infect, namely, macrophages and dendritic cells [190]. To address this in a direct fashion, we infected mice in which either XBP-1 or IRF4 was deleted only in B cells (XBP-1 $^{fl/fl}$ CD19$^{Cre/+}$ or IRF4 $^{fl/fl}$ CD19$^{Cre/+}$). Strikingly, infection of IRF4 knockouts, but not XBP-1 knockouts, showed a severe defect in establishment of latency as well as reactivation from latency (Matar CG, Rangaswamy US, Wakeman BM and Speck SH, manuscript in preparation). This clearly points to a critical role for IRF4 in MHV68 biology. Alternatively, it is possible that the severe defect observed in IRF4 knockouts are due to an indirect deficiency in germinal center B cells. This can be tested by using another knockout model where there is a defect in germinal center B cell formation as well as plasma cell formation.

M2 mediated changes in gene expression.

The microarray data presented in chapter 4 provides plethora of opportunities to identify signaling pathways mediated by M2. Although we focused on the IL-10 independent pathways, using the same data set, there is great promise in identifying other major signaling pathways mediated by M2 that are IL-10 dependent. Indeed, from the number of genes differentially changed in M2 vs M2stop expressing cells, it is clear that a vast majority of the pathways depend on IL-10. Further exploration and validation of the pathways in this subset of genes will prove highly useful in elucidating the requirements of IL-10 in M2 mediated functions. Indeed, CD23, a gene that we found to be among the top genes that was down-regulated in the microarray analysis (Rangaswamy US and Speck SH, unpublished data) was down-regulated significantly upon M2 expression in our flow cytometric analysis of primary murine B cells [190]. Indeed, the EBNA-2 gene product of EBV induces CD23 expression [255,256], which gets cleaved and shed and acts

as an autocrine growth factor for lymphoblastoid cell lines (LCLs) [257,258]. Therefore, future work to address other pathways manipulated by M2 in an IL-10 dependent manner would complement studies described in chapter 2.

Another avenue of research with the available microarray data would be to compare gene expression profiles of publicly available data from EBV and/or KSHV patients or gene expression analysis performed with available tissue culture-based cell lines [259-261]. Interestingly, since M2 up regulated SOCS2 expression in an IL-10 independent fashion, it would be important to characterize whether the human viruses encode proteins that modulate negative regulators of cytokine signaling. Indeed, SOCS2 has been shown to be up regulated in two gene expression studies in the analysis of latently infected EBV cells (reviewed in [262]).

CONCLUDING REMARKS

Fine tuning the mechanism of M2 mediated IL10 induction is instrumental to understanding how the virus uses this immunomodulatory mechanism as a means to maintain its niche in host cells. Identifying proteins and specific domains within the proteins that interact with M2 is crucial to gain a better physiological perspective of how MHV68 utilizes M2 to hijack the host cell signaling machinery to its own benefit. In conclusion, the results from these studies, as well as further studies aimed to characterize the biochemical properties of M2, will aid in understanding common strategies utilized by gammaherpesviruses to evade host immune response and anti-viral mechanisms.

REFERENCES

1. Davison AJ (2007) Overview of classification. In: Arvin A, Campadelli-Fiume G, Mocarski E, Moore PS, Roizman B et al., editors. Human Herpesviruses: Biology, Therapy, and Immunoprophylaxis. Cambridge.
2. Baines JD, Pellett PE (2007) Genetic comparison of human alphaherpesvirus genomes. In: Arvin A, Campadelli-Fiume G, Mocarski E, Moore PS, Roizman B et al., editors. Human Herpesviruses: Biology, Therapy, and Immunoprophylaxis. Cambridge.
3. Kondo K, Xu J, Mocarski ES (1996) Human cytomegalovirus latent gene expression in granulocyte-macrophage progenitors in culture and in seropositive individuals. Proc Natl Acad Sci U S A 93: 11137-11142.
4. Young LS, Murray PG (2003) Epstein-Barr virus and oncogenesis: from latent genes to tumours. Oncogene 22: 5108-5121.
5. Heller M, Kieff E (1981) Colinearity between the DNAs of Epstein-Barr virus and herpesvirus papio. J Virol 37: 821-826.
6. Chang Y, Cesarman E, Pessin MS, Lee F, Culpepper J, et al. (1994) Identification of herpesvirus-like DNA sequences in AIDS-associated Kaposi's sarcoma. Science 266: 1865-1869.
7. Longnecker R, Neipel F (2007) Introduction to the human gamma-herpesviruses. In: Arvin A, Campadelli-Fiume G, Mocarski E, Moore PS, Roizman B et al., editors. Human Herpesviruses: Biology, Therapy, and Immunoprophylaxis. Cambridge.
8. zur Hausen H, Schulte-Holthausen H, Klein G, Henle W, Henle G, et al. (1970) EBV DNA in biopsies of Burkitt tumours and anaplastic carcinomas of the nasopharynx. Nature 228: 1056-1058.
9. Young L, Alfieri C, Hennessy K, Evans H, O'Hara C, et al. (1989) Expression of Epstein-Barr virus transformation-associated genes in tissues of patients with EBV lymphoproliferative disease. N Engl J Med 321: 1080-1085.
10. Pathmanathan R, Prasad U, Chandrika G, Sadler R, Flynn K, et al. (1995) Undifferentiated, nonkeratinizing, and squamous cell carcinoma of the nasopharynx. Variants of Epstein-Barr virus-infected neoplasia. Am J Pathol 146: 1355-1367.
11. Glaser SL, Lin RJ, Stewart SL, Ambinder RF, Jarrett RF, et al. (1997) Epstein-Barr virus-associated Hodgkin's disease: epidemiologic characteristics in international data. Int J Cancer 70: 375-382.
12. Damania B (2007) DNA tumor viruses and human cancer. Trends Microbiol 15: 38-44.
13. Barton E, Mandal P, Speck SH (2011) Pathogenesis and host control of gammaherpesviruses: lessons from the mouse. Annu Rev Immunol 29: 351-397.
14. Martin JN (2007) The epidemiology of KSHV and its association with malignant disease. In: Arvin A, Campadelli-Fiume G, Mocarski E, Moore PS, Roizman B et al., editors. Human Herpesviruses: Biology, Therapy, and Immunoprophylaxis. Cambridge.
15. Blaskovic D, Stancekova M, Svobodova J, Mistrikova J (1980) Isolation of five strains of herpesviruses from two species of free living small rodents. Acta Virol 24: 468.
16. Blasdell K, McCracken C, Morris A, Nash AA, Begon M, et al. (2003) The wood mouse is a natural host for Murid herpesvirus 4. J Gen Virol 84: 111-113.

17. Telfer S, Bennett M, Carslake D, Helyar S, Begon M (2007) The dynamics of murid gammaherpesvirus 4 within wild, sympatric populations of bank voles and wood mice. J Wildl Dis 43: 32-39.
18. Rajcani J, Blaskovic D, Svobodova J, Ciampor F, Huckova D, et al. (1985) Pathogenesis of acute and persistent murine herpesvirus infection in mice. Acta Virol 29: 51-60.
19. Francois S, Vidick S, Sarlet M, Desmecht D, Drion P, et al. (2013) Illumination of murine gammaherpesvirus-68 cycle reveals a sexual transmission route from females to males in laboratory mice. PLoS Pathog 9: e1003292.
20. Jacoby MA, Virgin HWt, Speck SH (2002) Disruption of the M2 gene of murine gammaherpesvirus 68 alters splenic latency following intranasal, but not intraperitoneal, inoculation. J Virol 76: 1790-1801.
21. Herskowitz JH, Jacoby MA, Speck SH (2005) The murine gammaherpesvirus 68 M2 gene is required for efficient reactivation from latently infected B cells. J Virol 79: 2261-2273.
22. Tibbetts SA, Loh J, Van Berkel V, McClellan JS, Jacoby MA, et al. (2003) Establishment and maintenance of gammaherpesvirus latency are independent of infective dose and route of infection. J Virol 77: 7696-7701.
23. Virgin HWt, Latreille P, Wamsley P, Hallsworth K, Weck KE, et al. (1997) Complete sequence and genomic analysis of murine gammaherpesvirus 68. J Virol 71: 5894-5904.
24. Forrest J, Krug L, Speck S (2009) Murine Gammaherpesvirus 68 Infection of Mice: A Small Animal Model for Characterizing Basic Aspects of Gammaherpesvirus Pathogenesis. In: Damania B, Pipas J, editors. DNA Tumor Viruses: Springer US. pp. 735-775.
25. Moorman NJ, Lin CY, Speck SH (2004) Identification of candidate gammaherpesvirus 68 genes required for virus replication by signature-tagged transposon mutagenesis. J Virol 78: 10282-10290.
26. Song MJ, Hwang S, Wong WH, Wu TT, Lee S, et al. (2005) Identification of viral genes essential for replication of murine gamma-herpesvirus 68 using signature-tagged mutagenesis. Proc Natl Acad Sci U S A 102: 3805-3810.
27. Sunil-Chandra NP, Efstathiou S, Nash AA (1992) Murine gammaherpesvirus 68 establishes a latent infection in mouse B lymphocytes in vivo. J Gen Virol 73 (Pt 12): 3275-3279.
28. Sunil-Chandra NP, Efstathiou S, Arno J, Nash AA (1992) Virological and pathological features of mice infected with murine gamma-herpesvirus 68. J Gen Virol 73 (Pt 9): 2347-2356.
29. Usherwood EJ, Ross AJ, Allen DJ, Nash AA (1996) Murine gammaherpesvirus-induced splenomegaly: a critical role for CD4 T cells. J Gen Virol 77 (Pt 4): 627-630.
30. Usherwood EJ, Stewart JP, Robertson K, Allen DJ, Nash AA (1996) Absence of splenic latency in murine gammaherpesvirus 68-infected B cell-deficient mice. J Gen Virol 77 (Pt 11): 2819-2825.
31. Weck KE, Barkon ML, Yoo LI, Speck SH, Virgin HI (1996) Mature B cells are required for acute splenic infection, but not for establishment of latency, by murine gammaherpesvirus 68. J Virol 70: 6775-6780.
32. Flano E, Husain SM, Sample JT, Woodland DL, Blackman MA (2000) Latent murine gamma-herpesvirus infection is established in activated B cells, dendritic cells, and macrophages. J Immunol 165: 1074-1081.

33. Willer DO, Speck SH (2003) Long-term latent murine Gammaherpesvirus 68 infection is preferentially found within the surface immunoglobulin D-negative subset of splenic B cells in vivo. J Virol 77: 8310-8321.
34. Weck KE, Kim SS, Virgin HI, Speck SH (1999) B cells regulate murine gammaherpesvirus 68 latency. J Virol 73: 4651-4661.
35. Weck KE, Kim SS, Virgin HI, Speck SH (1999) Macrophages are the major reservoir of latent murine gammaherpesvirus 68 in peritoneal cells. J Virol 73: 3273-3283.
36. Kim IJ, Flano E, Woodland DL, Lund FE, Randall TD, et al. (2003) Maintenance of long term gamma-herpesvirus B cell latency is dependent on CD40-mediated development of memory B cells. J Immunol 171: 886-892.
37. Stewart JP, Usherwood EJ, Ross A, Dyson H, Nash T (1998) Lung epithelial cells are a major site of murine gammaherpesvirus persistence. J Exp Med 187: 1941-1951.
38. Krug LT, Moser JM, Dickerson SM, Speck SH (2007) Inhibition of NF-kappaB activation in vivo impairs establishment of gammaherpesvirus latency. PLoS Pathog 3: e11.
39. Suarez AL, van Dyk LF (2008) Endothelial cells support persistent gammaherpesvirus 68 infection. PLoS Pathog 4: e1000152.
40. Sunil-Chandra NP, Arno J, Fazakerley J, Nash AA (1994) Lymphoproliferative disease in mice infected with murine gammaherpesvirus 68. Am J Pathol 145: 818-826.
41. Tarakanova VL, Suarez F, Tibbetts SA, Jacoby MA, Weck KE, et al. (2005) Murine gammaherpesvirus 68 infection is associated with lymphoproliferative disease and lymphoma in BALB beta2 microglobulin-deficient mice. J Virol 79: 14668-14679.
42. Usherwood EJ, Stewart JP, Nash AA (1996) Characterization of tumor cell lines derived from murine gammaherpesvirus-68-infected mice. J Virol 70: 6516-6518.
43. Wu TT, Usherwood EJ, Stewart JP, Nash AA, Sun R (2000) Rta of murine gammaherpesvirus 68 reactivates the complete lytic cycle from latency. J Virol 74: 3659-3667.
44. Husain SM, Usherwood EJ, Dyson H, Coleclough C, Coppola MA, et al. (1999) Murine gammaherpesvirus M2 gene is latency-associated and its protein a target for CD8(+) T lymphocytes. Proc Natl Acad Sci U S A 96: 7508-7513.
45. Liang X, Paden CR, Morales FM, Powers RP, Jacob J, et al. (2011) Murine gamma-herpesvirus immortalization of fetal liver-derived B cells requires both the viral cyclin D homolog and latency-associated nuclear antigen. PLoS Pathog 7: e1002220.
46. Evans AG, Moser JM, Krug LT, Pozharskaya V, Mora AL, et al. (2008) A gammaherpesvirus-secreted activator of Vbeta4+ CD8+ T cells regulates chronic infection and immunopathology. J Exp Med 205: 669-684.
47. van Berkel V, Preiter K, Virgin HWt, Speck SH (1999) Identification and initial characterization of the murine gammaherpesvirus 68 gene M3, encoding an abundantly secreted protein. J Virol 73: 4524-4529.
48. van Berkel V, Barrett J, Tiffany HL, Fremont DH, Murphy PM, et al. (2000) Identification of a gammaherpesvirus selective chemokine binding protein that inhibits chemokine action. J Virol 74: 6741-6747.
49. Alexander JM, Nelson CA, van Berkel V, Lau EK, Studts JM, et al. (2002) Structural basis of chemokine sequestration by a herpesvirus decoy receptor. Cell 111: 343-356.

50. Evans AG, Moorman NJ, Willer DO, Speck SH (2006) The M4 gene of gammaHV68 encodes a secreted glycoprotein and is required for the efficient establishment of splenic latency. Virology 344: 520-531.
51. Virgin HWt, Presti RM, Li XY, Liu C, Speck SH (1999) Three distinct regions of the murine gammaherpesvirus 68 genome are transcriptionally active in latently infected mice. J Virol 73: 2321-2332.
52. Correia S, Ventura S, Parkhouse RM (2013) Identification and utility of innate immune system evasion mechanisms of ASFV. Virus Res 173: 87-100.
53. Liang X, Shin YC, Means RE, Jung JU (2004) Inhibition of interferon-mediated antiviral activity by murine gammaherpesvirus 68 latency-associated M2 protein. J Virol 78: 12416-12427.
54. Liang X, Pickering MT, Cho NH, Chang H, Volkert MR, et al. (2006) Deregulation of DNA damage signal transduction by herpesvirus latency-associated M2. J Virol 80: 5862-5874.
55. Madureira PA, Matos P, Soeiro I, Dixon LK, Simas JP, et al. (2005) Murine gamma-herpesvirus 68 latency protein M2 binds to Vav signaling proteins and inhibits B-cell receptor-induced cell cycle arrest and apoptosis in WEHI-231 B cells. J Biol Chem 280: 37310-37318.
56. Rodrigues L, Pires de Miranda M, Caloca MJ, Bustelo XR, Simas JP (2006) Activation of Vav by the gammaherpesvirus M2 protein contributes to the establishment of viral latency in B lymphocytes. J Virol 80: 6123-6135.
57. Pires de Miranda M, Alenquer M, Marques S, Rodrigues L, Lopes F, et al. (2008) The Gammaherpesvirus m2 protein manipulates the Fyn/Vav pathway through a multidocking mechanism of assembly. PLoS One 3: e1654.
58. Siegel AM, Herskowitz JH, Speck SH (2008) The MHV68 M2 protein drives IL-10 dependent B cell proliferation and differentiation. PLoS Pathog 4: e1000039.
59. Iwakoshi NN, Lee AH, Vallabhajosyula P, Otipoby KL, Rajewsky K, et al. (2003) Plasma cell differentiation and the unfolded protein response intersect at the transcription factor XBP-1. Nat Immunol 4: 321-329.
60. Liang X, Collins CM, Mendel JB, Iwakoshi NN, Speck SH (2009) Gammaherpesvirus-driven plasma cell differentiation regulates virus reactivation from latently infected B lymphocytes. PLoS Pathog 5: e1000677.
61. Pires de Miranda M, Lopes FB, McVey CE, Bustelo XR, Simas JP (2013) Role of Src homology domain binding in signaling complexes assembled by the murid gamma-herpesvirus M2 protein. J Biol Chem 288: 3858-3870.
62. Usherwood EJ, Roy DJ, Ward K, Surman SL, Dutia BM, et al. (2000) Control of gammaherpesvirus latency by latent antigen-specific CD8(+) T cells. J Exp Med 192: 943-952.
63. Macrae AI, Usherwood EJ, Husain SM, Flano E, Kim IJ, et al. (2003) Murid herpesvirus 4 strain 68 M2 protein is a B-cell-associated antigen important for latency but not lymphocytosis. J Virol 77: 9700-9709.
64. Simas JP, Marques S, Bridgeman A, Efstathiou S, Adler H (2004) The M2 gene product of murine gammaherpesvirus 68 is required for efficient colonization of splenic follicles but is not necessary for expansion of latently infected germinal centre B cells. J Gen Virol 85: 2789-2797.
65. Kurosaki T, Shinohara H, Baba Y (2010) B cell signaling and fate decision. Annu Rev Immunol 28: 21-55.
66. Harwood NE, Batista FD (2010) Early events in B cell activation. Annu Rev Immunol 28: 185-210.
67. Weber M, Treanor B, Depoil D, Shinohara H, Harwood NE, et al. (2008) Phospholipase C-gamma2 and Vav cooperate within signaling microclusters to

propagate B cell spreading in response to membrane-bound antigen. J Exp Med 205: 853-868.
68. Fu C, Turck CW, Kurosaki T, Chan AC (1998) BLNK: a central linker protein in B cell activation. Immunity 9: 93-103.
69. Dal Porto JM, Gauld SB, Merrell KT, Mills D, Pugh-Bernard AE, et al. (2004) B cell antigen receptor signaling 101. Mol Immunol 41: 599-613.
70. Dolmetsch RE, Lewis RS, Goodnow CC, Healy JI (1997) Differential activation of transcription factors induced by Ca2+ response amplitude and duration. Nature 386: 855-858.
71. Matsumoto M, Fujii Y, Baba A, Hikida M, Kurosaki T, et al. (2011) The calcium sensors STIM1 and STIM2 control B cell regulatory function through interleukin-10 production. Immunity 34: 703-714.
72. Baba Y, Matsumoto M, Kurosaki T (2013) Calcium signaling in B cells: Regulation of cytosolic Ca increase and its sensor molecules, STIM1 and STIM2. Mol Immunol.
73. Gires O, Zimber-Strobl U, Gonnella R, Ueffing M, Marschall G, et al. (1997) Latent membrane protein 1 of Epstein-Barr virus mimics a constitutively active receptor molecule. EMBO J 16: 6131-6140.
74. Kilger E, Kieser A, Baumann M, Hammerschmidt W (1998) Epstein-Barr virus-mediated B-cell proliferation is dependent upon latent membrane protein 1, which simulates an activated CD40 receptor. EMBO J 17: 1700-1709.
75. Caldwell RG, Wilson JB, Anderson SJ, Longnecker R (1998) Epstein-Barr virus LMP2A drives B cell development and survival in the absence of normal B cell receptor signals. Immunity 9: 405-411.
76. Kaye KM, Izumi KM, Kieff E (1993) Epstein-Barr virus latent membrane protein 1 is essential for B-lymphocyte growth transformation. Proc Natl Acad Sci U S A 90: 9150-9154.
77. Burkhardt AL, Bolen JB, Kieff E, Longnecker R (1992) An Epstein-Barr virus transformation-associated membrane protein interacts with src family tyrosine kinases. J Virol 66: 5161-5167.
78. Ding Y, Chen D, Tarcsafalvi A, Su R, Qin L, et al. (2003) Suppressor of cytokine signaling 1 inhibits IL-10-mediated immune responses. J Immunol 170: 1383-1391.
79. Miller CL, Lee JH, Kieff E, Longnecker R (1994) An integral membrane protein (LMP2) blocks reactivation of Epstein-Barr virus from latency following surface immunoglobulin crosslinking. Proc Natl Acad Sci U S A 91: 772-776.
80. Paine E, Scheinman RI, Baldwin AS, Jr., Raab-Traub N (1995) Expression of LMP1 in epithelial cells leads to the activation of a select subset of NF-kappa B/Rel family proteins. J Virol 69: 4572-4576.
81. Huen DS, Henderson SA, Croom-Carter D, Rowe M (1995) The Epstein-Barr virus latent membrane protein-1 (LMP1) mediates activation of NF-kappa B and cell surface phenotype via two effector regions in its carboxy-terminal cytoplasmic domain. Oncogene 10: 549-560.
82. Fukuda M, Longnecker R (2004) Latent membrane protein 2A inhibits transforming growth factor-beta 1-induced apoptosis through the phosphatidylinositol 3-kinase/Akt pathway. J Virol 78: 1697-1705.
83. Lagunoff M, Majeti R, Weiss A, Ganem D (1999) Deregulated signal transduction by the K1 gene product of Kaposi's sarcoma-associated herpesvirus. Proc Natl Acad Sci U S A 96: 5704-5709.
84. Lee H, Guo J, Li M, Choi JK, DeMaria M, et al. (1998) Identification of an immunoreceptor tyrosine-based activation motif of K1 transforming protein of Kaposi's sarcoma-associated herpesvirus. Mol Cell Biol 18: 5219-5228.

85. Lee BS, Lee SH, Feng P, Chang H, Cho NH, et al. (2005) Characterization of the Kaposi's sarcoma-associated herpesvirus K1 signalosome. J Virol 79: 12173-12184.
86. Prakash O, Tang ZY, Peng X, Coleman R, Gill J, et al. (2002) Tumorigenesis and aberrant signaling in transgenic mice expressing the human herpesvirus-8 K1 gene. J Natl Cancer Inst 94: 926-935.
87. Brinkmann MM, Glenn M, Rainbow L, Kieser A, Henke-Gendo C, et al. (2003) Activation of mitogen-activated protein kinase and NF-kappaB pathways by a Kaposi's sarcoma-associated herpesvirus K15 membrane protein. J Virol 77: 9346-9358.
88. Wang L, Brinkmann MM, Pietrek M, Ottinger M, Dittrich-Breiholz O, et al. (2007) Functional characterization of the M-type K15-encoded membrane protein of Kaposi's sarcoma-associated herpesvirus. J Gen Virol 88: 1698-1707.
89. Glenn M, Rainbow L, Aurade F, Davison A, Schulz TF (1999) Identification of a spliced gene from Kaposi's sarcoma-associated herpesvirus encoding a protein with similarities to latent membrane proteins 1 and 2A of Epstein-Barr virus. J Virol 73: 6953-6963.
90. Jung JU, Trimble JJ, King NW, Biesinger B, Fleckenstein BW, et al. (1991) Identification of transforming genes of subgroup A and C strains of Herpesvirus saimiri. Proc Natl Acad Sci U S A 88: 7051-7055.
91. Duboise SM, Guo J, Czajak S, Desrosiers RC, Jung JU (1998) STP and Tip are essential for herpesvirus saimiri oncogenicity. J Virol 72: 1308-1313.
92. Lee H, Choi JK, Li M, Kaye K, Kieff E, et al. (1999) Role of cellular tumor necrosis factor receptor-associated factors in NF-kappaB activation and lymphocyte transformation by herpesvirus Saimiri STP. J Virol 73: 3913-3919.
93. Lund T, Medveczky MM, Medveczky PG (1997) Herpesvirus saimiri Tip-484 membrane protein markedly increases p56lck activity in T cells. J Virol 71: 378-382.
94. Lund TC, Prator PC, Medveczky MM, Medveczky PG (1999) The Lck binding domain of herpesvirus saimiri tip-484 constitutively activates Lck and STAT3 in T cells. J Virol 73: 1689-1694.
95. Guo J, Duboise M, Lee H, Li M, Choi JK, et al. (1997) Enhanced downregulation of Lck-mediated signal transduction by a Y114 mutation of herpesvirus Saimiri tip. J Virol 71: 7092-7096.
96. Moore KW, Vieira P, Fiorentino DF, Trounstine ML, Khan TA, et al. (1990) Homology of cytokine synthesis inhibitory factor (IL-10) to the Epstein-Barr virus gene BCRFI. Science 248: 1230-1234.
97. Miyazaki I, Cheung RK, Dosch HM (1993) Viral interleukin 10 is critical for the induction of B cell growth transformation by Epstein-Barr virus. J Exp Med 178: 439-447.
98. Suzuki T, Tahara H, Narula S, Moore KW, Robbins PD, et al. (1995) Viral interleukin 10 (IL-10), the human herpes virus 4 cellular IL-10 homologue, induces local anergy to allogeneic and syngeneic tumors. J Exp Med 182: 477-486.
99. Zeidler R, Eissner G, Meissner P, Uebel S, Tampe R, et al. (1997) Downregulation of TAP1 in B lymphocytes by cellular and Epstein-Barr virus-encoded interleukin-10. Blood 90: 2390-2397.
100. Nicholas J, Ruvolo VR, Burns WH, Sandford G, Wan X, et al. (1997) Kaposi's sarcoma-associated human herpesvirus-8 encodes homologues of macrophage inflammatory protein-1 and interleukin-6. Nat Med 3: 287-292.
101. Jones KD, Aoki Y, Chang Y, Moore PS, Yarchoan R, et al. (1999) Involvement of interleukin-10 (IL-10) and viral IL-6 in the spontaneous growth of Kaposi's

sarcoma herpesvirus-associated infected primary effusion lymphoma cells. Blood 94: 2871-2879.
102. Molden J, Chang Y, You Y, Moore PS, Goldsmith MA (1997) A Kaposi's sarcoma-associated herpesvirus-encoded cytokine homolog (vIL-6) activates signaling through the shared gp130 receptor subunit. J Biol Chem 272: 19625-19631.
103. Boshoff C, Endo Y, Collins PD, Takeuchi Y, Reeves JD, et al. (1997) Angiogenic and HIV-inhibitory functions of KSHV-encoded chemokines. Science 278: 290-294.
104. Stine JT, Wood C, Hill M, Epp A, Raport CJ, et al. (2000) KSHV-encoded CC chemokine vMIP-III is a CCR4 agonist, stimulates angiogenesis, and selectively chemoattracts TH2 cells. Blood 95: 1151-1157.
105. Polizzotto MN, Uldrick TS, Wang V, Aleman K, Wyvill KM, et al. (2013) Human and viral interleukin-6 and other cytokines in Kaposi sarcoma herpesvirus-associated multicentric Castleman disease. Blood 122: 4189-4198.
106. Nicholas J (2005) Human gammaherpesvirus cytokines and chemokine receptors. J Interferon Cytokine Res 25: 373-383.
107. Fiorentino DF, Bond MW, Mosmann TR (1989) Two types of mouse T helper cell. IV. Th2 clones secrete a factor that inhibits cytokine production by Th1 clones. J Exp Med 170: 2081-2095.
108. Fiorentino DF, Zlotnik A, Vieira P, Mosmann TR, Howard M, et al. (1991) IL-10 acts on the antigen-presenting cell to inhibit cytokine production by Th1 cells. J Immunol 146: 3444-3451.
109. Saraiva M, O'Garra A (2010) The regulation of IL-10 production by immune cells. Nat Rev Immunol 10: 170-181.
110. Burdin N, Rousset F, Banchereau J (1997) B-cell-derived IL-10: production and function. Methods 11: 98-111.
111. Malisan F, Briere F, Bridon JM, Harindranath N, Mills FC, et al. (1996) Interleukin-10 induces immunoglobulin G isotype switch recombination in human CD40-activated naive B lymphocytes. J Exp Med 183: 937-947.
112. Briere F, Servet-Delprat C, Bridon JM, Saint-Remy JM, Banchereau J (1994) Human interleukin 10 induces naive surface immunoglobulin D+ (sIgD+) B cells to secrete IgG1 and IgG3. J Exp Med 179: 757-762.
113. Burdin N, Van Kooten C, Galibert L, Abrams JS, Wijdenes J, et al. (1995) Endogenous IL-6 and IL-10 contribute to the differentiation of CD40-activated human B lymphocytes. J Immunol 154: 2533-2544.
114. Matthes T, Werner-Favre C, Tang H, Zhang X, Kindler V, et al. (1993) Cytokine mRNA expression during an in vitro response of human B lymphocytes: kinetics of B cell tumor necrosis factor alpha, interleukin (IL)6, IL-10, and transforming growth factor beta 1 mRNAs. J Exp Med 178: 521-528.
115. Levy Y, Brouet JC (1994) Interleukin-10 prevents spontaneous death of germinal center B cells by induction of the bcl-2 protein. J Clin Invest 93: 424-428.
116. Li L, Krajewski S, Reed JC, Choi YS (1997) The apoptosis and proliferation of SAC-activated B cells by IL-10 are associated with changes in Bcl-2, Bcl-xL, and Mcl-1 expression. Cell Immunol 178: 33-41.
117. O'Garra A, Stapleton G, Dhar V, Pearce M, Schumacher J, et al. (1990) Production of cytokines by mouse B cells: B lymphomas and normal B cells produce interleukin 10. Int Immunol 2: 821-832.
118. O'Garra A, Chang R, Go N, Hastings R, Haughton G, et al. (1992) Ly-1 B (B-1) cells are the main source of B cell-derived interleukin 10. Eur J Immunol 22: 711-717.

119. Ishida H, Hastings R, Kearney J, Howard M (1992) Continuous anti-interleukin 10 antibody administration depletes mice of Ly-1 B cells but not conventional B cells. J Exp Med 175: 1213-1220.
120. Fillatreau S, Sweenie CH, McGeachy MJ, Gray D, Anderton SM (2002) B cells regulate autoimmunity by provision of IL-10. Nat Immunol 3: 944-950.
121. Blair PA, Norena LY, Flores-Borja F, Rawlings DJ, Isenberg DA, et al. (2010) CD19(+)CD24(hi)CD38(hi) B cells exhibit regulatory capacity in healthy individuals but are functionally impaired in systemic Lupus Erythematosus patients. Immunity 32: 129-140.
122. Yoshizaki A, Miyagaki T, DiLillo DJ, Matsushita T, Horikawa M, et al. (2012) Regulatory B cells control T-cell autoimmunity through IL-21-dependent cognate interactions. Nature 491: 264-268.
123. Yanaba K, Bouaziz JD, Haas KM, Poe JC, Fujimoto M, et al. (2008) A regulatory B cell subset with a unique CD1dhiCD5+ phenotype controls T cell-dependent inflammatory responses. Immunity 28: 639-650.
124. Yanaba K, Bouaziz JD, Matsushita T, Tsubata T, Tedder TF (2009) The development and function of regulatory B cells expressing IL-10 (B10 cells) requires antigen receptor diversity and TLR signals. J Immunol 182: 7459-7472.
125. Poe JC, Smith SH, Haas KM, Yanaba K, Tsubata T, et al. (2011) Amplified B lymphocyte CD40 signaling drives regulatory B10 cell expansion in mice. PLoS One 6: e22464.
126. Iwata Y, Matsushita T, Horikawa M, Dilillo DJ, Yanaba K, et al. (2011) Characterization of a rare IL-10-competent B-cell subset in humans that parallels mouse regulatory B10 cells. Blood 117: 530-541.
127. Maseda D, Smith SH, DiLillo DJ, Bryant JM, Candando KM, et al. (2012) Regulatory B10 cells differentiate into antibody-secreting cells after transient IL-10 production in vivo. J Immunol 188: 1036-1048.
128. Kalampokis I, Yoshizaki A, Tedder TF (2013) IL-10-producing regulatory B cells (B10 cells) in autoimmune disease. Arthritis Res Ther 15 Suppl 1: S1.
129. Horikawa M, Minard-Colin V, Matsushita T, Tedder TF (2011) Regulatory B cell production of IL-10 inhibits lymphoma depletion during CD20 immunotherapy in mice. J Clin Invest 121: 4268-4280.
130. Charles Janeway PT, Mark Walport, Mark Shlomchik (2001) Immunobiology: The Immune System in Health and Disease. Garland Science: Taylor & Francis.
131. Levine MH, Haberman AM, Sant'Angelo DB, Hannum LG, Cancro MP, et al. (2000) A B-cell receptor-specific selection step governs immature to mature B cell differentiation. Proc Natl Acad Sci U S A 97: 2743-2748.
132. Pillai S, Cariappa A, Moran ST (2005) Marginal zone B cells. Annu Rev Immunol 23: 161-196.
133. Klein U, Dalla-Favera R (2008) Germinal centres: role in B-cell physiology and malignancy. Nat Rev Immunol 8: 22-33.
134. Sze DM, Toellner KM, Garcia de Vinuesa C, Taylor DR, MacLennan IC (2000) Intrinsic constraint on plasmablast growth and extrinsic limits of plasma cell survival. J Exp Med 192: 813-821.
135. Slifka MK, Antia R, Whitmire JK, Ahmed R (1998) Humoral immunity due to long-lived plasma cells. Immunity 8: 363-372.
136. Turner CA, Jr., Mack DH, Davis MM (1994) Blimp-1, a novel zinc finger-containing protein that can drive the maturation of B lymphocytes into immunoglobulin-secreting cells. Cell 77: 297-306.

137. Shaffer AL, Lin KI, Kuo TC, Yu X, Hurt EM, et al. (2002) Blimp-1 orchestrates plasma cell differentiation by extinguishing the mature B cell gene expression program. Immunity 17: 51-62.
138. Shapiro-Shelef M, Lin KI, McHeyzer-Williams LJ, Liao J, McHeyzer-Williams MG, et al. (2003) Blimp-1 is required for the formation of immunoglobulin secreting plasma cells and pre-plasma memory B cells. Immunity 19: 607-620.
139. Sciammas R, Shaffer AL, Schatz JH, Zhao H, Staudt LM, et al. (2006) Graded expression of interferon regulatory factor-4 coordinates isotype switching with plasma cell differentiation. Immunity 25: 225-236.
140. Klein U, Casola S, Cattoretti G, Shen Q, Lia M, et al. (2006) Transcription factor IRF4 controls plasma cell differentiation and class-switch recombination. Nat Immunol 7: 773-782.
141. Mittrucker HW, Matsuyama T, Grossman A, Kundig TM, Potter J, et al. (1997) Requirement for the transcription factor LSIRF/IRF4 for mature B and T lymphocyte function. Science 275: 540-543.
142. Cattoretti G, Shaknovich R, Smith PM, Jack HM, Murty VV, et al. (2006) Stages of germinal center transit are defined by B cell transcription factor coexpression and relative abundance. J Immunol 177: 6930-6939.
143. Lin L, Gerth AJ, Peng SL (2004) Active inhibition of plasma cell development in resting B cells by microphthalmia-associated transcription factor. J Exp Med 200: 115-122.
144. Ochiai K, Maienschein-Cline M, Simonetti G, Chen J, Rosenthal R, et al. (2013) Transcriptional regulation of germinal center B and plasma cell fates by dynamical control of IRF4. Immunity 38: 918-929.
145. Gupta S, Jiang M, Anthony A, Pernis AB (1999) Lineage-specific modulation of interleukin 4 signaling by interferon regulatory factor 4. J Exp Med 190: 1837-1848.
146. Kallies A, Nutt SL (2007) Terminal differentiation of lymphocytes depends on Blimp-1. Curr Opin Immunol 19: 156-162.
147. Pernis AB (2002) The role of IRF-4 in B and T cell activation and differentiation. J Interferon Cytokine Res 22: 111-120.
148. De Silva NS, Simonetti G, Heise N, Klein U (2012) The diverse roles of IRF4 in late germinal center B-cell differentiation. Immunol Rev 247: 73-92.
149. Lohoff M, Mittrucker HW, Prechtl S, Bischof S, Sommer F, et al. (2002) Dysregulated T helper cell differentiation in the absence of interferon regulatory factor 4. Proc Natl Acad Sci U S A 99: 11808-11812.
150. Brustle A, Heink S, Huber M, Rosenplanter C, Stadelmann C, et al. (2007) The development of inflammatory T(H)-17 cells requires interferon-regulatory factor 4. Nat Immunol 8: 958-966.
151. Bollig N, Brustle A, Kellner K, Ackermann W, Abass E, et al. (2012) Transcription factor IRF4 determines germinal center formation through follicular T-helper cell differentiation. Proc Natl Acad Sci U S A 109: 8664-8669.
152. Cretney E, Xin A, Shi W, Minnich M, Masson F, et al. (2011) The transcription factors Blimp-1 and IRF4 jointly control the differentiation and function of effector regulatory T cells. Nat Immunol 12: 304-311.
153. Lee CG, Kang KH, So JS, Kwon HK, Son JS, et al. (2009) A distal cis-regulatory element, CNS-9, controls NFAT1 and IRF4-mediated IL-10 gene activation in T helper cells. Mol Immunol 46: 613-621.
154. Rengarajan J, Mowen KA, McBride KD, Smith ED, Singh H, et al. (2002) Interferon regulatory factor 4 (IRF4) interacts with NFATc2 to modulate interleukin 4 gene expression. J Exp Med 195: 1003-1012.

155. Crawford DH, Ando I (1986) EB virus induction is associated with B-cell maturation. Immunology 59: 405-409.
156. Laichalk LL, Thorley-Lawson DA (2005) Terminal differentiation into plasma cells initiates the replicative cycle of Epstein-Barr virus in vivo. J Virol 79: 1296-1307.
157. Sun CC, Thorley-Lawson DA (2007) Plasma cell-specific transcription factor XBP-1s binds to and transactivates the Epstein-Barr virus BZLF1 promoter. J Virol 81: 13566-13577.
158. Bhende PM, Dickerson SJ, Sun X, Feng WH, Kenney SC (2007) X-box-binding protein 1 activates lytic Epstein-Barr virus gene expression in combination with protein kinase D. J Virol 81: 7363-7370.
159. Wilson SJ, Tsao EH, Webb BL, Ye H, Dalton-Griffin L, et al. (2007) X box binding protein XBP-1s transactivates the Kaposi's sarcoma-associated herpesvirus (KSHV) ORF50 promoter, linking plasma cell differentiation to KSHV reactivation from latency. J Virol 81: 13578-13586.
160. Yu F, Feng J, Harada JN, Chanda SK, Kenney SC, et al. (2007) B cell terminal differentiation factor XBP-1 induces reactivation of Kaposi's sarcoma-associated herpesvirus. FEBS Lett 581: 3485-3488.
161. Jenner RG, Maillard K, Cattini N, Weiss RA, Boshoff C, et al. (2003) Kaposi's sarcoma-associated herpesvirus-infected primary effusion lymphoma has a plasma cell gene expression profile. Proc Natl Acad Sci U S A 100: 10399-10404.
162. Herskowitz JH, Siegel AM, Jacoby MA, Speck SH (2008) Systematic mutagenesis of the murine gammaherpesvirus 68 M2 protein identifies domains important for chronic infection. J Virol 82: 3295-3310.
163. Baba Y, Kurosaki T (2011) Impact of Ca2+ signaling on B cell function. Trends Immunol 32: 589-594.
164. Wakkach A, Cottrez F, Groux H (2000) Can interleukin-10 be used as a true immunoregulatory cytokine? Eur Cytokine Netw 11: 153-160.
165. Damania B (2004) Oncogenic gamma-herpesviruses: comparison of viral proteins involved in tumorigenesis. Nat Rev Microbiol 2: 656-668.
166. Moser JM, Upton JW, Allen RD, 3rd, Wilson CB, Speck SH (2005) Role of B-cell proliferation in the establishment of gammaherpesvirus latency. J Virol 79: 9480-9491.
167. Warming S, Costantino N, Court DL, Jenkins NA, Copeland NG (2005) Simple and highly efficient BAC recombineering using galK selection. Nucleic Acids Res 33: e36.
168. de Oliveira VL, Almeida SC, Soares HR, Parkhouse RM (2013) Selective B-cell expression of the MHV-68 latency-associated M2 protein regulates T-dependent antibody response and inhibits apoptosis upon viral infection. J Gen Virol 94: 1613-1623.
169. Xuan Y, Liu L, Shen S, Deng H, Gao G (2012) Zinc finger antiviral protein inhibits murine gammaherpesvirus 68 M2 expression and regulates viral latency in cultured cells. J Virol 86: 12431-12434.
170. Berland R, Wortis HH (2003) Normal B-1a cell development requires B cell-intrinsic NFATc1 activity. Proc Natl Acad Sci U S A 100: 13459-13464.
171. Winslow MM, Gallo EM, Neilson JR, Crabtree GR (2006) The calcineurin phosphatase complex modulates immunogenic B cell responses. Immunity 24: 141-152.
172. Ahyi AN, Chang HC, Dent AL, Nutt SL, Kaplan MH (2009) IFN regulatory factor 4 regulates the expression of a subset of Th2 cytokines. J Immunol 183: 1598-1606.

173. Honma K, Kimura D, Tominaga N, Miyakoda M, Matsuyama T, et al. (2008) Interferon regulatory factor 4 differentially regulates the production of Th2 cytokines in naive vs. effector/memory CD4+ T cells. Proc Natl Acad Sci U S A 105: 15890-15895.
174. Lee CG, Hwang W, Maeng KE, Kwon HK, So JS, et al. (2011) IRF4 regulates IL-10 gene expression in CD4(+) T cells through differential nuclear translocation. Cell Immunol 268: 97-104.
175. Ito S, Ansari P, Sakatsume M, Dickensheets H, Vazquez N, et al. (1999) Interleukin-10 inhibits expression of both interferon alpha- and interferon gamma-induced genes by suppressing tyrosine phosphorylation of STAT1. Blood 93: 1456-1463.
176. Choe J, Choi YS (1998) IL-10 interrupts memory B cell expansion in the germinal center by inducing differentiation into plasma cells. Eur J Immunol 28: 508-515.
177. Itoh K, Hirohata S (1995) The role of IL-10 in human B cell activation, proliferation, and differentiation. J Immunol 154: 4341-4350.
178. Kobayashi N, Nagumo H, Agematsu K (2002) IL-10 enhances B-cell IgE synthesis by promoting differentiation into plasma cells, a process that is inhibited by CD27/CD70 interaction. Clin Exp Immunol 129: 446-452.
179. Paden CR, Forrest JC, Tibbetts SA, Speck SH (2012) Unbiased mutagenesis of MHV68 LANA reveals a DNA-binding domain required for LANA function in vitro and in vivo. PLoS Pathog 8: e1002906.
180. Collins CM, Speck SH (2012) Tracking murine gammaherpesvirus 68 infection of germinal center B cells in vivo. PLoS One 7: e33230.
181. Brightbill HD, Plevy SE, Modlin RL, Smale ST (2000) A prominent role for Sp1 during lipopolysaccharide-mediated induction of the IL-10 promoter in macrophages. J Immunol 164: 1940-1951.
182. Wang ZY, Sato H, Kusam S, Sehra S, Toney LM, et al. (2005) Regulation of IL-10 gene expression in Th2 cells by Jun proteins. J Immunol 174: 2098-2105.
183. Macian F, Garcia-Rodriguez C, Rao A (2000) Gene expression elicited by NFAT in the presence or absence of cooperative recruitment of Fos and Jun. EMBO J 19: 4783-4795.
184. Young LS, Rickinson AB (2004) Epstein-Barr virus: 40 years on. Nat Rev Cancer 4: 757-768.
185. Krutzik PO, Clutter MR, Nolan GP (2005) Coordinate analysis of murine immune cell surface markers and intracellular phosphoproteins by flow cytometry. J Immunol 175: 2357-2365.
186. Xuan Y, Gong D, Qi J, Han C, Deng H, et al. (2013) ZAP inhibits murine gammaherpesvirus 68 ORF64 expression and is antagonized by RTA. J Virol 87: 2735-2743.
187. Finbloom DS, Winestock KD (1995) IL-10 induces the tyrosine phosphorylation of tyk2 and Jak1 and the differential assembly of STAT1 alpha and STAT3 complexes in human T cells and monocytes. J Immunol 155: 1079-1090.
188. Krutzik PO, Hale MB, Nolan GP (2005) Characterization of the murine immunological signaling network with phosphospecific flow cytometry. J Immunol 175: 2366-2373.
189. Welte T, Leitenberg D, Dittel BN, al-Ramadi BK, Xie B, et al. (1999) STAT5 interaction with the T cell receptor complex and stimulation of T cell proliferation. Science 283: 222-225.
190. Rangaswamy US, Speck SH (2014) Murine gammaherpesvirus M2 protein induction of IRF4 via the NFAT pathway leads to IL-10 expression in B cells. PLoS Pathog 10: e1003858.

191. Krug LT, Collins CM, Gargano LM, Speck SH (2009) NF-kappaB p50 plays distinct roles in the establishment and control of murine gammaherpesvirus 68 latency. J Virol 83: 4732-4748.
192. Grumont RJ, Gerondakis S (2000) Rel induces interferon regulatory factor 4 (IRF-4) expression in lymphocytes: modulation of interferon-regulated gene expression by rel/nuclear factor kappaB. J Exp Med 191: 1281-1292.
193. Jones EA, Flavell RA (2005) Distal enhancer elements transcribe intergenic RNA in the IL-10 family gene cluster. J Immunol 175: 7437-7446.
194. Bhattacharyya S, Deb J, Patra AK, Thuy Pham DA, Chen W, et al. (2011) NFATc1 affects mouse splenic B cell function by controlling the calcineurin--NFAT signaling network. J Exp Med 208: 823-839.
195. Gupta S, Anthony A, Pernis AB (2001) Stage-specific modulation of IFN-regulatory factor 4 function by Kruppel-type zinc finger proteins. J Immunol 166: 6104-6111.
196. Matsushita T, Tedder TF (2011) Identifying regulatory B cells (B10 cells) that produce IL-10 in mice. Methods Mol Biol 677: 99-111.
197. Yoshimura A, Naka T, Kubo M (2007) SOCS proteins, cytokine signalling and immune regulation. Nat Rev Immunol 7: 454-465.
198. Inagaki-Ohara K, Kondo T, Ito M, Yoshimura A (2013) SOCS, inflammation, and cancer. JAKSTAT 2: e24053.
199. Cassatella MA, Gasperini S, Bovolenta C, Calzetti F, Vollebregt M, et al. (1999) Interleukin-10 (IL-10) selectively enhances CIS3/SOCS3 mRNA expression in human neutrophils: evidence for an IL-10-induced pathway that is independent of STAT protein activation. Blood 94: 2880-2889.
200. Berlato C, Cassatella MA, Kinjyo I, Gatto L, Yoshimura A, et al. (2002) Involvement of suppressor of cytokine signaling-3 as a mediator of the inhibitory effects of IL-10 on lipopolysaccharide-induced macrophage activation. J Immunol 168: 6404-6411.
201. Goldfeld AE, Liu P, Liu S, Flemington EK, Strominger JL, et al. (1995) Cyclosporin A and FK506 block induction of the Epstein-Barr virus lytic cycle by anti-immunoglobulin. Virology 209: 225-229.
202. Liu S, Liu P, Borras A, Chatila T, Speck SH (1997) Cyclosporin A-sensitive induction of the Epstein-Barr virus lytic switch is mediated via a novel pathway involving a MEF2 family member. EMBO J 16: 143-153.
203. Zoeteweij JP, Moses AV, Rinderknecht AS, Davis DA, Overwijk WW, et al. (2001) Targeted inhibition of calcineurin signaling blocks calcium-dependent reactivation of Kaposi sarcoma-associated herpesvirus. Blood 97: 2374-2380.
204. Lukac DM, Renne R, Kirshner JR, Ganem D (1998) Reactivation of Kaposi's sarcoma-associated herpesvirus infection from latency by expression of the ORF 50 transactivator, a homolog of the EBV R protein. Virology 252: 304-312.
205. Ganem D (2006) KSHV infection and the pathogenesis of Kaposi's sarcoma. Annu Rev Pathol 1: 273-296.
206. DeZalia M, Speck SH (2008) Identification of closely spaced but distinct transcription initiation sites for the murine gammaherpesvirus 68 latency-associated M2 gene. J Virol 82: 7411-7421.
207. Carsetti R, Kohler G, Lamers MC (1995) Transitional B cells are the target of negative selection in the B cell compartment. J Exp Med 181: 2129-2140.
208. Stinski MF, Meier JL (2007) Immediate-early viral gene regulation and function. In: Arvin A, Campadelli-Fiume G, Mocarski E, Moore PS, Roizman B et al., editors. Human Herpesviruses: Biology, Therapy, and Immunoprophylaxis. Cambridge.
209. Wehinger J, Gouilleux F, Groner B, Finke J, Mertelsmann R, et al. (1996) IL-10 induces DNA binding activity of three STAT proteins (Stat1, Stat3, and Stat5) and

their distinct combinatorial assembly in the promoters of selected genes. FEBS Lett 394: 365-370.
210. Collins CM, Boss JM, Speck SH (2009) Identification of infected B-cell populations by using a recombinant murine gammaherpesvirus 68 expressing a fluorescent protein. J Virol 83: 6484-6493.
211. Siegel AM, Rangaswamy US, Napier RJ, Speck SH (2010) Blimp-1-dependent plasma cell differentiation is required for efficient maintenance of murine gammaherpesvirus latency and antiviral antibody responses. J Virol 84: 674-685.
212. Mandal P, Krueger BE, Oldenburg D, Andry KA, Beard RS, et al. (2011) A gammaherpesvirus cooperates with interferon-alpha/beta-induced IRF2 to halt viral replication, control reactivation, and minimize host lethality. PLoS Pathog 7: e1002371.
213. Marques S, Alenquer M, Stevenson PG, Simas JP (2008) A single CD8+ T cell epitope sets the long-term latent load of a murid herpesvirus. PLoS Pathog 4: e1000177.
214. Cheng SM, Li JC, Lin SS, Lee DC, Liu L, et al. (2009) HIV-1 transactivator protein induction of suppressor of cytokine signaling-2 contributes to dysregulation of IFN{gamma} signaling. Blood 113: 5192-5201.
215. Hashimoto K, Ishibashi K, Ishioka K, Zhao D, Sato M, et al. (2009) RSV replication is attenuated by counteracting expression of the suppressor of cytokine signaling (SOCS) molecules. Virology 391: 162-170.
216. Koeberlein B, zur Hausen A, Bektas N, Zentgraf H, Chin R, et al. (2010) Hepatitis B virus overexpresses suppressor of cytokine signaling-3 (SOCS3) thereby contributing to severity of inflammation in the liver. Virus Res 148: 51-59.
217. Kundu K, Dutta K, Nazmi A, Basu A (2013) Japanese encephalitis virus infection modulates the expression of suppressors of cytokine signaling (SOCS) in macrophages: implications for the hosts' innate immune response. Cell Immunol 285: 100-110.
218. Lee J, Lim S, Kang SM, Min S, Son K, et al. (2012) Saponin inhibits hepatitis C virus propagation by up-regulating suppressor of cytokine signaling 2. PLoS One 7: e39366.
219. Oshansky CM, Krunkosky TM, Barber J, Jones LP, Tripp RA (2009) Respiratory syncytial virus proteins modulate suppressors of cytokine signaling 1 and 3 and the type I interferon response to infection by a toll-like receptor pathway. Viral Immunol 22: 147-161.
220. Pauli EK, Schmolke M, Wolff T, Viemann D, Roth J, et al. (2008) Influenza A virus inhibits type I IFN signaling via NF-kappaB-dependent induction of SOCS-3 expression. PLoS Pathog 4: e1000196.
221. Pothlichet J, Chignard M, Si-Tahar M (2008) Cutting edge: innate immune response triggered by influenza A virus is negatively regulated by SOCS1 and SOCS3 through a RIG-I/IFNAR1-dependent pathway. J Immunol 180: 2034-2038.
222. Ramirez-Martinez G, Cruz-Lagunas A, Jimenez-Alvarez L, Espinosa E, Ortiz-Quintero B, et al. (2013) Seasonal and pandemic influenza H1N1 viruses induce differential expression of SOCS-1 and RIG-I genes and cytokine/chemokine production in macrophages. Cytokine 62: 151-159.
223. Xu X, Zheng J, Zheng K, Hou Y, Zhao F, et al. (2014) Respiratory Syncytial Virus NS1 Protein Degrades STAT2 by Inducing SOCS1 Expression. Intervirology.
224. Zhang X, Wang J, Cheng J, Ding S, Li M, et al. (2013) An integrated analysis of SOCS1 down-regulation in HBV infection-related hepatocellular carcinoma. J Viral Hepat.

225. Forrest JC, Paden CR, Allen RD, 3rd, Collins J, Speck SH (2007) ORF73-null murine gammaherpesvirus 68 reveals roles for mLANA and p53 in virus replication. J Virol 81: 11957-11971.
226. Ruben S, Perkins A, Purcell R, Joung K, Sia R, et al. (1989) Structural and functional characterization of human immunodeficiency virus tat protein. J Virol 63: 1-8.
227. Stoiber D, Kovarik P, Cohney S, Johnston JA, Steinlein P, et al. (1999) Lipopolysaccharide induces in macrophages the synthesis of the suppressor of cytokine signaling 3 and suppresses signal transduction in response to the activating factor IFN-gamma. J Immunol 163: 2640-2647.
228. Hsu DH, Moore KW, Spits H (1992) Differential effects of IL-4 and IL-10 on IL-2-induced IFN-gamma synthesis and lymphokine-activated killer activity. Int Immunol 4: 563-569.
229. Galizia G, Orditura M, Romano C, Lieto E, Castellano P, et al. (2002) Prognostic significance of circulating IL-10 and IL-6 serum levels in colon cancer patients undergoing surgery. Clin Immunol 102: 169-178.
230. Schloot NC, Hanifi-Moghaddam P, Goebel C, Shatavi SV, Flohe S, et al. (2002) Serum IFN-gamma and IL-10 levels are associated with disease progression in non-obese diabetic mice. Diabetes Metab Res Rev 18: 64-70.
231. Peacock JW, Bost KL (2001) Murine gammaherpesvirus-68-induced interleukin-10 increases viral burden, but limits virus-induced splenomegaly and leukocytosis. Immunology 104: 109-117.
232. Tannahill GM, Elliott J, Barry AC, Hibbert L, Cacalano NA, et al. (2005) SOCS2 can enhance interleukin-2 (IL-2) and IL-3 signaling by accelerating SOCS3 degradation. Mol Cell Biol 25: 9115-9126.
233. Boverhof DR, Tam E, Harney AS, Crawford RB, Kaminski NE, et al. (2004) 2,3,7,8-Tetrachlorodibenzo-p-dioxin induces suppressor of cytokine signaling 2 in murine B cells. Mol Pharmacol 66: 1662-1670.
234. Metcalf D, Greenhalgh CJ, Viney E, Willson TA, Starr R, et al. (2000) Gigantism in mice lacking suppressor of cytokine signalling-2. Nature 405: 1069-1073.
235. Greenhalgh CJ, Metcalf D, Thaus AL, Corbin JE, Uren R, et al. (2002) Biological evidence that SOCS-2 can act either as an enhancer or suppressor of growth hormone signaling. J Biol Chem 277: 40181-40184.
236. Spence S, Fitzsimons A, Boyd CR, Kessler J, Fitzgerald D, et al. (2013) Suppressors of cytokine signaling 2 and 3 diametrically control macrophage polarization. Immunity 38: 66-78.
237. Song MM, Shuai K (1998) The suppressor of cytokine signaling (SOCS) 1 and SOCS3 but not SOCS2 proteins inhibit interferon-mediated antiviral and antiproliferative activities. J Biol Chem 273: 35056-35062.
238. Platanias LC (2005) Mechanisms of type-I- and type-II-interferon-mediated signalling. Nat Rev Immunol 5: 375-386.
239. Der SD, Zhou A, Williams BR, Silverman RH (1998) Identification of genes differentially regulated by interferon alpha, beta, or gamma using oligonucleotide arrays. Proc Natl Acad Sci U S A 95: 15623-15628.
240. Jacobs SR, Damania B (2011) The viral interferon regulatory factors of KSHV: immunosuppressors or oncogenes? Front Immunol 2: 19.
241. Schmidt K, Wies E, Neipel F (2011) Kaposi's sarcoma-associated herpesvirus viral interferon regulatory factor 3 inhibits gamma interferon and major histocompatibility complex class II expression. J Virol 85: 4530-4537.

242. Paden CR, Forrest JC, Moorman NJ, Speck SH (2010) Murine gammaherpesvirus 68 LANA is essential for virus reactivation from splenocytes but not long-term carriage of viral genome. J Virol 84: 7214-7224.
243. Fejer G, Medveczky MM, Horvath E, Lane B, Chang Y, et al. (2003) The latency-associated nuclear antigen of Kaposi's sarcoma-associated herpesvirus interacts preferentially with the terminal repeats of the genome in vivo and this complex is sufficient for episomal DNA replication. J Gen Virol 84: 1451-1462.
244. Viejo-Borbolla A, Ottinger M, Bruning E, Burger A, Konig R, et al. (2005) Brd2/RING3 interacts with a chromatin-binding domain in the Kaposi's Sarcoma-associated herpesvirus latency-associated nuclear antigen 1 (LANA-1) that is required for multiple functions of LANA-1. J Virol 79: 13618-13629.
245. Correia B, Cerqueira SA, Beauchemin C, Pires de Miranda M, Li S, et al. (2013) Crystal structure of the gamma-2 herpesvirus LANA DNA binding domain identifies charged surface residues which impact viral latency. PLoS Pathog 9: e1003673.
246. Domsic JF, Chen HS, Lu F, Marmorstein R, Lieberman PM (2013) Molecular basis for oligomeric-DNA binding and episome maintenance by KSHV LANA. PLoS Pathog 9: e1003672.
247. Hellert J, Weidner-Glunde M, Krausze J, Richter U, Adler H, et al. (2013) A structural basis for BRD2/4-mediated host chromatin interaction and oligomer assembly of Kaposi sarcoma-associated herpesvirus and murine gammaherpesvirus LANA proteins. PLoS Pathog 9: e1003640.
248. Marques S, Efstathiou S, Smith KG, Haury M, Simas JP (2003) Selective gene expression of latent murine gammaherpesvirus 68 in B lymphocytes. J Virol 77: 7308-7318.
249. Longnecker R, Kieff E (1990) A second Epstein-Barr virus membrane protein (LMP2) is expressed in latent infection and colocalizes with LMP1. J Virol 64: 2319-2326.
250. Swart R, Ruf IK, Sample J, Longnecker R (2000) Latent membrane protein 2A-mediated effects on the phosphatidylinositol 3-Kinase/Akt pathway. J Virol 74: 10838-10845.
251. Merchant M, Caldwell RG, Longnecker R (2000) The LMP2A ITAM is essential for providing B cells with development and survival signals in vivo. J Virol 74: 9115-9124.
252. Engels N, Merchant M, Pappu R, Chan AC, Longnecker R, et al. (2001) Epstein-Barr virus latent membrane protein 2A (LMP2A) employs the SLP-65 signaling module. J Exp Med 194: 255-264.
253. Hsu DH, de Waal Malefyt R, Fiorentino DF, Dang MN, Vieira P, et al. (1990) Expression of interleukin-10 activity by Epstein-Barr virus protein BCRF1. Science 250: 830-832.
254. Lee BS, Paulose-Murphy M, Chung YH, Connlole M, Zeichner S, et al. (2002) Suppression of tetradecanoyl phorbol acetate-induced lytic reactivation of Kaposi's sarcoma-associated herpesvirus by K1 signal transduction. J Virol 76: 12185-12199.
255. Wang F, Gregory CD, Rowe M, Rickinson AB, Wang D, et al. (1987) Epstein-Barr virus nuclear antigen 2 specifically induces expression of the B-cell activation antigen CD23. Proc Natl Acad Sci U S A 84: 3452-3456.
256. Thorley-Lawson DA, Mann KP (1985) Early events in Epstein-Barr virus infection provide a model for B cell activation. J Exp Med 162: 45-59.

257. Swendeman S, Thorley-Lawson DA (1987) The activation antigen BLAST-2, when shed, is an autocrine BCGF for normal and transformed B cells. EMBO J 6: 1637-1642.
258. Lacy J, Roth G, Shieh B (1994) Regulation of the human IgE receptor (Fc epsilon RII/CD23) by EBV. Localization of an intron EBV-responsive enhancer and characterization of its cognate GC-box binding factors. J Immunol 153: 5537-5548.
259. Portis T, Dyck P, Longnecker R (2003) Epstein-Barr Virus (EBV) LMP2A induces alterations in gene transcription similar to those observed in Reed-Sternberg cells of Hodgkin lymphoma. Blood 102: 4166-4178.
260. Vockerodt M, Morgan SL, Kuo M, Wei W, Chukwuma MB, et al. (2008) The Epstein-Barr virus oncoprotein, latent membrane protein-1, reprograms germinal centre B cells towards a Hodgkin's Reed-Sternberg-like phenotype. J Pathol 216: 83-92.
261. Shi W, Bastianutto C, Li A, Perez-Ordonez B, Ng R, et al. (2006) Multiple dysregulated pathways in nasopharyngeal carcinoma revealed by gene expression profiling. Int J Cancer 119: 2467-2475.
262. Robertson ES (2010) Epstein-Barr virus : latency and transformation. Wymondham, Norfolk, UK: Caister Academic Press.